

PROPIONYL COENZYME A CARBOXYLASE FROM RHODOSPIRILLUM RUBRUM:

KINETIC STUDIES AND MECHANISM OF ACTION

by

MICHAEL GUTWAKS

A dissertation submitted to the Faculty of Graduate Studies of
the University of Manitoba in partial fulfillment of the requirements
of the degree of

MASTER OF SCIENCE

© 1975

Permission has been granted to the LIBRARY OF THE UNIVERSITY OF MANITOBA to lend or sell copies of this dissertation, to the NATIONAL LIBRARY OF CANADA to microfilm this dissertation and to lend or sell copies of the film, and UNIVERSITY MICROFILMS to publish an abstract of this dissertation.

The author reserves other publication rights, and neither the dissertation nor extensive extracts from it may be printed or otherwise reproduced without the author's written permission.



TO MY BROTHER AND MY PARENTS

ACKNOWLEDGEMENTS

The author wishes to express his deep gratitude to Dr. D. N. Burton, Department of Microbiology, University of Manitoba, whose extreme patience, unfailing enthusiasm, and receptive guidance throughout this study have aided enormously in the preparation of this thesis.

In addition, sincere thanks are extended to Dr. I. Suzuki and the staff and graduate students of the Department of Microbiology for their unselfish assistance and for many enlightening discussions.

ABSTRACT

The enzyme, propionyl CoA carboxylase (propionyl CoA : carbon dioxide ligase (ADP), EC 6.4.1.3), was extracted and partially purified from a microaerophilic culture of Rhodospirillum rubrum grown in the light. Product formation by propionyl CoA carboxylase from R. rubrum displayed a linear proportionality with time and protein concentration. The pH optimum of the enzyme was determined to be 7.9 - 8.1 with a temperature optimum of 30° - 32°. Propionyl CoA carboxylase was subject to heat denaturation, with the loss of all activity occurring at 50°. This enzyme was shown to be a biotin-containing enzyme by its inactivation by avidin and protection against such inactivation by excess biotin. The effects of cations and anions on the activity were also examined in this study, using Na⁺, K⁺, SO₄⁼, PO₄⁼, and Cl⁻ ions.

Apparent and true Michaelis constants were determined for the substrates involved in the reaction; propionyl CoA, HCO₃⁻, ATP, and Mg⁺⁺. As a result of this study, propionyl CoA carboxylase was shown to display a distinct homotropic effect with MgATP. Product in-

hibition studies were carried out with each product, (methylmalonyl CoA, MgADP, and P_i), in combination with every substrate, (propionyl CoA, HCO_3^- , and MgATP). From the kinetic results, a mechanism was proposed for the action of propionyl CoA carboxylase which involves two separate active sites on the enzyme; one for each partial reaction. The two catalytic sites were assumed to be linked by the biotinyl residue, functioning as a carboxyl carrier between the two sites. Propionyl CoA, the substrate for site II, was assumed to interact in the vicinity of site I at high concentrations. This mechanism satisfactorily explains most of the kinetic data obtained in this study.

TABLE OF CONTENTS

	Page
INTRODUCTION	1
HISTORICAL	3
MATERIALS AND METHODS	19
Chemicals	19
Growth and Maintenance of Culture	20
Harvesting and Storage of <u>R. rubrum</u> cells	22
Preparation of <u>R. rubrum</u> Cell-free Extracts	23
Enzyme Assays	24
Purification of Propionyl CoA Carboxylase	25
RESULTS	27
Purification of Propionyl CoA Carboxylase	27
Protein Concentration and Time Dependence of Propionyl CoA Carboxylase	29
pH Optimum	29
Temperature Optimum and Heat Stability of Propionyl CoA Carboxylase	33

Table of Contents Continued

	Page
Effects of Avidin and Biotin	33
Effect of Cations and Anions on Propionyl CoA Carboxylase Activity	36
Kinetics of Propionyl CoA Carboxylase From <u>Rhodospirillum rubrum</u>	38
Determination of Apparent K_m values for Reaction Components	40
1. Apparent K_m for Propionyl CoA	40
2. Apparent K_m for Bicarbonate	40
3. Apparent K_m for MgATP	45
The Influence of Free Mg^{++} on Propionyl CoA Carboxylase Activity Using MgATP as Variable Substrate	49
Determination of True K_m values for Reaction Components	51
1. Propionyl CoA : MgATP	54
2. Propionyl CoA : Bicarbonate	57
3. MgATP : Bicarbonate	62
Product Inhibition Studies	69
1. P_i : MgATP	70
2. P_i : Bicarbonate	70
3. P_i : Propionyl CoA	70

Table of Contents Continued

	Page
4. MgADP : MgATP	77
5. MgADP : Bicarbonate	77
6. MgADP : Propionyl CoA	77
7. Methylmalonyl CoA : MgATP	77
8. Methylmalonyl CoA : Bicarbonate	86
9. Methylmalonyl CoA : Propionyl CoA	86
DISCUSSION	91
General Discussion	91
Effect of pH on Propionyl CoA Carboxylase Activity	91
Effect of Various Cations and Anions on Propionyl CoA Carboxylase Activity	92
Inhibition by Avidin and Protection by Biotin ..	94
Kinetic Constants of Propionyl CoA Carboxylase..	96
Effect of Free Mg^{++} on Propionyl CoA Carboxylase Activity	96
Discussion of Mechanism of Action of Propionyl CoA Carboxylase	102
REFERENCES	115

LIST OF TABLES

	Page
TABLE	
I Purification of Propionyl CoA Carboxylase From <u>Rhodospirillum rubrum</u>	28
II Effects of Avidin and Biotin on Propionyl CoA Carboxylase Activity	37
III Effect of Cations and Anions on Propionyl CoA Carboxylase Activity	39
IV Influence of Free Mg^{++} Concentration on "n" Values of Hill Plots	53
V Comparison of pH Optima of Propionyl CoA Carboxylases from Various Sources	93
VI Comparison of Effects of Various Ions on Propionyl CoA Carboxylase From Several Sources	95
VII Comparison of Michaelis Constants For Propionyl CoA Carboxylase From Several Sources	97
VIII Summary of Kinetic Data For Propionyl CoA Carboxylase From <u>R. rubrum</u>	103

LIST OF FIGURES

	Page
Figure 1. Dependence of reaction rate on protein concentration for <u>R. rubrum</u> propionyl CoA carboxylase	30
Figure 2. Dependence of $\text{H}^{14}\text{CO}_3^-$ incorporation on time for <u>R. rubrum</u> propionyl CoA carboxylase.....	31
Figure 3. pH dependence of <u>R. rubrum</u> propionyl CoA carboxylase.	32
Figure 4. Dependence of reaction on temperature	34
Figure 5. Heat Stability of <u>R. rubrum</u> propionyl CoA carboxylase	35
Figure 6. Rate-concentration plot, using propionyl CoA as variable substrate	41
Figure 7. Lineweaver-Burk Plot, using propionyl CoA as variable substrate	42
Figure 8. Rate-concentration plot, using HCO_3^- as variable substrate	43
Figure 9. Lineweaver-Burk plot, using HCO_3^- as variable substrate	44
Figure 10. Rate-concentration plot, using MgATP as variable substrate in the absence of free Mg^{++}	46
Figure 11. Rate-concentration plot, using MgATP as variable substrate in the presence of free Mg^{++} (2.25mM)	47

List of Figures Continued

	page
Figure 12. Lineweaver-Burk plot, using MgATP as variable substrate in the presence of free Mg^{++} (2.25mM)	48
Figure 13. Rate-concentration plot, using MgATP as variable substrate at various levels of free Mg^{++}	50
Figure 14. Hill plots obtained using MgATP as variable substrate at various levels of free Mg^{++}	52
Figure 15. Lineweaver-Burk plots obtained using propionyl CoA as variable and MgATP as fixed variable	55
Figure 16. Replot of intercepts obtained from Figure 15 as a function of the reciprocal of MgATP concentration.	56
Figure 17. Lineweaver-Burk plots obtained using MgATP as variable and propionyl CoA as fixed variable	58
Figure 18. Replot of intercepts obtained from Figure 17, as a function of the reciprocal of propionyl CoA concentration	59
Figure 19. Lineweaver-Burk plots obtained using propionyl CoA as variable and HCO_3^- as fixed variable	60
Figure 19a. Replot of intercepts obtained from Figure 19 as a function of the reciprocal of HCO_3^- concentration ..	61
Figure 20. Lineweaver-Burk plots obtained using HCO_3^- as variable and propionyl CoA as fixed variable	63

List of Figures Continued

	page
Figure 21. Replot of intercepts obtained from Figure 20 as a function of the reciprocal of propionyl CoA concentration	64
Figure 22. Lineweaver -Burk plots obtained using MgATP as variable and HCO_3^- as fixed variable	65
Figure 23. Replots of slopes and intercepts obtained from Figure 22 as a function of the reciprocal of HCO_3^- concentration	66
Figure 24. Lineweaver-Burk plots obtained using HCO_3^- as variable and MgATP as fixed variable	67
Figure 25. Replots of slopes and intercepts obtained from Figure 24 as a function of the reciprocal of MgATP concentration	68
Figure 26. Lineweaver-Burk plots of inhibition by potassium phosphate, using MgATP as variable substrate	71
Figure 27. Replot of slopes obtained from Figure 26, as a function of phosphate concentration	72
Figure 28. Lineweaver-Burk plots of inhibition by potassium phosphate, using HCO_3^- as variable substrate	73

List of Figures Continued

	page
Figure 29. Replots of slopes and intercepts obtained from Figure 28, as a function of phosphate concentration	74
Figure 30. Lineweaver-Burk plots of inhibition by potassium phosphate, using propionyl CoA as variable substrate	75
Figure 31. Replot of slopes obtained from Figure 30, as a function of phosphate concentration	76
Figure 32. Lineweaver-Burk plots of inhibition by MgADP, using MgATP as variable substrate	78
Figure 33. Replot of slopes obtained from Figure 32 as a function of MgADP concentration	79
Figure 34. Lineweaver-Burk plots of inhibition by MgADP using HCO_3^- as variable substrate	80
Figure 35. Replots of slopes and intercepts obtained from Figure 34, as a function of MgADP concentration	81
Figure 36. Lineweaver-Burk plots of inhibition by MgADP, using propionyl CoA as variable substrate	82
Figure 37. Replot of slopes obtained from Figure 36, as a function of MgADP concentration	83

List of Figures Continued

	page
Figure 38. Lineweaver-Burk plots of inhibition by methylmalonyl CoA, using MgATP as variable substrate	84
Figure 39. Replots of slopes and intercepts obtained from Figure 38, as a function of methyl- malonyl CoA concentration	85
Figure 40. Lineweaver-Burk plots of inhibition by methylmalonyl CoA, using HCO_3^- as variable substrate	87
Figure 41. Replots of slopes and intercepts obtained from Figure 40, as a function of methylmalonyl CoA concentration	88
Figure 42. Lineweaver-Burk plots of inhibition by methylmalonyl CoA, using propionyl CoA as variable substrate	89
Figure 43. Replot of slopes obtained from Figure 42, as a function of methylmalonyl CoA concentration	90
Figure 44. Diagramatic representation of the proposed kinetic mechanism for propionyl CoA carboxylase from <u>R. rubrum</u>	108

INTRODUCTION

Biotin carboxylases, in general, have been extensively studied for the past twenty years using acetyl CoA carboxylase and pyruvate carboxylase as model enzymes. However, two carboxylases, β -methylcrotonyl CoA carboxylase and propionyl CoA carboxylase, have not been studied in as much detail as have the other biotin carboxylases. In fact, of the above mentioned enzymes, only those from eukaryotic sources have been used for studying kinetic behavior. An attempt to study the kinetics of such an enzyme from a prokaryotic source would therefore facilitate comparison with previously studied enzymes from eukaryotic sources.

The enzyme, propionyl CoA carboxylase, catalyzes the formation of D₅-methylmalonyl CoA by the direct carboxylation of propionyl CoA utilizing energy supplied by the breakdown of ATP to ADP and P_i. Propionyl CoA carboxylase is an enzyme which functions as a key anaplerotic distributary for the reactions of the TCA cycle. The kinetic behavior and physiological features of this enzyme have only been studied briefly from microbial sources (1). Therefore, it was of interest to

determine the kinetic behavior of propionyl CoA carboxylase from Rhodospirillum rubrum and to assess both the physical and kinetic properties obtained from such a study.

Furthermore, if possible, a mechanism of action of this enzyme would be proposed; using the nomenclature of Cleland (2, 3, 4); and this would be compared with mechanisms for other biotin carboxylase enzyme systems, already known.

HISTORICAL

Propionic acid arises from the oxidation of fatty acids with an odd number of carbon atoms, catabolism of branched-chain amino acids, and fermentation by the gastrointestinal flora of ruminants and other animals. Propionate is metabolized by a number of pathways depending on the system studied (5). One such pathway directly involves a biotin-dependent enzyme; propionyl CoA carboxylase, which converts propionyl CoA to D₅-methylmalonyl CoA.

The fate of propionate and its metabolic importance have been examined in great detail over the last sixty years. Initially, propionate was thought to be a key glycolytic compound which was eventually converted through acrylate and lactate to pyruvate (6). Later work by Lorber *et al* (7) suggested that randomization of propionate occurred, resulting in the formation of glycogen, acetyl groups, or lactate. However, with the demonstration of a pathway of propionate metabolism involving carboxylation, in Chlorobium thiosulphatophilum (8),

investigations were initiated to examine this mode of propionate metabolism further.

Lardy and Peanasky (9), using extracts of acetone-dried mitochondria from rats, showed that propionate could be utilized via an ATP- and divalent cation-dependent carboxylation reaction, yielding succinate as the final product. In addition, it was observed that this carboxylating activity was markedly depressed in liver mitochondrial extracts from biotin-deficient rats as compared to mitochondria of normal rats, thereby first implicating biotin involvement in propionate carboxylation in animal tissues. Subsequently, Ochoa and his co-workers (10, 11, 12), working with preparations from animal tissues, showed that the actual substrate of this carboxylation reaction was propionyl CoA and that the product thus formed was D₅-methylmalonyl CoA. This latter compound was then converted by the action of a separate enzyme, methylmalonyl CoA isomerase, into succinyl CoA. The carboxylation of propionate to succinate is therefore dependent on propionyl CoA carboxylase, an enzyme associated with biotin in some way.

The discovery of propionyl CoA carboxylase in animal tissues prompted investigations into propionate carboxylation in other systems, and the reaction was looked for in many prokaryotes.

One such prokaryote examined was the photosynthetic bacterium Rhodospirillum rubrum. The studies of Elsdon and Ormerod (13) on the effect of monofluoroacetate on the photometabolism of propionate and succinate by R. rubrum, suggested that these compounds were metabolized by a common pathway. Subsequently Ormerod (14), proposed that carbon dioxide played a special role in the photometabolism of propionate. The role of carbon dioxide was further emphasized by the work of Clayton et al (15, 16) who showed that the metabolic pathway of propionate in R. rubrum in both light and dark probably involved a preliminary carboxylation to succinate. The work of Elsdon (17), strongly suggested that propionate was metabolized via succinate after propionate assimilation. Further studies carried out by Gibson and Knight (18), and later by Knight (19), using crude extracts of R. rubrum indicated the formation of methylmalonate and succinate from propionyl CoA, ATP, and CO₂. The reaction quite closely resembled that found in animal tissues, being inhibited in the presence of avidin, a biotin antagonist.

Further investigation of propionyl CoA carboxylase in R. rubrum was later performed by Olsen and Merrick (1). When R. rubrum was grown on acetate, succinate, glutamate or yeast extract, the microorganism displayed relatively high levels of propionyl CoA carboxylase. Furthermore, photoheterotrophic growth on acetate resulted in an accumulation of propionate which, could be used as a CO₂ acceptor during acetate assimilation into cellular material. Results from ¹⁴CO₂- fixation experiments obtained under these growth conditions indicated that a propionyl CoA carboxylase reaction existed in R. rubrum with methylmalonate and succinate clearly being identified as the end products of the reaction. Later, studies by Burton (20), demonstrated that propionate accumulation also resulted when R. rubrum was grown photoheterotrophically, on malate or succinate. Under these conditions, not only did propionate accumulate, but propionyl CoA carboxylase displayed high activity as compared with that in cells grown on acetate. Therefore, the presence of propionyl CoA carboxylase in R. rubrum has been demonstrated. However, questions as to how propionate accumulates, or what role propionate plays in the synthesis of cellular material still remain unsolved.

With the initial discovery by Larsen in 1951, of a new carboxylation pathway for propionate metabolism, as mentioned previously, attention was shifted slightly to examine certain metabolic possibilities offered by this new pathway. However, since specific evidence regarding the enzymes directly involved in this pathway did not exist, the significance of the new route for propionate utilization was unclear. Alternative pathways for propionate metabolism had already been proposed at that time (5), so that studies carried out on this carboxylation pathway were only one of several avenues to be explored. However, more recently, the importance of this carboxylation pathway and correspondingly, that of propionyl CoA carboxylase has become clearer.

Hsia and his co-workers (21, 22), using fibroblasts from propionyl CoA carboxylase-lacking children, have shown that the lack of this enzyme through an inborn metabolic defect, resulted in severe metabolic disorders and early death to patients with this hereditary condition (23, 24). Further tests revealed that a high concentration of propionate developed in the plasma and urine of these patients since propionate could not be oxidized to CO_2 . Hence, propionyl CoA

carboxylase was essential for proper metabolic function and consequently, life itself.

Lynen and Tada (25) as well as Wawszkiewicz and Lynen (26) have suggested that propionyl CoA carboxylase was also important in erythronolide synthesis, the ground structure of erythromycin A. They observed that propionyl CoA acted as a primer in a condensation decarboxylation reaction between units of methylmalonyl CoA. Further evidence by Kanada and Corcoran (27) and also by Grisebach et al (28) clearly supported this proposal.

The importance of propionyl CoA carboxylase is also quite evident in photosynthetic bacteria. Evans and his co-workers (29) demonstrated an alternative pathway for the assimilation of carbon dioxide in photosynthetic cells and in autotrophic bacteria, besides the already known reductive pentose phosphate cycle. In this cycle, it is suggested that photosynthetic bacteria, like R. rubrum, are able to carry out the reversal of two normally irreversible reactions of carbohydrate metabolism. This is accomplished using reduced ferredoxin generated photochemically by the organism. One such reaction is the conversion of succinyl CoA to α -ketoglutarate by a ferredoxin-dependent carboxylation reaction. Propionyl CoA carboxylase, being present in microorganisms like R. rubrum, therefore

could replenish the cycle with succinyl CoA, thereby being a key anaplerotic enzyme in this ferredoxin-dependent carbon reduction cycle. However, the route of formation of the propionate used in the propionyl CoA carboxylase reaction is not known as yet and is still under investigation.

Kinetic examination of the behavior of biotin carboxylases, including propionyl CoA carboxylase, has been a topic of research for many years. Extensive studies have been conducted to determine the molecular and kinetic properties of such enzymes in an effort to establish the mechanism of the carboxylase reaction. Although the majority of the work done on propionyl CoA carboxylase has made use of mitochondrial extracts from pig heart (10, 12, 30-35), propionyl CoA carboxylase has also been isolated and purified from mitochondrial extracts from bovine liver (36-40), and from rat liver (41). In addition, the existence of this enzyme has been established in many microbial sources including extracts of Mycobacterium smegmatis (42), Rhodospirillum rubrum (1, 19), Nocardia corallina (43), Streptomyces erythraeus (26), Pseudomonas citronellolis (44), Mycobacterium phlei (44) and Bacillus cereus (44).

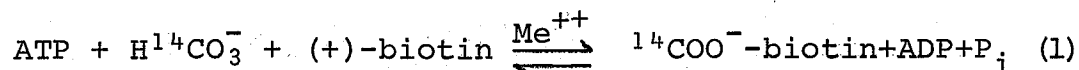
Studies with propionyl CoA carboxylase from pig heart mitochondria (5, 32-34, 45) demonstrated that the enzyme had a molecular weight of 700,000 daltons. It contained one mole of bound biotin per 175,000 grams of enzyme, suggesting the existence of four subunits per enzyme molecule, each having a molecular weight of 175,000 daltons. The enzyme had a sedimentation coefficient of 19.7 S and in the presence of 7 M urea, dissociated into inactive subunits of the 2.5 S variety, of undetermined molecular weight. Similar molecular characteristics were observed with the bovine liver mitochondrial enzyme (36-38), although characterization of the enzyme was not as extensive as was the case using the pig heart source.

Avidin inhibition has been verified for the propionyl CoA carboxylase from all sources thus far studied. This inhibition is almost complete in all cases and can be prevented by preincubation of the avidin with biotin. These results demonstrated that propionyl CoA carboxylase is a biotin-containing enzyme. The fact that this co-factor had a function in CO₂ fixation had long been postulated since it had been observed in many systems that CO₂ fixation was decreased in biotin deficiencies (45).

Lardy and Peanasky (9) first illustrated biotin involvement in the propionyl CoA carboxylase reaction. Later, work by Kosow and Lane (46) verified these findings and showed that incubation of liver slices from biotin deficient rats with (+)-biotin led to a rapid restoration of enzyme activity. Furthermore, incubation of partially purified preparations obtained from livers of biotin deficient rats with ATP and (+)-[^{14}C] biotin yielded propionyl CoA carboxylase labeled with ^{14}C -biotin (47, 48). This evidence not only suggested biotin involvement in the propionyl CoA carboxylase reaction but indicated the presence of bound biotin in the enzyme itself. Through further investigation, many more carboxylases, besides the propionyl CoA carboxylase system, were shown to have a co-relation with biotin in their reaction schemes. It now seemed possible to generalize all biotin-containing carboxylases into one class. In this respect, at least four other carboxylases appeared similar to propionyl CoA carboxylase; β -methylcrotonyl CoA carboxylase (49), acetyl CoA carboxylase (50), pyruvate carboxylase (51), and the transcarboxylase, methylmalonyl-oxalacetic transcarboxylase (52).

Much of the present knowledge of the mechanism

of action of biotin carboxylases was derived from the work of Lynen and his co-workers (49) using β -methylcrotonyl CoA carboxylase. In 1959, Lynen first demonstrated that the biotin content of carboxylase enzyme preparations was directly proportional to the enzyme activity and was inhibited specifically by avidin which formed a complex with the biotin bound to the carboxylase (49). β -methylcrotonyl CoA carboxylase catalyzed a model reaction with free (+)-biotin; reaction (1) (49, 53):



This model reaction provided the means for obtaining direct evidence as to the mode of linkage of HCO_3^- to biotin, resulting in the formation of carboxybiotin, an unstable reaction intermediate.

By 1961, a more general reaction mechanism had been established for all biotin-containing carboxylases (45). The general mechanism involved two partial reactions and will be mentioned later.

Further insight into the structure and mechanism of action of biotin-containing carboxylases was obtained principally through investigation of pyruvate and acetyl CoA carboxylases. These findings may be summarized as follows:-

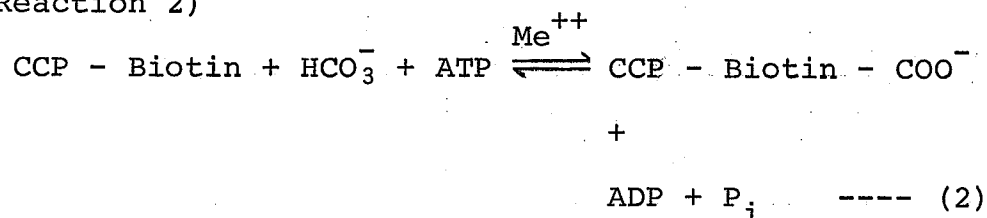
1. Molecular Structure

The bulk of the information concerning molecular structure has been obtained by the groups of P. R. Vagelos and of M. D. Lane, using the E. coli acetyl CoA carboxylase. The system consists of the following types of proteins:

(a) Biotin Carboxyl Carrier Protein: This is a low molecular weight protein, which contains a covalently bound biotinyl group, but which has no catalytic activity (54, 55). The biotin carboxyl carrier protein from E. coli has a molecular weight of 45,000 daltons, and consists of two similar polypeptide chains of molecular weight equal to 22,500 daltons. This "native" form is extremely susceptible to proteolytic modification during isolation (56, 57).

(b) A biotin carboxylase which can carboxylate the biotinyl residue of biotin carboxyl carrier protein, and catalyzes the following reaction:-

(Reaction 2)



This enzyme has been crystallized and exists as a dimer composed of apparently identical 51,000 dalton subunits (58, 59, 60).

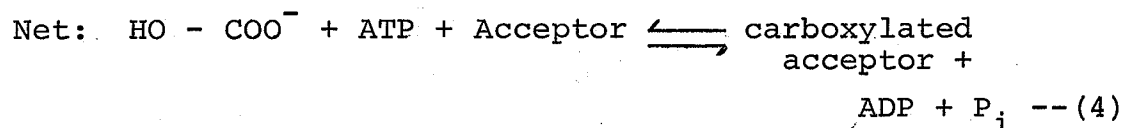
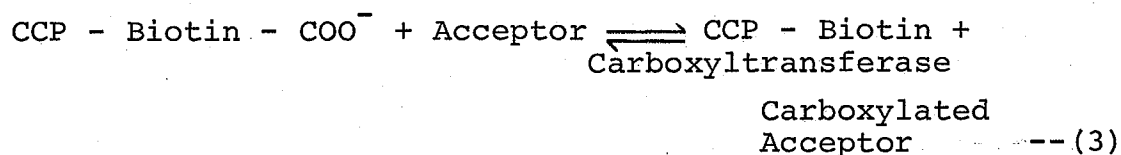
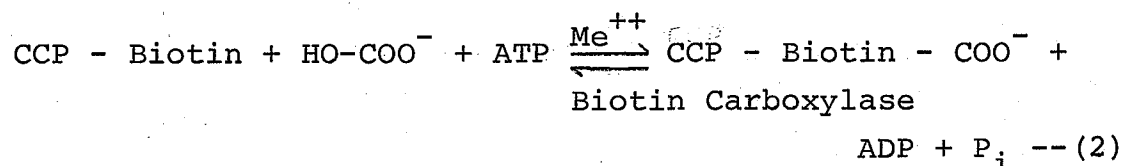
the carboxylation of acetyl CoA. This is similar to the situation in the avian system in which the protomer is tetrameric.

Pyruvate carboxylases from avian liver and from yeast (*S. cerevisiae*) are also known to have tetrameric structures, and are presumably similar in this respect to acetyl CoA carboxylases (63).

2. Mechanism of Action

Without going into detailed discussion of individual carboxylase systems, the following generalizations can be made concerning the mechanism of action of biotin carboxylases.

The overall reaction catalyzed is the sum of the individual reactions discussed above:



From extensive kinetic analyses, principally using pyruvate carboxylase from a variety of sources, complex

kinetic mechanisms have been derived. The bulk of the work has come from the laboratories of Lardy and of Scrutton and Utter.

In essence the mechanism can be described as a nonclassical, Ping Pong, Bi Bi, Uni Uni scheme. The nonclassical feature is the proposal that each active site on the enzyme is composed of two separate and functionally distinct, catalytic sites i.e. a separate catalytic site exists for the reactants of each partial reaction shown above (Reactions 2 and 3). The two catalytic sites are proposed to be linked by a mobile biotinyl residue which functions as a carboxyl carrier (45, 64-70). A more thorough discussion of this mechanism in the light of the findings detailed in this thesis is to be found later in the text (See Figure 44). These mechanisms have not shed light on the coupling of ATP hydrolysis to CO_2 fixation, and it is noteworthy that Ashman and Keech (71) have recently considered three possible mechanisms by which such coupling may occur.

3. Regulation

The regulatory properties of biotin-containing carboxylases have been the subject of extensive investigation. For information on the regulation of pyruvate and acetyl CoA carboxylases the reader is referred to reviews by Scrutton and Young (63) and

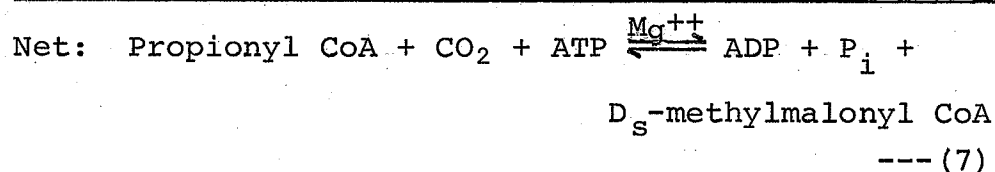
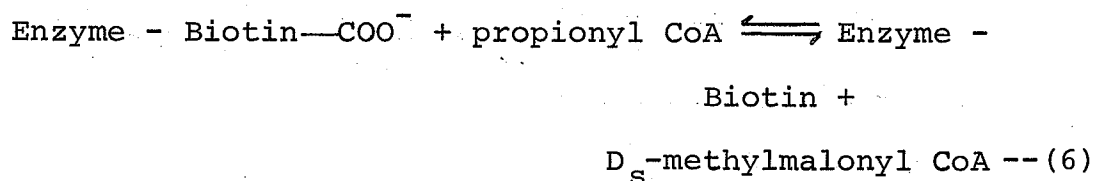
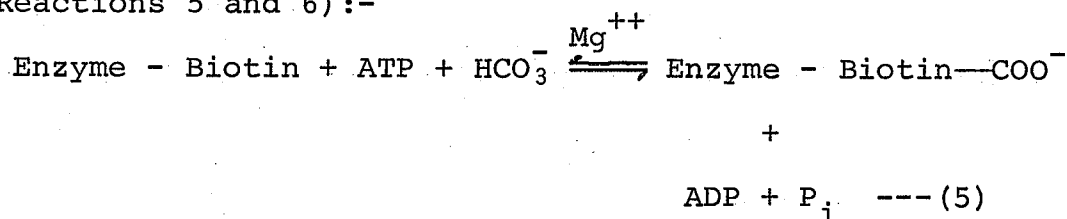
Lane and his co-workers (72-75). A recent observation which has not yet entered the review literature (76) is that the acetyl CoA carboxylase of E. coli is under stringent control, and may be regulated by guanosine-5'-diphosphate-3'-diphosphate (ppGpp).

Of interest in the context of the results presented in this thesis are the effects of metal ions and metabolite-metal complexes eg. Mg-ATP, on pyruvate carboxylases.

Pyruvate carboxylase from chicken liver is activated by both uni- and divalent cations. Mg^{++} , in addition to its role as a substrate (in MgATP), specifically activates the reaction in which carboxylation of the biotinyl residue occurs (77). In contrast, the univalent activator, K^+ , appears to act at both the carboxylation site and the carboxyl-transferase subsite. Similar effects with Mg^{++} have been found using rat liver (69) and sheep kidney (78) pyruvate carboxylases. K^+ activation and Na^+ inhibition were observed with pyruvate carboxylase from A. niger (70). Evidence implicating Mg^{++} , and perhaps MgATP, as possible allosteric effectors using pyruvate carboxylase from baker's yeast (79), and pigeon kidney (80), has been presented.

According to the general mechanism discussed above, the reaction mechanism for propionyl CoA carboxylase may now be written in two steps

(Reactions 5 and 6):-



The net reaction is given in (7).

This thesis presents an attempt to establish the kinetic mechanism of action of propionyl CoA carboxylase from R. rubrum. The results show a close degree of agreement with what would be expected in the light of the above discussion. In addition however, the data obtained using propionyl CoA carboxylase from R. rubrum are complicated by the existence of unusual behavior with respect to the substrate Mg^{++} and ATP, and this behavior may be allosteric in nature.

MATERIALS AND METHODS

Chemicals

Propionyl CoA was prepared from CoA and propionic anhydride using the procedure described by Simon and Shemin (81).

The following chemicals were obtained from P-L Biochemicals, Inc.:

CoA, lithium salt, ~~Chromatopure~~.

Methylmalonyl CoA

DTT

ADP from equine muscle, disodium salt, Grade I

ATP from equine muscle, disodium salt, crystalline

The following chemicals were obtained from

Nutritional Biochemicals Corporation:

Avidin, 2273 units/g

D-biotin (Vitamin H), crystalline

The following chemical was obtained from Schwarz/

Mann Corporation:

Mannex DEAE-cellulose

The following chemical was obtained from Amersham/

Searle Corporation:

$\text{NaH}^{14}\text{CO}_3$, aqueous solution, 59.3 mCi/mmol

All other chemicals were of analytical grade, and were purchased from standard chemical suppliers.

Growth and Maintenance of Culture

A culture of Rhodospirillum rubrum, obtained from Dr. Jack Preiss, Department of Biochemistry and Biophysics, University of California, Davis, California 95616, was used throughout this study. Cultures of R. rubrum were maintained in stabs and, for experimental work, were grown microaerophically in liquid cultures. The basic medium used for both types of culture was essentially that described by Cohen-Bazire et al. (82). The constituents were prepared in three parts. Part A contained: EDTA, 0.25 g; $\text{ZnSO}_4 \cdot 7\text{H}_2\text{O}$, 1.095 g; $\text{FeSO}_4 \cdot 7\text{H}_2\text{O}$, 0.50 g; $\text{MnSO}_4 \cdot \text{H}_2\text{O}$, 0.154 g; $\text{CuSO}_4 \cdot 5\text{H}_2\text{O}$, 39.2 mg; $\text{Co}(\text{NO}_3)_2 \cdot 6\text{H}_2\text{O}$, 24.8 mg; $\text{NaB}_4\text{O}_7 \cdot 10\text{H}_2\text{O}$, 17.7 mg; a few drops of H_2SO_4 ; and distilled water, 100 ml. Part B contained: KP_i 1.0 M buffer, pH 6.8^a. Part C contained: EDTA, 10.0 g, dissolved and neutralized with approximately 7.3 g KOH; MgSO_4 , 14.5 g; CaCl_2 , 2.55 g; $(\text{NH}_4)_6\text{Mo}_7\text{O}_{24} \cdot 4\text{H}_2\text{O}$, 9.3 mg; $\text{FeSO}_4 \cdot 7\text{H}_2\text{O}$, 99 mg; nicotinic acid, 50 mg; thiamine-HCl, 25 mg; biotin, 0.5 mg; Part A, 50 ml; and distilled water, to 1.0 litre. The pH of Part C was adjusted to 6.8. The complete defined liquid medium was now made up as follows:

^aThe abbreviation used is KP_i , potassium phosphate.

PART B	20 ml
PART C	20 ml
$(\text{NH}_4)_2\text{SO}_4$	0.2% (w/v)
DL-malate	2.68 g

Distilled water to 1.0 litre

The pH of this complete liquid medium was then adjusted to 6.8 and it was autoclaved at 121° for 45 minutes.

Stock cultures were maintained in stabs in which 2.5% agar (Bacto-Agar, Difco Laboratories, Detroit) was added to the basic liquid medium and the resulting solution distributed in 10 ml aliquots into screw-cap test-tubes, then autoclaved as before. Inoculation into stabs was performed aseptically, using a platinum wire and a fully developed liquid culture of R. rubrum or another stab. Addition of approximately a 0.25 ml liquid culture layer onto each stab provided a substantial supplement for luxuriant growth of the organism to arise in each stab. Luxuriant growth was obtained after 4 days incubation at 30° in a Conviron Model E7 incubator (Controlled Environments) under continual fluorescent and incandescent lighting conditions. The stabs were then stored at 4° and subcultured approximately every month to six weeks thereafter.

This defined medium was also used for growth of R. rubrum on a larger scale for later experimental

purposes. A 1.0 ml inoculum from a fully grown R. rubrum liquid culture was aseptically transferred to a 150 ml sterile screw-cap milk-dilution bottle filled to the neck with medium. This was then placed in the Convicon incubator and the microorganism allowed to grow under the same conditions previously indicated. Approximately 75 ml of this liquid culture were aseptically transferred to a 3 litre carboy containing the same liquid medium filled up to the neck. Incubation was repeated in the Convicon incubator under the same conditions as in the case of the milk-dilution flask or stab cultures. After 3 to 4 days, the 3 litre carboy of R. rubrum liquid culture was used as an inoculum for a 40 litre carboy filled with the basic liquid medium. A sterile gas outlet tube was attached to the stoppered 40 litre carboy to allow the escape of any hydrogen gas produced by R. rubrum during the growth period. The inoculated 40 litre carboy was then incubated as before in a Convicon Model PGW-36 incubator (Controlled Environments) until stationary phase was reached (about 48 hr).

Harvesting and Storage of R. rubrum Cells

The cells were harvested using the Sharples Super Centrifuge Model T 1-P at a centrifugal force of 20,000 x g and a flow rate of 8-10 litres/hr. The cells were washed

twice with 500 ml of 20 mM KP_i pH 7.0 buffer and collected by centrifugation. The wet weight of the cells was determined and they were then resuspended in a 20% (w/v) ratio using 20 mM KP_i pH 7.0 buffer. Once resuspended, the cells were dispensed in 10 ml aliquots and frozen at -76°C .

Preparation of *R. rubrum* Cell-free Extracts

All procedures were carried out at $0^\circ\text{--}4^\circ\text{C}$. The cell suspension was thawed and the suspending buffer was removed by centrifugation. After weighing, the cells were resuspended in homogenizing buffer (20 mM KP_i pH 7.0 + 2 mM DTT) in a 20% (w/v) ratio using a hand-operated glass Ten-Broeck homogenizer. The cell suspension was then sonicated in a Raytheon DF 101 Sonic Oscillator for 8-10 minutes. The sonicated cells were centrifuged at $48,000 \times g$ for 10 minutes and the supernatant - the cell-free extract - was carefully removed. Negatively stained smears of this supernatant were prepared, and observed under the light microscope to ensure that all whole cells were in fact disrupted and were no longer present in the extract. This was then used for further purification.

Enzyme Assays

The enzymatic activity of propionyl CoA carboxylase was measured by following the rate of propionyl CoA-dependent $\text{H}^{14}\text{CO}_3^-$ incorporation into acid-stable non-volatile material. Under the assay conditions used, ^{14}C is incorporated into D_5 -methylmalonyl CoA (1,83). Spectrophotometric techniques could not be used as the assay procedure, since the presence of contaminating NADH oxidase in the enzyme preparation did not allow any coupling of the propionyl CoA carboxylase reaction with other NAD-dependent enzyme systems.

The following mixture was used for measuring propionyl CoA carboxylase activity (Final concentrations are given): Tris-HCl buffer pH 8.0, 50 mM; ATP, 2.25 mM; MgCl_2 , 4.5 mM; DTT, 5.0 mM; $\text{KH}^{14}\text{CO}_3$, 12.6 mM; propionyl CoA, 1.5 mM; and enzyme (18 μg); in a total volume of 0.5 ml. After equilibration at 30° , the reaction was initiated by the addition of the enzyme. After 10 minutes incubation, the reaction was terminated by the addition of 50 μl of 3N HCl. 200 μl aliquots of the assay mixture were added to scintillation vials and after air-drying to remove any $\text{H}^{14}\text{CO}_3^-$ not incorporated, the samples were redissolved in 0.5 ml water. 10 ml of scintillation fluid, prepared according to Bray (84), were then added to each sample and the radioactivity was quantitated in a

Beckman Model LS-230 liquid scintillation spectrometer.

One unit of propionyl CoA carboxylase activity was defined as that amount of the preparation which catalyzes the incorporation of 1 nmole of $\text{H}^{14}\text{CO}_3^-$ into acid-stable non-volatile material per minute. Specific activity was expressed per mg protein. Protein concentration was determined by the method described by Lowry et al. (85).

Purification of Propionyl CoA Carboxylase

All steps were carried out at $0^\circ\text{-}4^\circ$. The purification procedure was basically a modified version of that described by Olsen and Merrick (1).). The crude extract was centrifuged in a Beckman 60 Ti rotor for about 1 hr at $177,000 \times g$ in a Beckman Model L Ultracentrifuge. Solid ammonium sulfate was added to the supernatant to bring the final concentration to 50% saturation. After fifteen minutes stirring, the cloudy suspension was centrifuged ($48,000 \times g$, 10 minutes) and the pellet was dissolved in a minimal volume of the homogenizing buffer (20 mM KP_i pH 7.0 buffer + 2 mM DTT) and dialyzed overnight against the same buffer. After dialysis, the ammonium sulfate fraction was mixed batchwise, with DEAE-cellulose which had been previously equilibrated with the

standard homogenizing buffer. The mixture was centrifuged at 5,400 x g for 10 minutes and the pellet was washed with approximately 250 ml of the homogenizing buffer. This washing and centrifugation procedure was repeated twice more using a 0.1 M KP_i pH 7.0 buffer + 2 mM DTT and a 0.2 M KP_i pH 7.0 buffer + 2 mM DTT as the washing buffers (250 ml per buffer). After centrifugation, the 0.2 M eluate supernatant was brought to 90% of saturation using solid ammonium sulfate. After stirring for 15 minutes, the cloudy suspension was centrifuged at 48,000 x g for 10 minutes and the resulting pellet was resuspended in as small a volume of homogenizing buffer as possible. Dialysis against the same buffer was carried out overnight. After dialysis, insoluble material was removed by centrifugation at 48,000 x g for 10 minutes. The resulting supernatant was removed carefully and frozen in 0.2 ml aliquots at -76° . The propionyl CoA carboxylase enzyme, present in this supernatant fraction, was the enzyme form used for all the kinetic and physical studies. An outline of the purification procedures is presented in Table I.

RESULTS

Purification of Propionyl CoA Carboxylase

A 2-fold purification of propionyl CoA carboxylase was obtained with a combination of procedures involving ultracentrifugation, ammonium sulfate precipitation, and batch DEAE-cellulose chromatography. Table I presents the purification steps of propionyl CoA carboxylase from R. rubrum.

The activity of propionyl CoA carboxylase for all subsequent results presented in this study, was expressed in terms of initial velocity, v , in unit values; unless specified otherwise. One unit of propionyl CoA carboxylase activity was defined as that amount of the preparation which catalyzes the incorporation of 1 nmole of $\text{H}^{14}\text{CO}_3^-$ into acid-stable non-volatile material per minute.

TABLE I

Purification of propionyl CoA carboxylase from Rhodospirillum rubrum

Stage	Total Protein (mg)	Total Activity (units)	Recovery (%)	Specific Activity (units/mg)
I Cell-free extract	1501.2	57,586	100	38.4
II (NH ₄) ₂ SO ₄ precipitate, 0-50%	445.1	12,000	20.8	40.3
III 0.2 M buffer eluate from DEAE-washing	71.8	5,385	9.4	70.8
IV (NH ₄) ₂ SO ₄ precipitate, 0-90%	48.9	3,814	6.6	78.4

Protein Concentration and Time Dependence of Propionyl CoA Carboxylase

As shown in Fig. 1, propionyl CoA carboxylase activity was proportional to the amount of protein added. A concentration of 18 μg of protein per assay was selected as the concentration of enzyme for all subsequent assays.

Activity was also linear with time, for at least 12 minutes, with the protein concentration used (Fig. 2). A 10 minute incubation time period was selected as the standard assay period. Although this time interval seemed rather close to the non-linear portion of the curve, the 10 minute time allotment permitted sufficient $\text{H}^{14}\text{CO}_3^-$ - incorporation to occur in the reaction system to ensure reproducibility of results.

pH Optimum

As shown in Fig. 3, the pH optimum for propionyl CoA carboxylase was 7.9 - 8.1. This curve was determined using two different buffers; KP_i buffer and Tris-HCl buffer. Although KP_i buffer was used in the purification of propionyl CoA carboxylase from R. rubrum,

Figure 1. Dependence of reaction rate on
protein concentration for R. rubrum
propionyl CoA carboxylase.

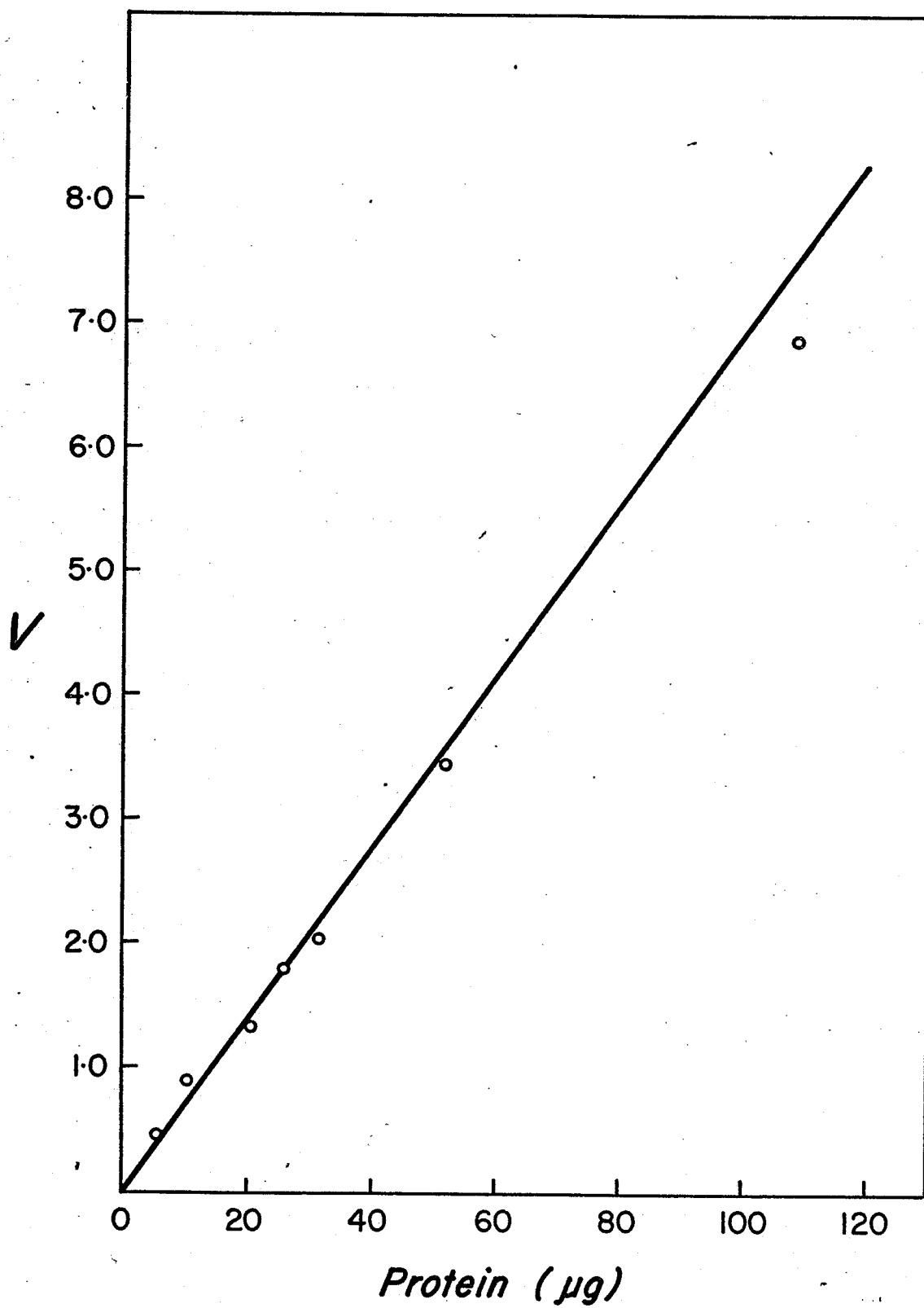


Figure 2. Dependence of $\text{H}^{14}\text{CO}_3^-$ incorporation
on time for R. rubrum propionyl
CoA carboxylase.

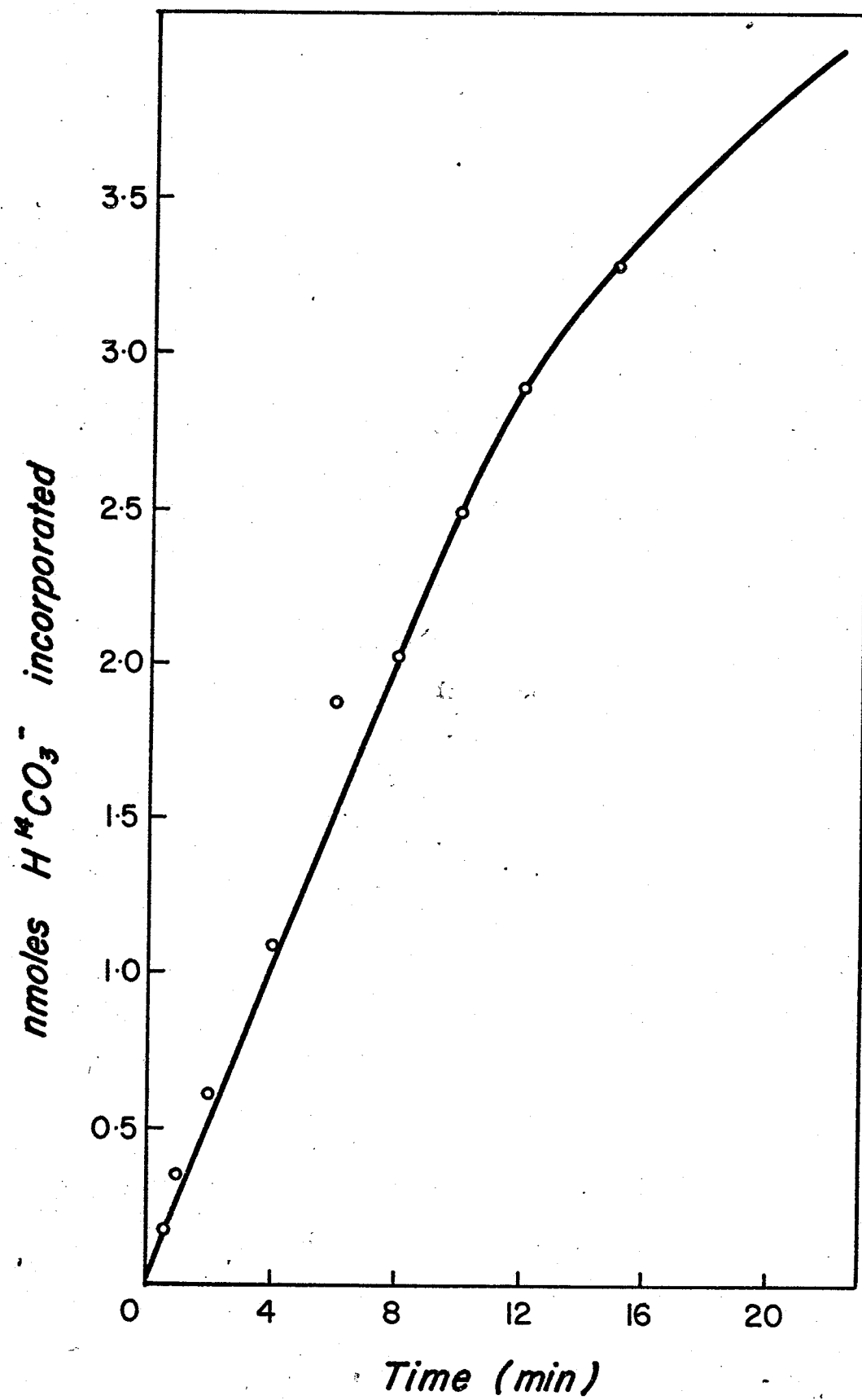
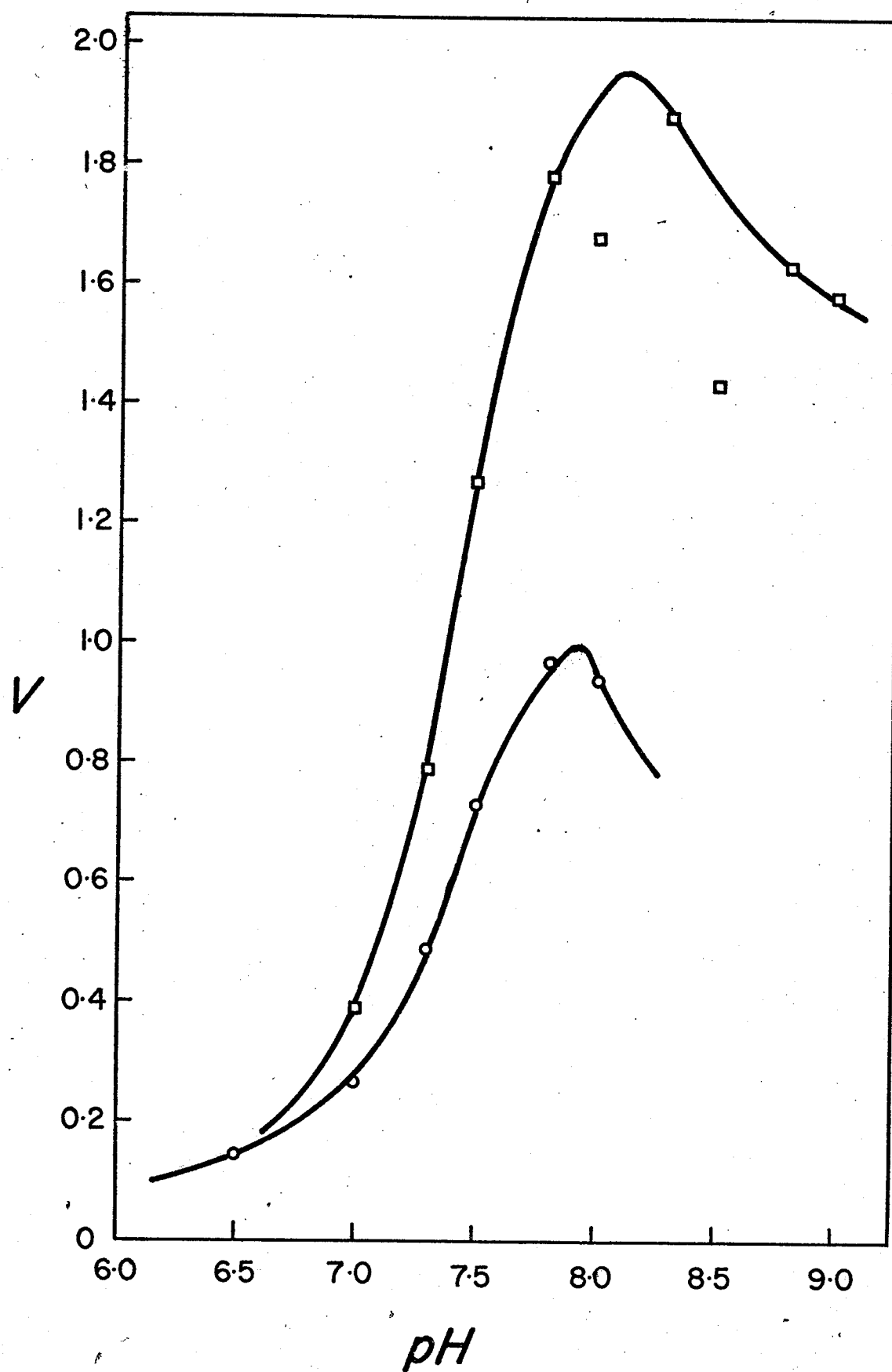


Figure 3. pH dependence of R. rubrum propionyl
CoA carboxylase.

▣ —▣ Tris-HCl buffer (50 mM)

○ —○ Potassium phosphate buffer (50
(50 mM)



Tris-HCl buffer was found to give higher enzyme activity at the pH optimum than KP_i buffer, and was therefore used for all subsequent studies.

All buffers used in this section were of a final concentration of 50 mM.

Temperature Optimum and Heat Stability of Propionyl CoA Carboxylase

As shown in Fig. 4, the temperature optimum for maximal propionyl CoA carboxylase activity was 30° - 32° . Furthermore, (Fig. 5), a rapid decline in enzyme activity was observed starting at 38° with a resultant loss of almost all enzyme activity at 50° . 30° was selected as the standard assay temperature for all subsequent assays.

Effects of Avidin and Biotin

Propionyl CoA carboxylase, like all other biotin carboxylases thus far studied, has been found to be inhibited by avidin. This inhibition was eliminated if the enzyme was protected by pre-incubation with biotin.

Figure 4. Dependence of Reaction on Temperature.

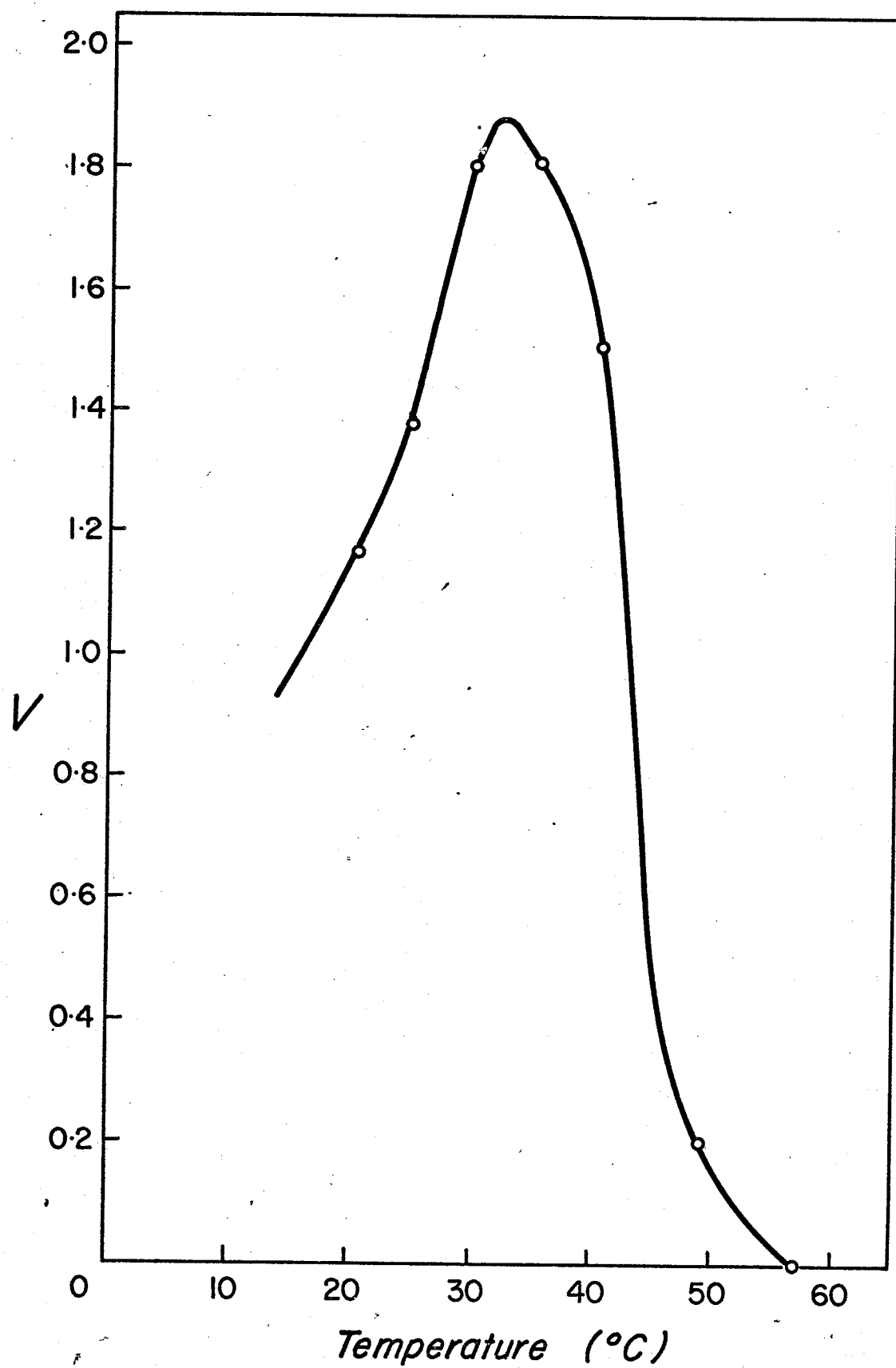
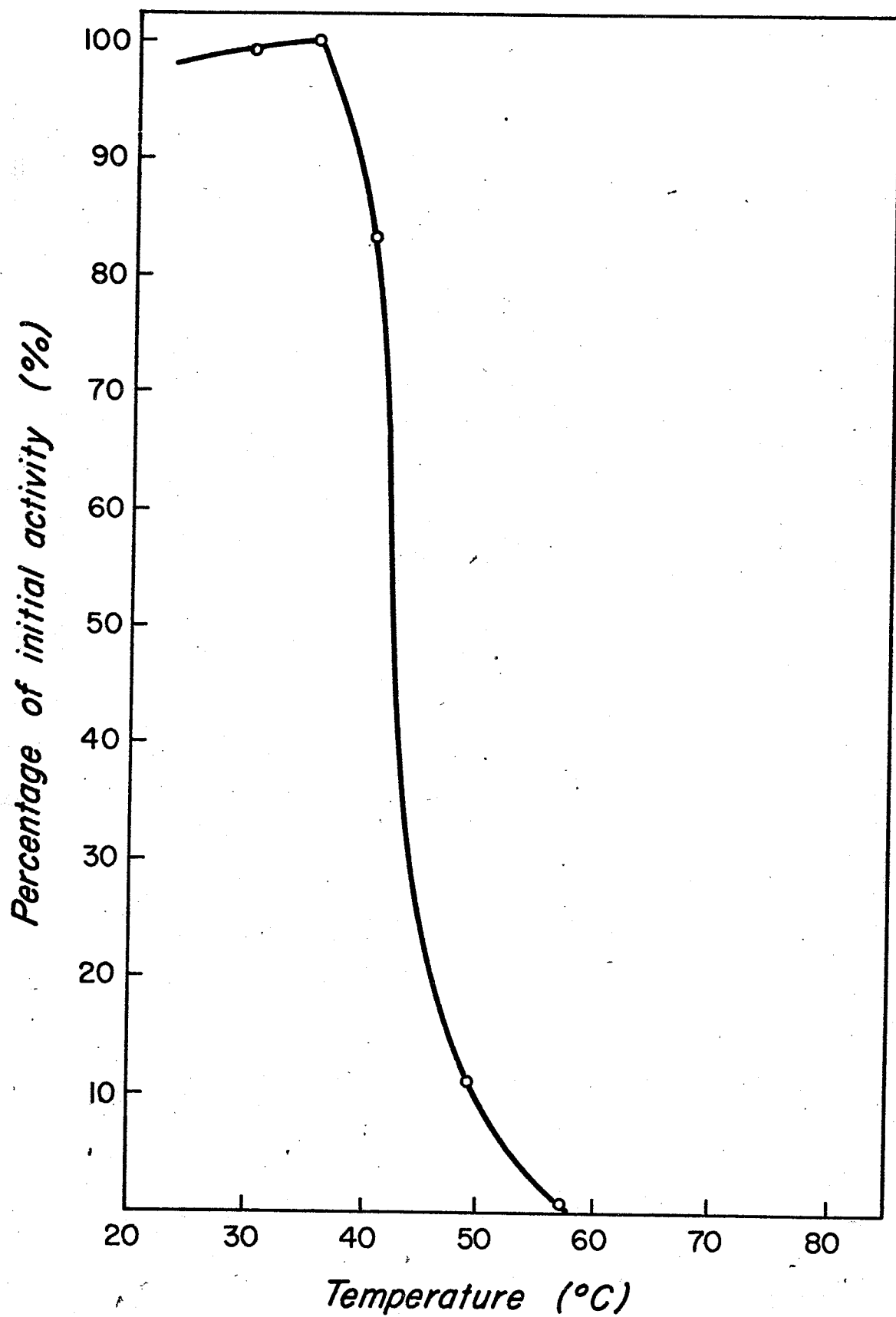


Figure 5. Heat Stability of R. rubrum
propionyl CoA carboxylase.



The effects of these compounds on R. rubrum propionyl CoA carboxylase were tested. The assays were carried out using the standard procedure except for the avidin and biotin additions. Avidin was incubated for 2 minutes with the enzyme at the assay temperature before addition of the latter to the reaction mixture. When biotin was employed, it was added to the avidin 2 minutes before the latter was mixed with the enzyme.

The results of this study are shown in Table II. Inhibition of activity by avidin and protection against this effect by preincubation with biotin, are demonstrated in this table. Although the inhibitory effect is not as large as one might expect, the fact that some inhibition and protection against inhibition by using avidin and biotin are observed, indicates that propionyl CoA carboxylase from R. rubrum is a biotin-containing enzyme as is the case of other biotin carboxylases (70, 86-89).

Effect of Cations and Anions on Propionyl CoA Carboxylase Activity

The effects of various cations and anions on R. rubrum propionyl CoA carboxylase activity were

TABLE II

Effects of avidin and biotin on propionyl CoA carboxylase activity^a

Additions	Enzyme Activity (units)
None	6.42
Avidin (0.10 units) ^b	5.97
Avidin (0.21 units)	5.10
Avidin (0.34 units)	4.90
Biotin (25 µg)	6.20
Biotin (25 µg) + Avidin (0.34 units)	6.19

^aEnzyme activity was measured as described in "Materials and Methods".^b1 unit of avidin is that amount which binds 1 µg of D-biotin.

studied using Na^+ , K^+ , Cl^- , P_i , and $\text{SO}_4^{=}$ ions. The results are presented in Table III. Standard assay conditions were used with the exception that the KHCO_3 final concentration was approximately 4 mM. The various anions and cations were then added to the assay system as indicated in the table. It was found that 50 mM NaCl had a slight inhibitory effect on enzyme activity while 50 mM KCl caused 18% stimulation of the enzyme. 50 mM KP_i resulted in a 28% inhibition while 50 mM NaP_i inhibited enzyme activity by approximately 45%. K_2SO_4 displayed a 12% stimulatory effect at 50 mM while Na_2SO_4 at 50 mM resulted in a 5% inhibition of activity.

Kinetics of Propionyl CoA Carboxylase from
Rhodospirillum rubrum

The initial velocity data, unless stated otherwise, were plotted in the double reciprocal form ($1/v$ versus $1/s$) according to Lineweaver and Burk (90), where v is the initial velocity and S is the concentration of the variable substrate. The nomenclature of reaction mechanisms and definitions of kinetic constants were those proposed by Cleland (2).

TABLE III
Effect of cations and anions on propionyl CoA carboxylase activity^a

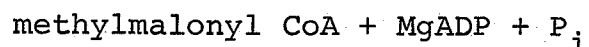
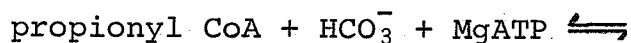
Additive	Concentration of Ion	
	10 mM	50 mM
NaCl	102.7%	96.5%
KCl	107.2%	118.1%
KP ₁	102.4%	72.1%
NaP ₁	93.9%	54.8%
K ₂ SO ₄	108.4%	112.5%
Na ₂ SO ₄	98.6%	94.9%

^aStandard conditions were employed (see "Materials and Methods") except that the KH₁⁴CO₃ was approximately 4 mM. Note therefore that all the above results were obtained with a minimum of 4 mM K⁺ in the reaction mixture. Activity is expressed as a percentage of that observed in the absence of added ions.

Determination of Apparent K_m Values for Reaction

Components

Propionyl CoA carboxylase catalyzes the reaction:



The apparent K_m values for various substrates were calculated from the intercepts at the horizontal axis of double reciprocal plots according to the equation:

$$1/v = 1/v^1 + K_m^1 / v^1 (1/s)$$

where K_m^1 is the apparent K_m value for the variable substrate S, and v^1 is the apparent maximum velocity.

1. Apparent K_m for propionyl CoA

The plots for v versus S and 1/v versus 1/S are shown in Figs. 6 and 7, respectively. The apparent K_m for propionyl CoA was calculated to be 1.33×10^{-4} M.

2. Apparent K_m for bicarbonate

The plots for v versus S and 1/v versus 1/s are shown in Figs. 8 and 9 respectively. The endogenous bicarbonate concentration was assumed to

Figure 6. Rate-concentration plot, using
propionyl CoA as variable
substrate.

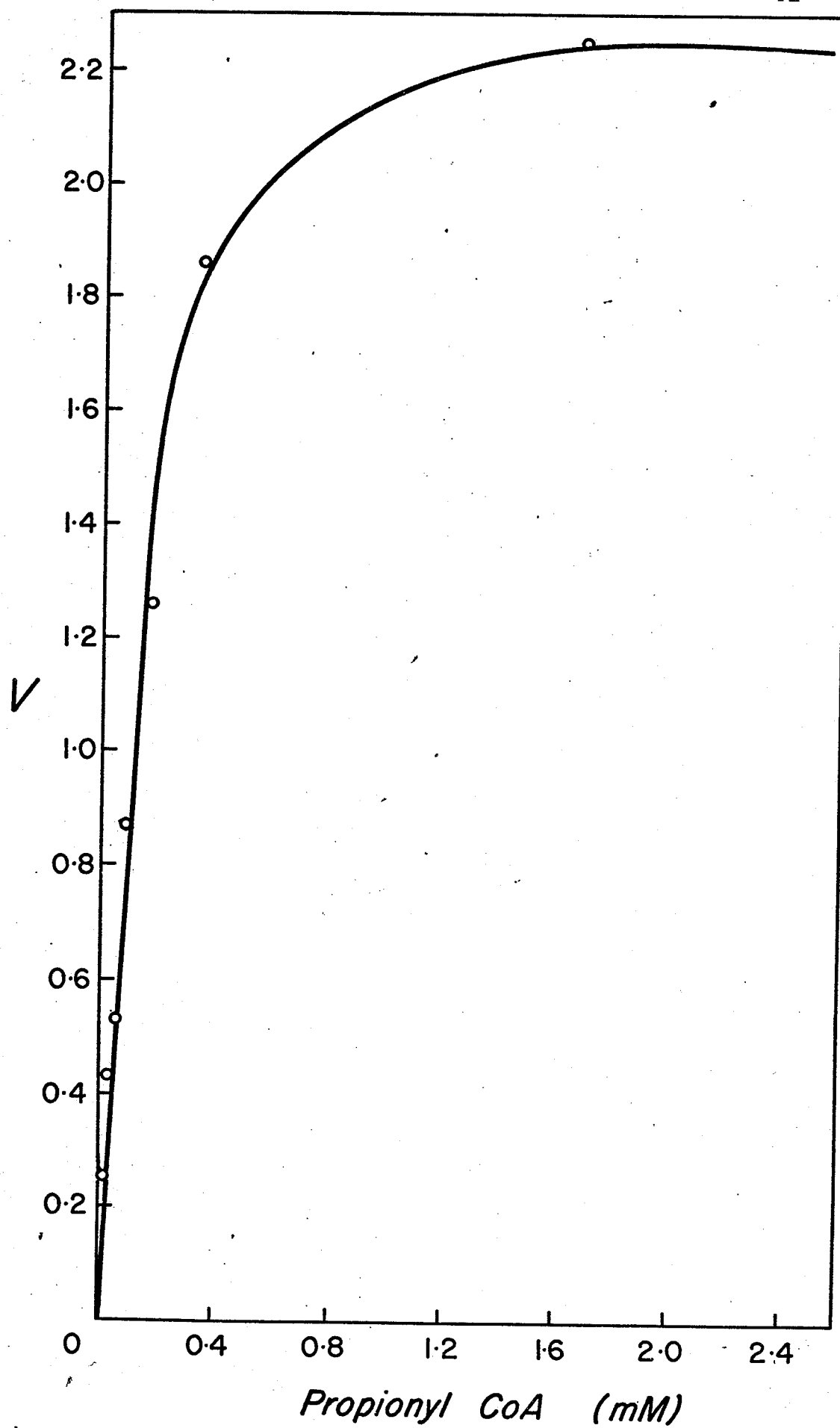


Figure 7. Lineweaver-Burk plot using propionyl
CoA as variable substrate.

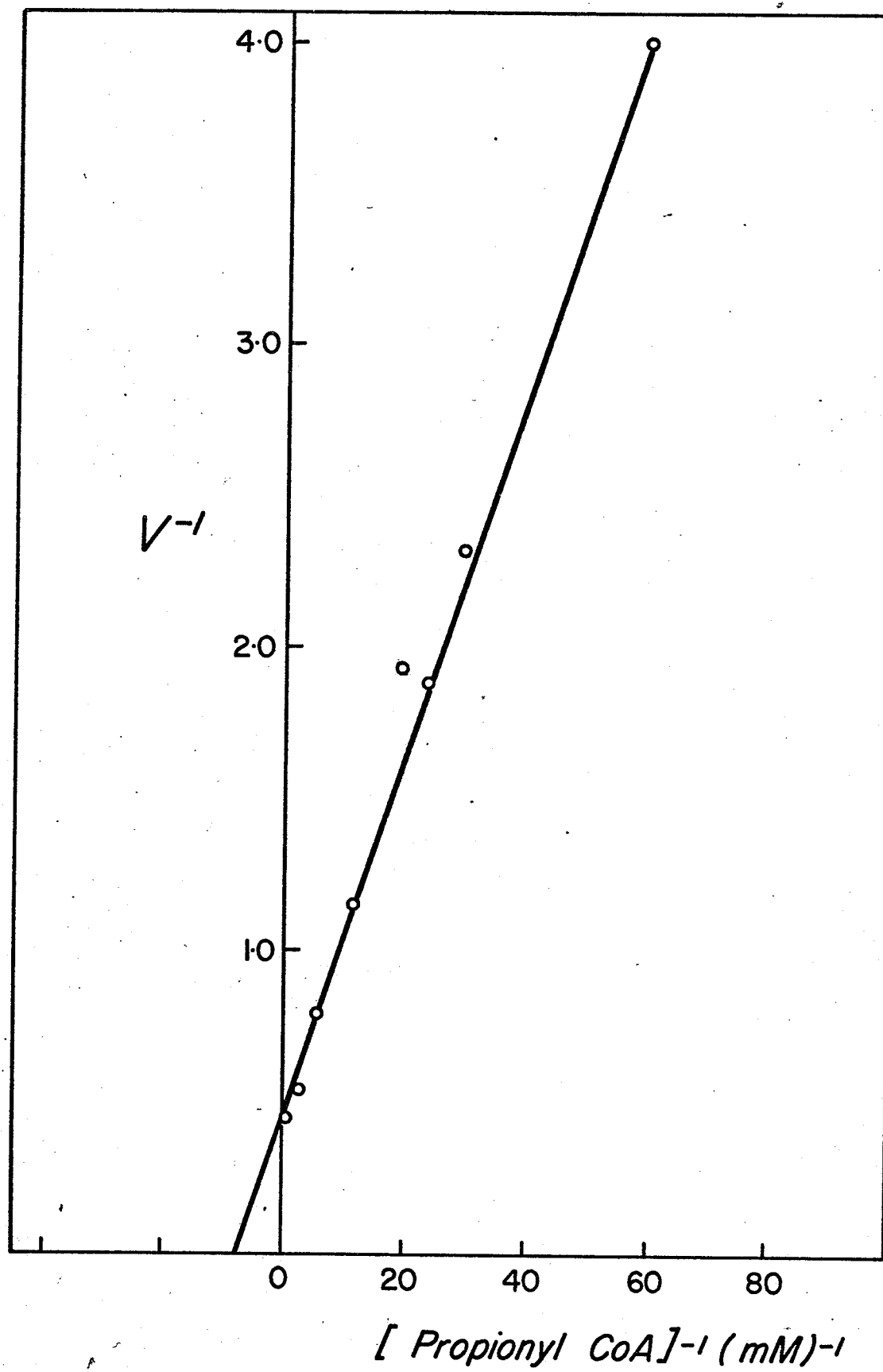


Figure 8. Rate-concentration plot, using
 HCO_3^- as variable substrate.

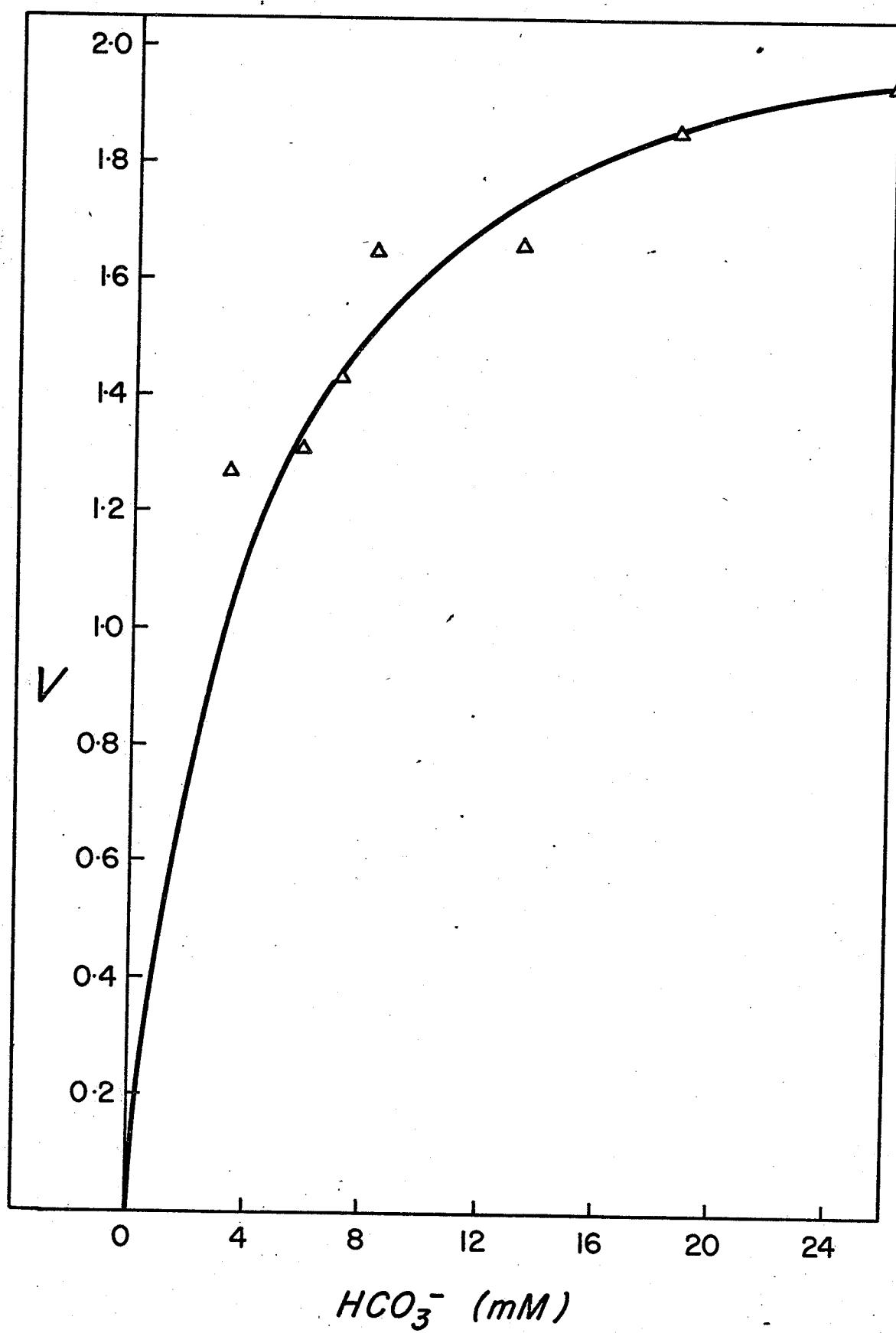
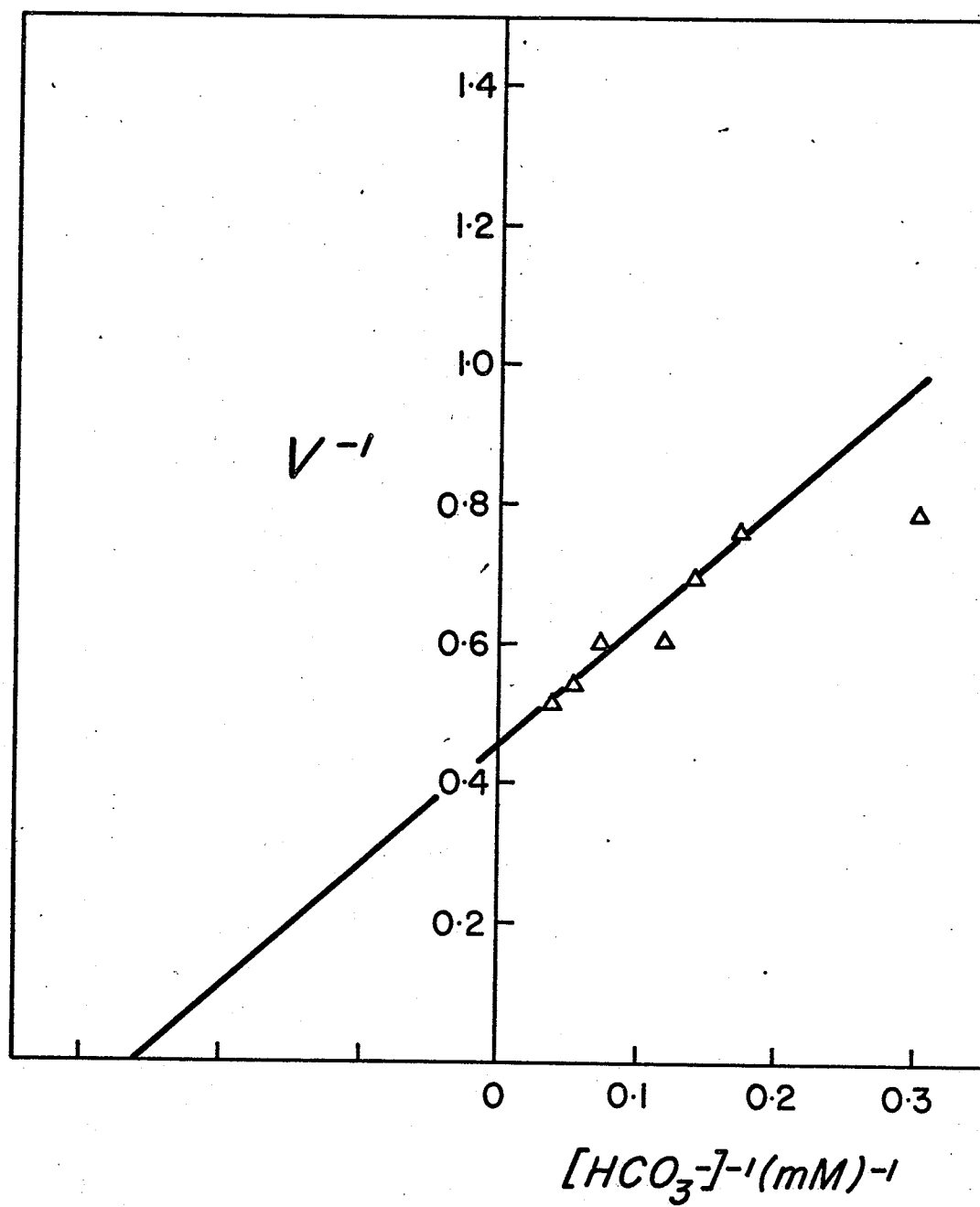


Figure 9. Lineweaver-Burk plot, using
 HCO_3^- as variable substrate.



be 0.8 mM (70, 91). The apparent K_m for bicarbonate was 2.8 mM.

3. Apparent K_m for MgATP

In apparent K_m studies with propionyl CoA, and HCO_3^- , it was found that the presence or absence of free Mg^{++} did not influence the reaction kinetics. In the absence of free Mg^{++} , propionyl CoA and HCO_3^- displayed Michaelis-Menten kinetics, i.e. hyperbolic v versus S plots. Lineweaver-Burk replots for these substrates were linear and gave apparent K_m values similar to those obtained under standard assay conditions (i.e. 2.25 mM free Mg^{++}).

However, as seen in Fig. 10, the plot for v versus S for MgATP, carried out in the absence of free Mg^{++} is sigmoid, in nature. $1/v$ versus $1/S$ replots for this data were non-linear in shape. Thus, apparent K_m values could not be determined under these conditions. However, in the presence of 2.25 mM free Mg^{++} , (standard assay conditions), the plots for v versus S and $1/v$ versus $1/S$ (Figs. 11 and 12) became of Michaelis-Menten type. The apparent K_m value of MgATP was calculated to be 0.176 mM.

Figure 10. Rate-concentration plot, using MgATP
as variable substrate, in the absence
of free Mg^{++} .

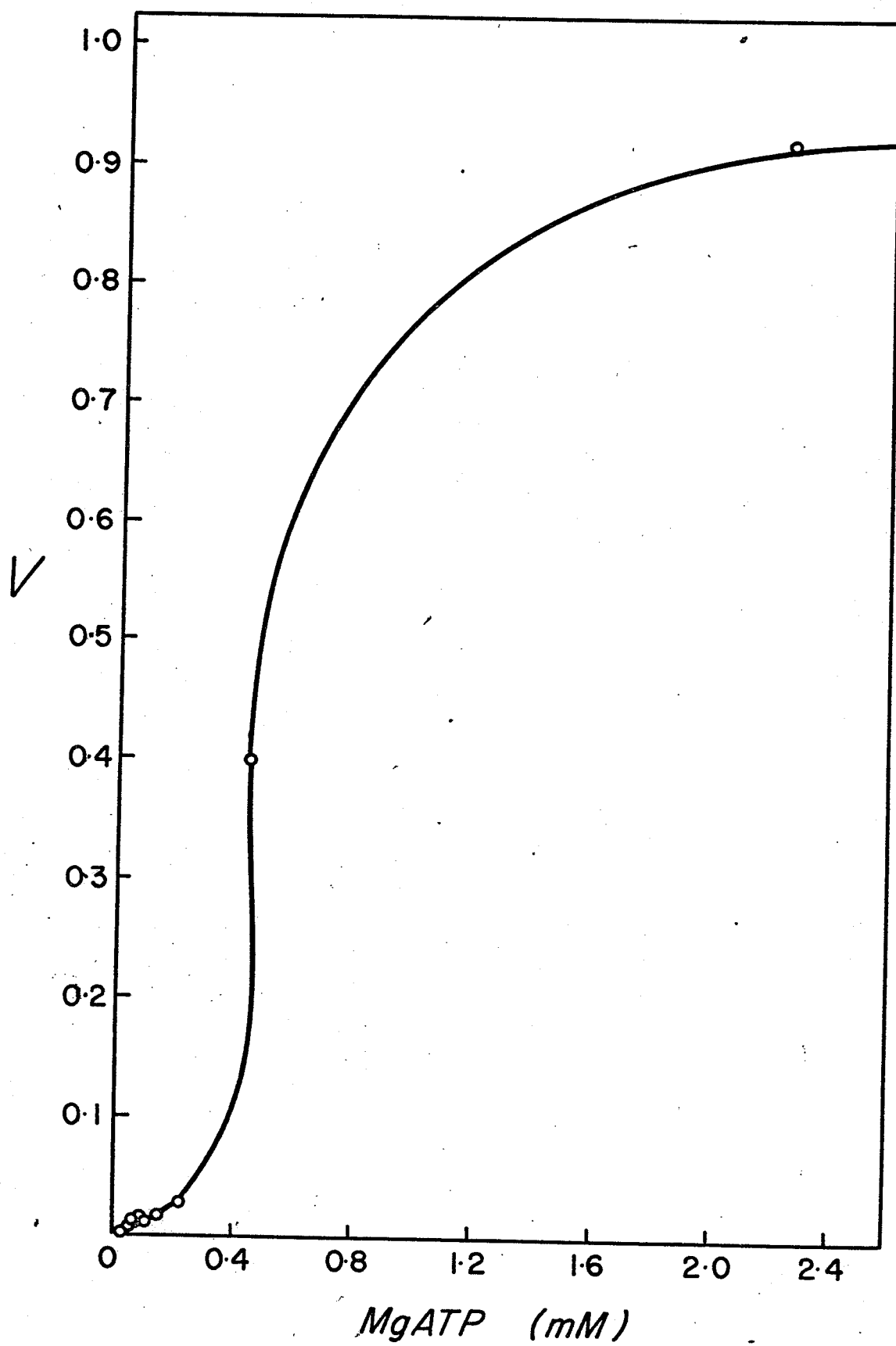


Figure 11. Rate-concentration plot, using MgATP
as variable substrate, in the presence
of free Mg^{++} (2.25mM).

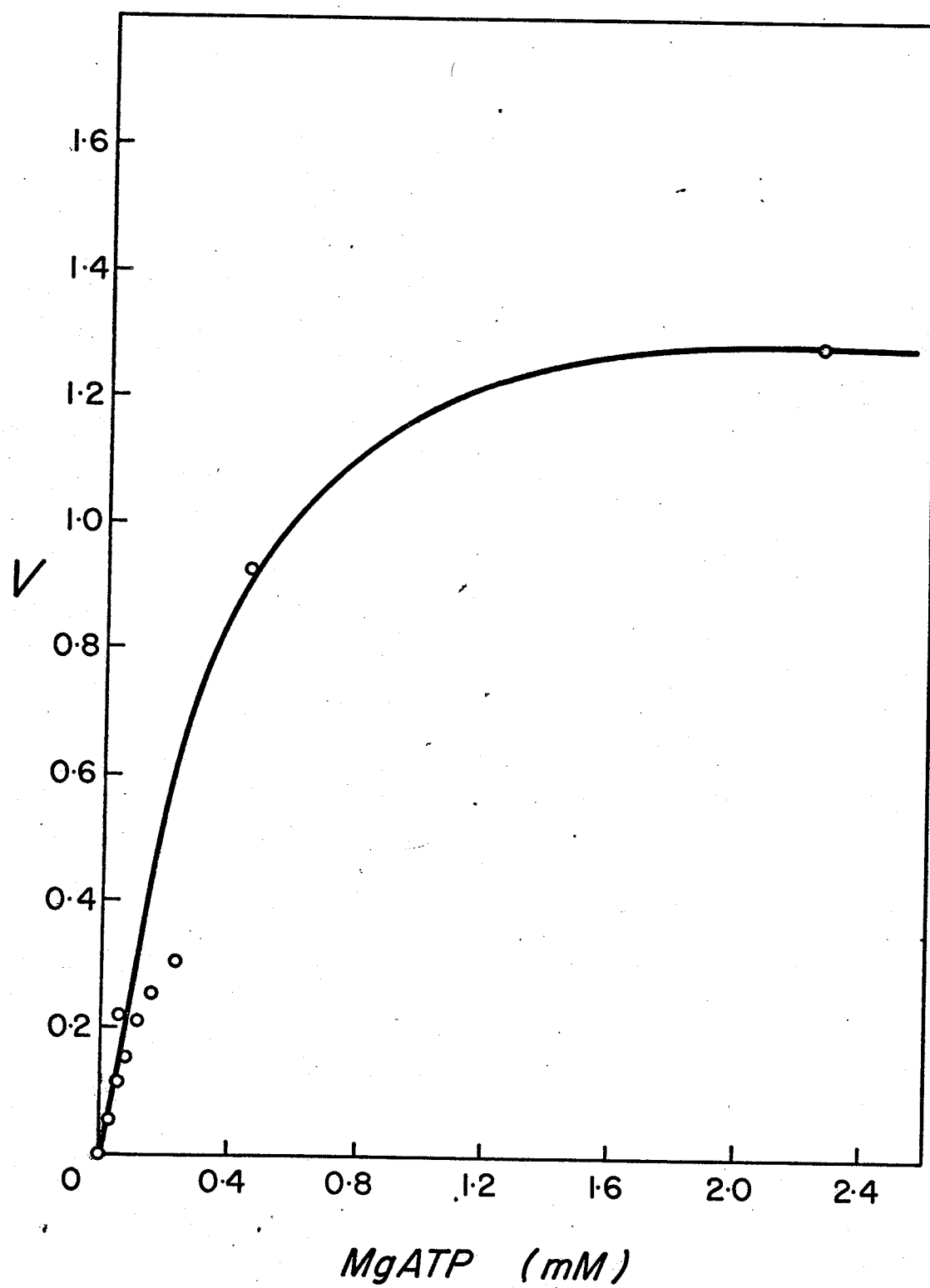
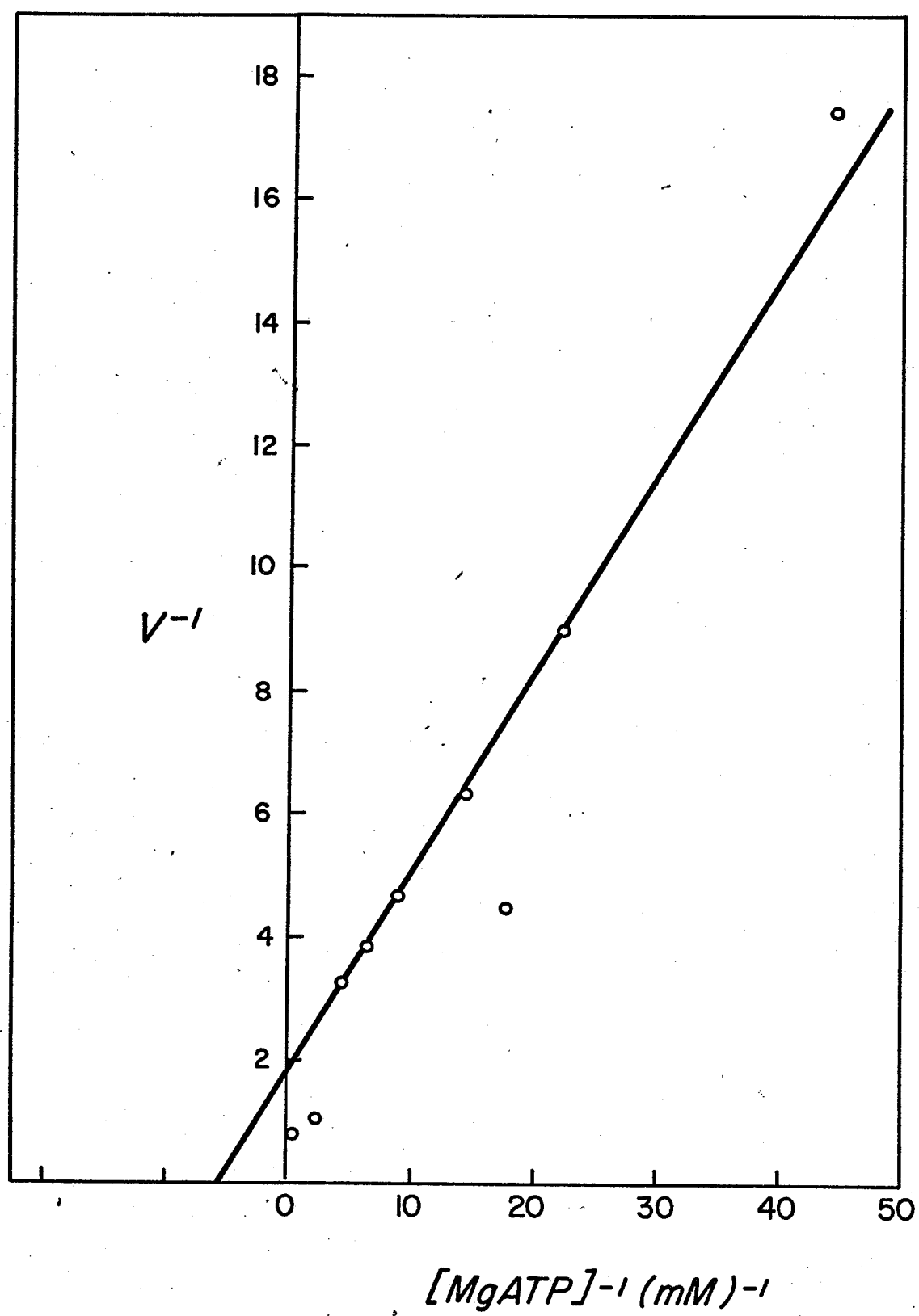


Figure 12. Lineweaver-Burk plot, using MgATP
as variable substrate, in the
presence of free Mg^{++} (2.25 mM).



The Influence of Free Mg^{++} on Propionyl CoA
Carboxylase Activity Using MgATP as Variable Substrate^a

As stated previously (Fig. 10), when free Mg^{++} is absent from the reaction mixture, the plot for v versus S (where S is MgATP) is sigmoidal in shape, suggesting the existence of an allosteric effect. Furthermore, when standard assay conditions were employed, the v versus S plot for MgATP became of Michaelis-Menten type. To further investigate this homotropic effect in which MgATP apparently acts as both a substrate and allosteric effector, a Hill plot was prepared.

Standard assay conditions were employed with the exception that the $KH^{14}CO_3$ concentration was approximately 4 mM not 13 mM as in the standard conditions. The amount of free Mg^{++} was gradually increased from zero to a final concentration of 2.25 mM (standard conditions). Plots of v versus S for MgATP, (Fig. 13), formed a series of lines, varying from a sigmoidal plot at zero free Mg^{++} to a hyperbolic plot at 2.25 mM free Mg^{++} . At concentrations between the two extremes, the lines fell between the sigmoidal and hyperbolic plots. When the data was now applied to the Hill equation:

^aThe reader is referred to the additional material following page 101 for further consideration of this subject.

Figure 13. Rate-concentration plot, using MgATP as variable substrate, at various levels of free Mg^{++} .

o—o, 0 mM;

■—■, 0.05 mM;

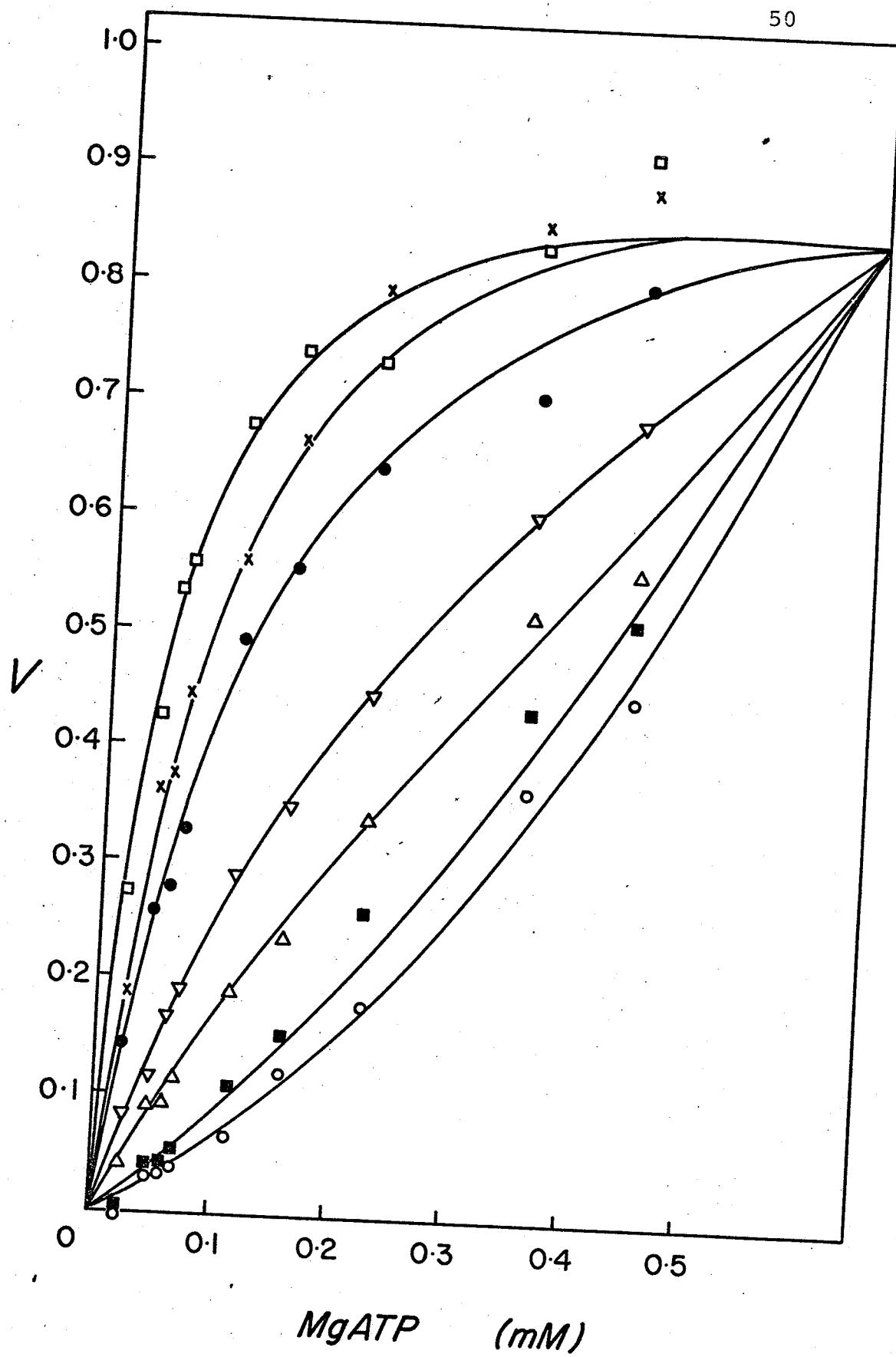
Δ—Δ, 0.10 mM;

▽—▽, 0.25 mM;

●—●, 0.5 mM;

x—x, 1.0 mM;

□—□, 2.25 mM.



$$\log \frac{v}{V_{\max} - v} = n \log S - \log K$$

where n = number of interacting sites

v = velocity at any point on the curve

V_{\max} = maximum velocity

S = concentration of variable substrate

and K = equilibrium constant for the reaction

and the $\log \frac{v}{V_{\max} - v}$ was plotted as a function of $\log S$, a series of straight lines was observed with the slopes of the lines varying from $n \approx 2$ in the absence of free Mg^{++} to $n \approx 1$ under the standard assay conditions (2.25 mM free Mg^{++}). The maximum velocity, V_{\max} , had been determined from a Lineweaver-Burk double reciprocal plot of Figure 13 and had demonstrated the same maximum velocity no matter what concentration of free Mg^{++} if any, was present in the assay system. The values of n for those lines between the upper and lower limits fell between the values obtained at the two extremes (i.e. between $n = 1$ and $n = 2$). The Hill plot is presented in Figure 14 and the data is summarized in Table IV.

Determination of True K_m Values for Reaction Components

True Michaelis constants (K_m 's) were determined by measuring initial velocities at varied concentrations

Figure 14. Hill plots obtained using MgATP as variable substrate at various levels of free Mg^{++} .

- , 0 mM;
- , 0.05 mM;
- △—△, 0.1 mM;
- ▼—▼, 0.25 mM;
- , 0.5 mM;
- x—x, 1.0 mM;
- , 2.25 mM.

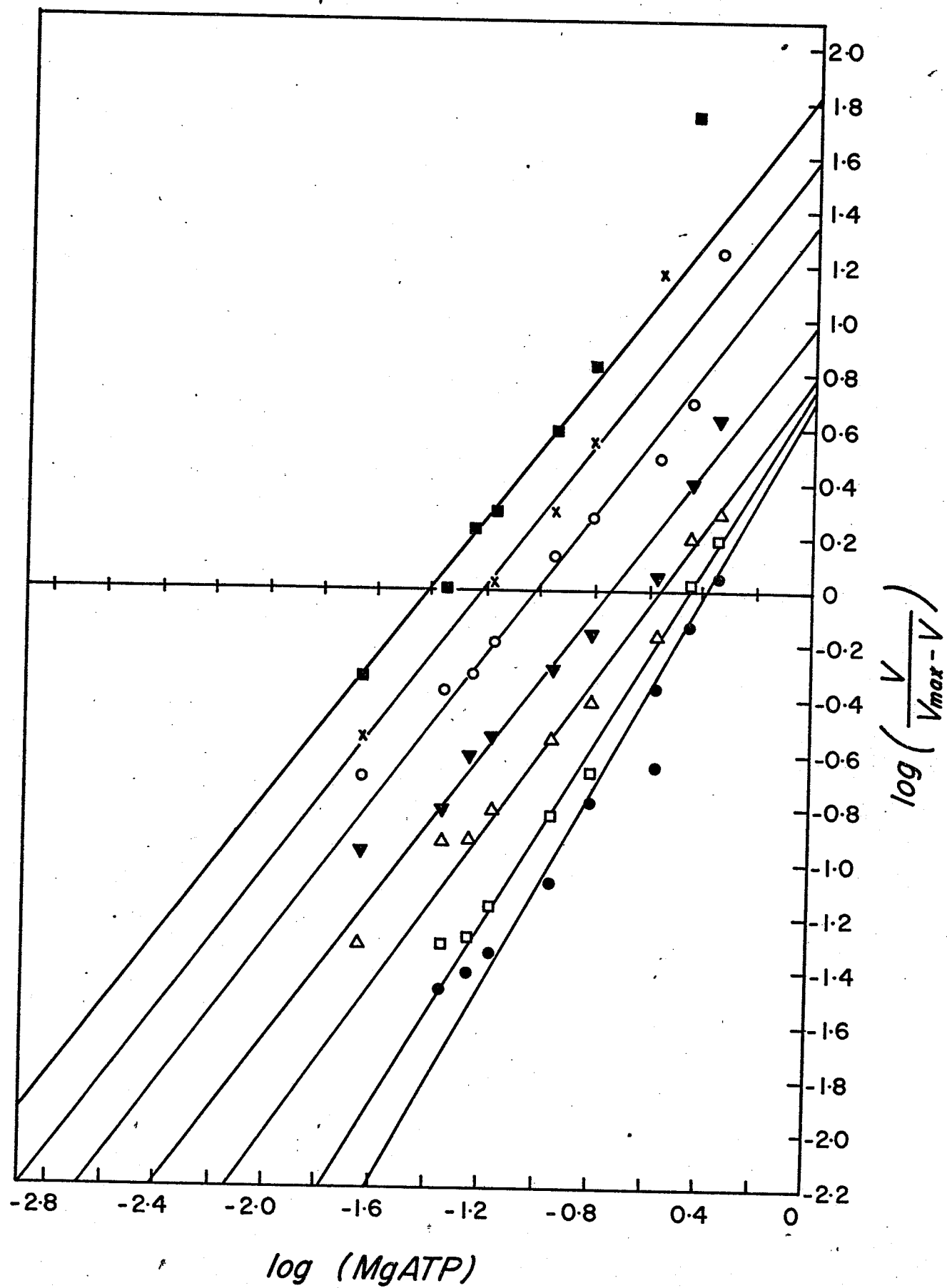


TABLE IV

Influence of free Mg^{++} concentration on "n" values of Hill plots^a

Free Mg^{++} concentration (mM)	n Value
0	1.85
0.05	1.64
0.10	1.40
0.25	1.33
0.50	1.33
1.00	1.30
2.25	1.28

^aThe Hill plots were prepared as described in "Results" section.

of one substrate and several fixed concentrations of the second substrate. The third substrate was kept at the concentration used for the standard assays. The only exception to standard assay conditions was that the $\text{KH}^{14}\text{CO}_3$ used throughout this study was approximately 4 mM final concentration not 14 mM as in the standard conditions. At higher $\text{KH}^{14}\text{CO}_3$ concentrations, i.e. at 14 mM, inhibition by $\text{KH}^{14}\text{CO}_3$ was observed resulting in very complex kinetic behavior.

From the double reciprocal plots, the intercepts ($1/v^1$) and slopes (K_m^1/v^1) were replotted against the reciprocal of the fixed substrate concentration (92). K_m values were obtained from the intercepts at the horizontal axis.

1. Propionyl CoA:MgATP

When propionyl CoA was used as the variable substrate at several fixed concentrations of MgATP, the double reciprocal plots (Fig. 15) were linear. The replot of values for intercepts against reciprocals of MgATP concentrations was also linear (Fig. 16) and yielded a true K_m for MgATP of 0.111 mM. However at high propionyl CoA concentrations, the parallel lines lost their linearity and became concave upward, in nature.

With MgATP as the variable and propionyl CoA the fixed variable substrate, the double reciprocal

Figure 15. Lineweaver-Burk plots obtained using propionyl CoA as variable and MgATP as fixed variable.

○—○, 0.05 mM;

x—x, 0.1 mM;

Δ—Δ, 0.15 mM;

●—●, 0.25 mM;

□—□, 0.5 mM;

▽—▽, 2.25 mM.

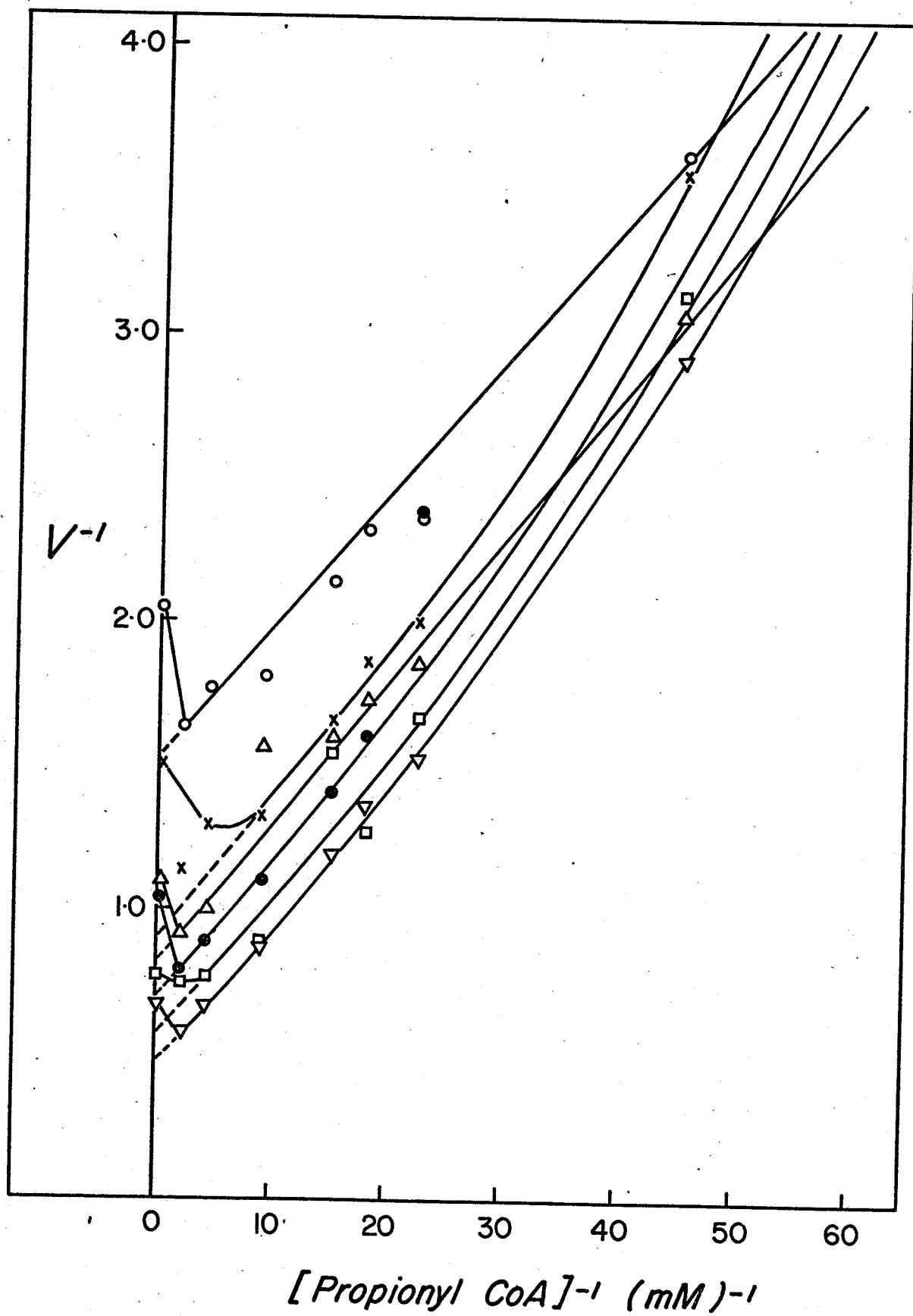
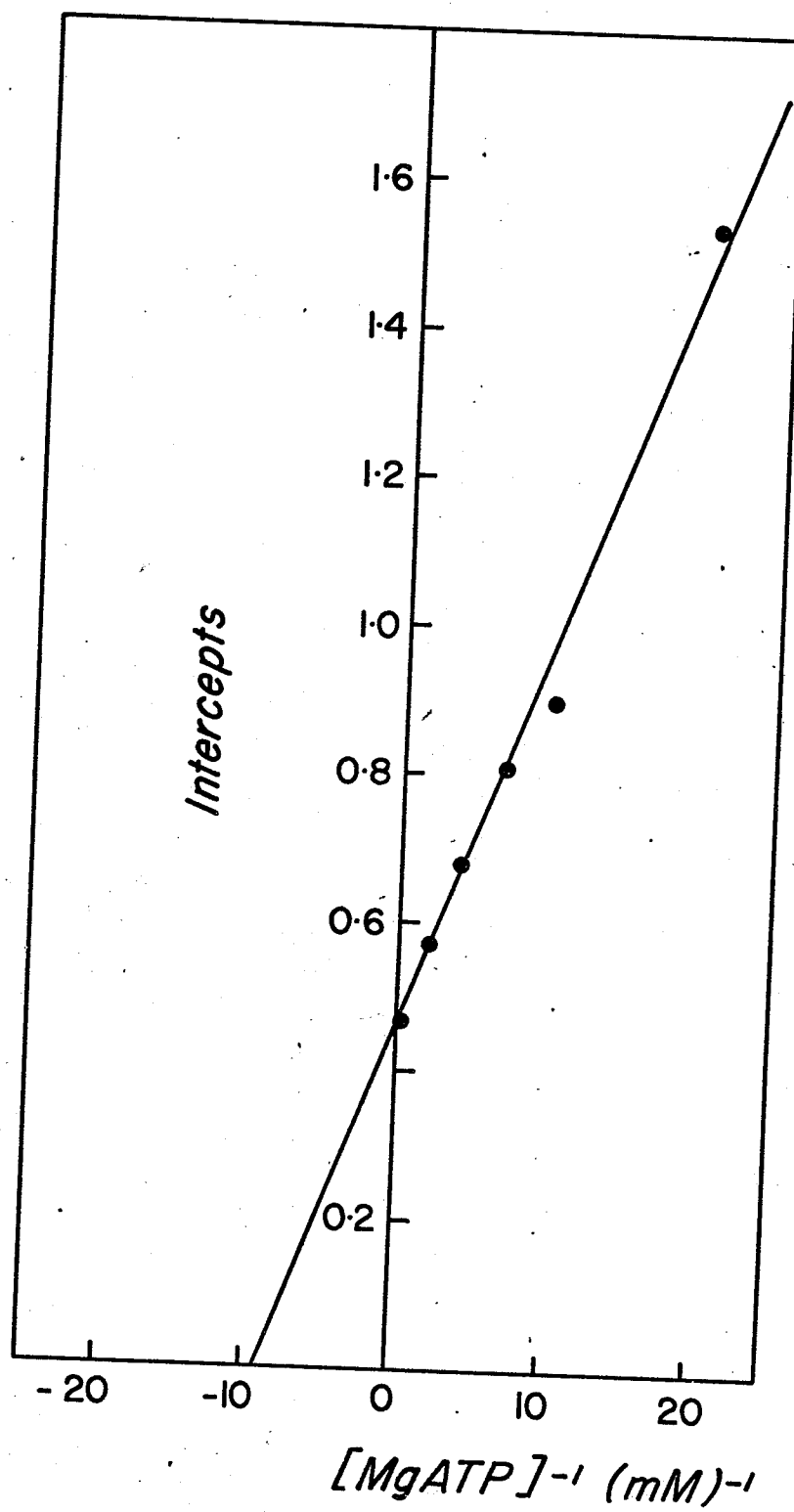


Figure 16. Replot of intercepts obtained from Figure 15, as a function of the reciprocal of MgATP concentration.



plots (Fig. 17) and replot of ($1/v^1$) against reciprocals of propionyl CoA concentrations were linear (Fig. 18). The intercept replot yielded a true K_m for propionyl CoA of 91 μ M.

2. Propionyl CoA : bicarbonate

Double reciprocal plots obtained when propionyl CoA was varied at several fixed concentrations of bicarbonate yielded a set of lines which were biphasic, being linear at low propionyl CoA concentrations and curved downward at high propionyl CoA concentrations, indicating complex kinetic behavior. The basic pattern was intersecting but the lines became closer to parallel in nature at higher HCO_3^- concentrations (see "Discussion"). The linear portions of the curves (Fig. 19) were used for the determination of the true K_m of the fixed variable substrate, HCO_3^- . Thus the replot of values for ($1/v^1$) against reciprocals of bicarbonate concentrations was linear (Fig. 19A) and yielded a true K_m for bicarbonate of 5.20 mM.

When bicarbonate was varied at several fixed concentrations of propionyl CoA, the double reciprocal plots were essentially parallel at high propionyl CoA concentrations and intersecting at low propionyl CoA concentration values (Fig. 20). The replot of the

Figure 17. Lineweaver-Burk plots obtained using MgATP as variable and propionyl CoA as fixed variable.

○—○, 0.022 mM;

●—●, 0.044 mM;

△—△, 0.056 mM;

▽—▽, 0.067 mM;

◻—◻, 0.111 mM;

x—x, 0.22 mM;

+ —⁺⁺+, 2.25 mM.

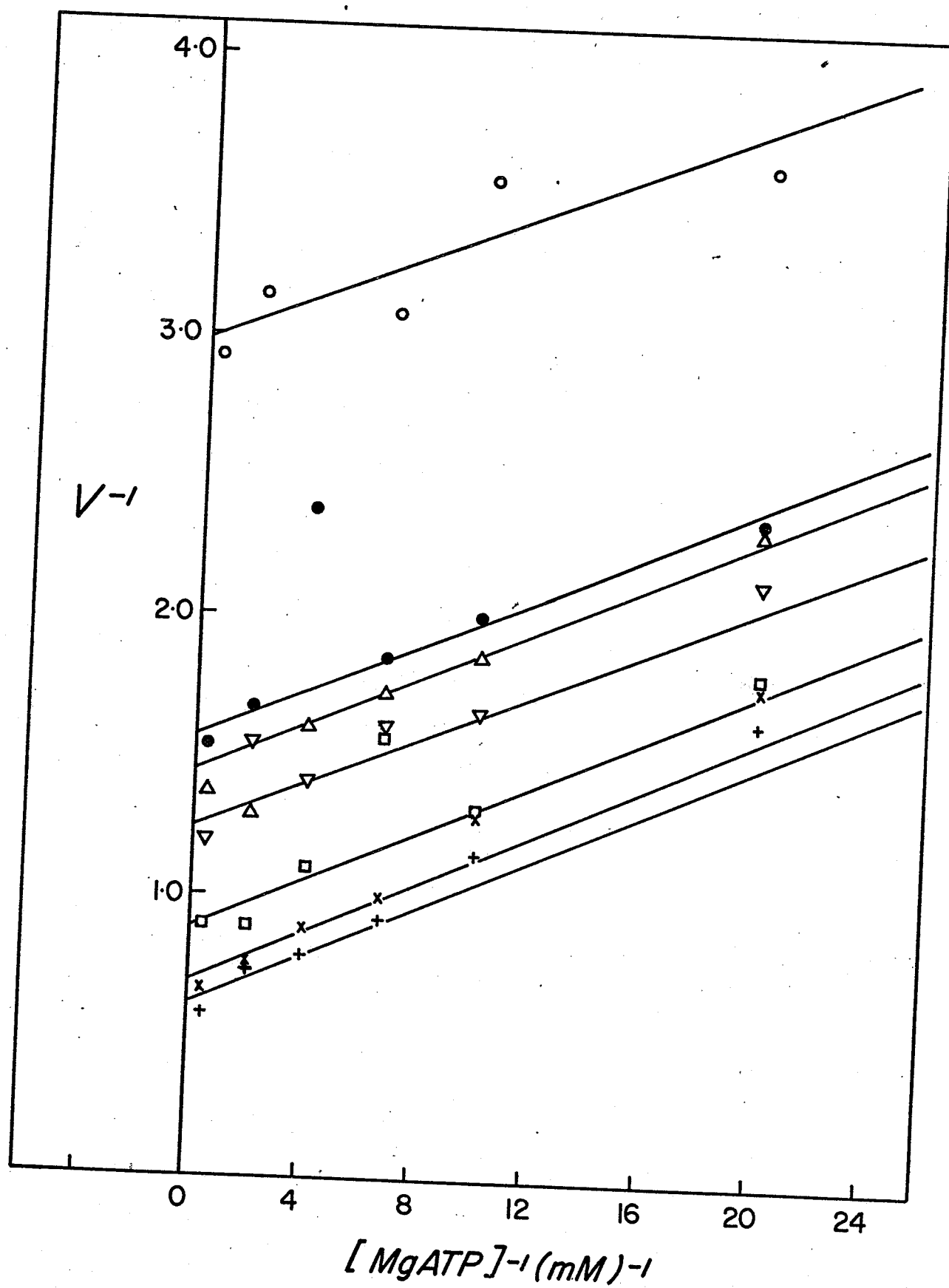


Figure 18. Replot of intercepts obtained from Figure 17, as a function of the reciprocal of propionyl CoA concentration.

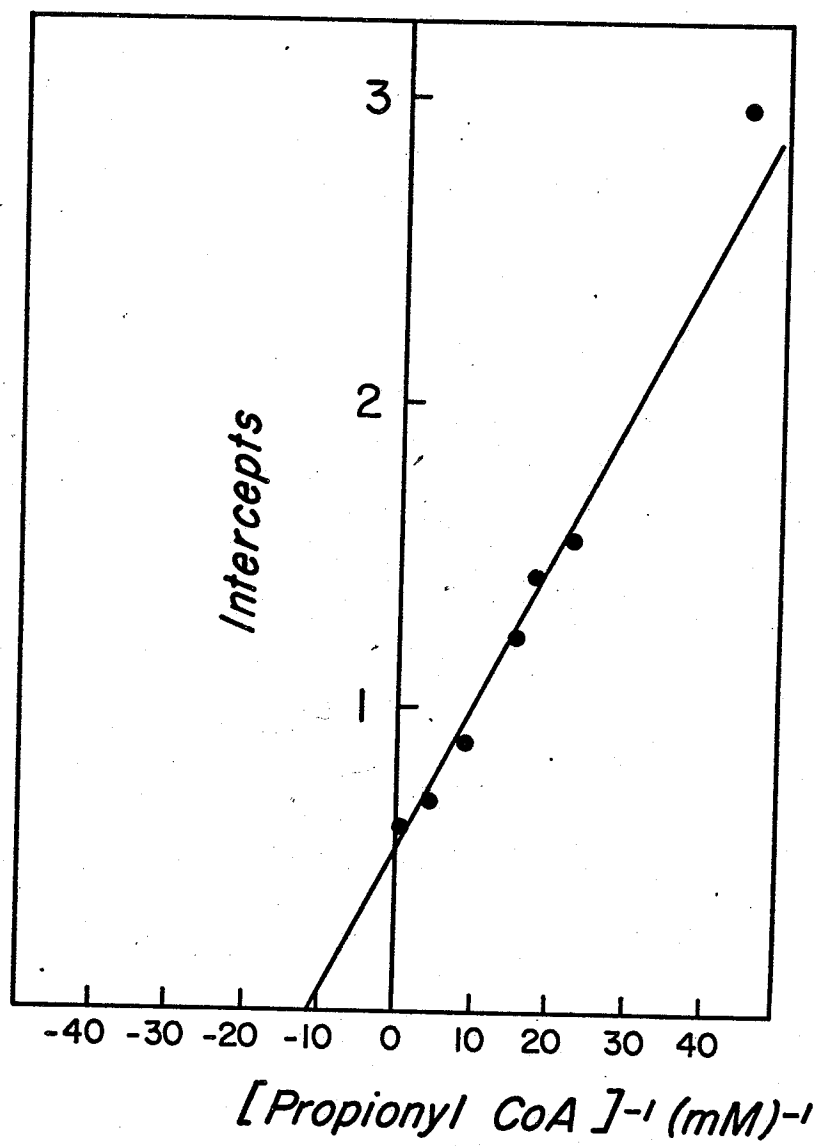


Figure 19. Lineweaver-Burk plots obtained
using propionyl CoA as variable,
and HCO_3^- as fixed variable.

△—△, 3.93 mM;

⊗—⊗, 7.43 mM;

▽—▽, 13.9 mM.

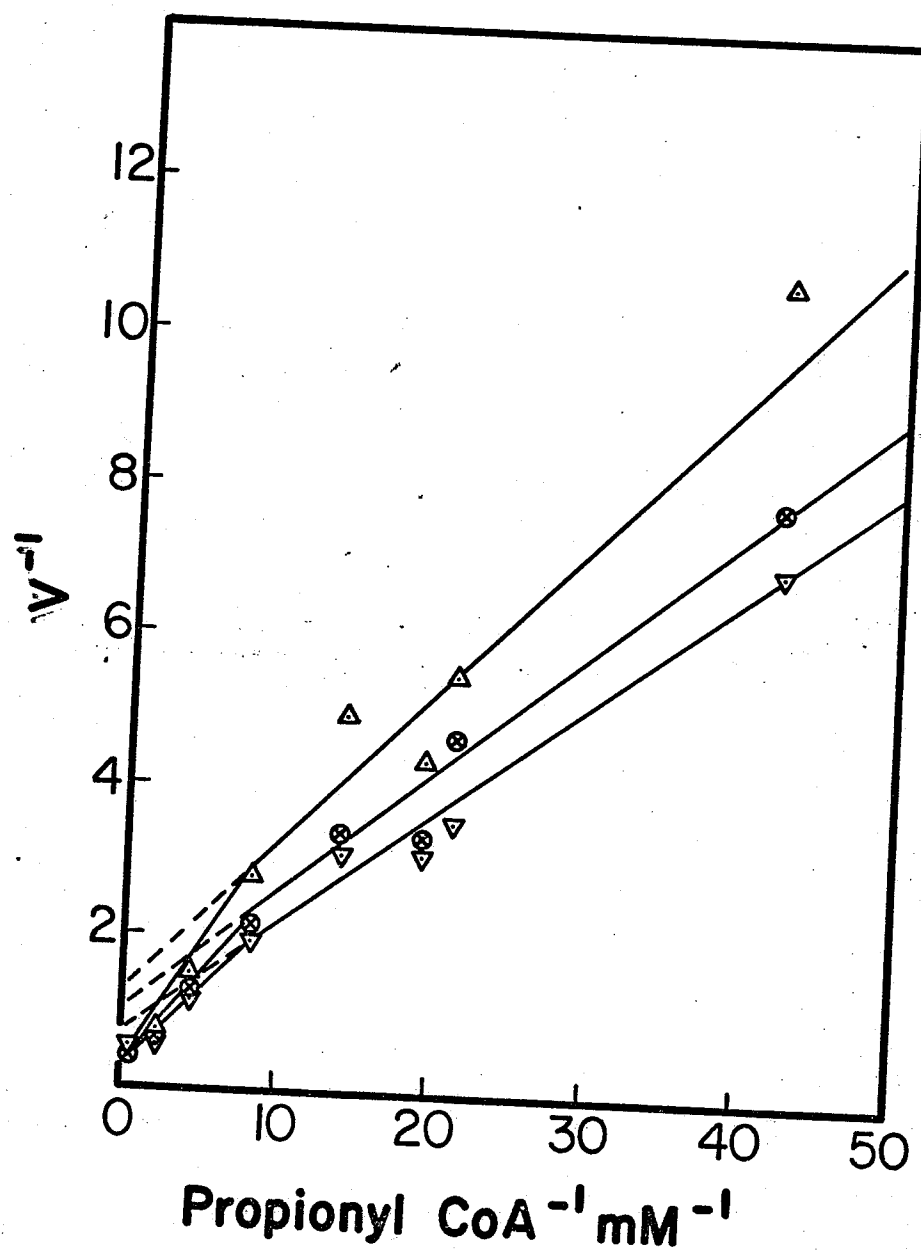
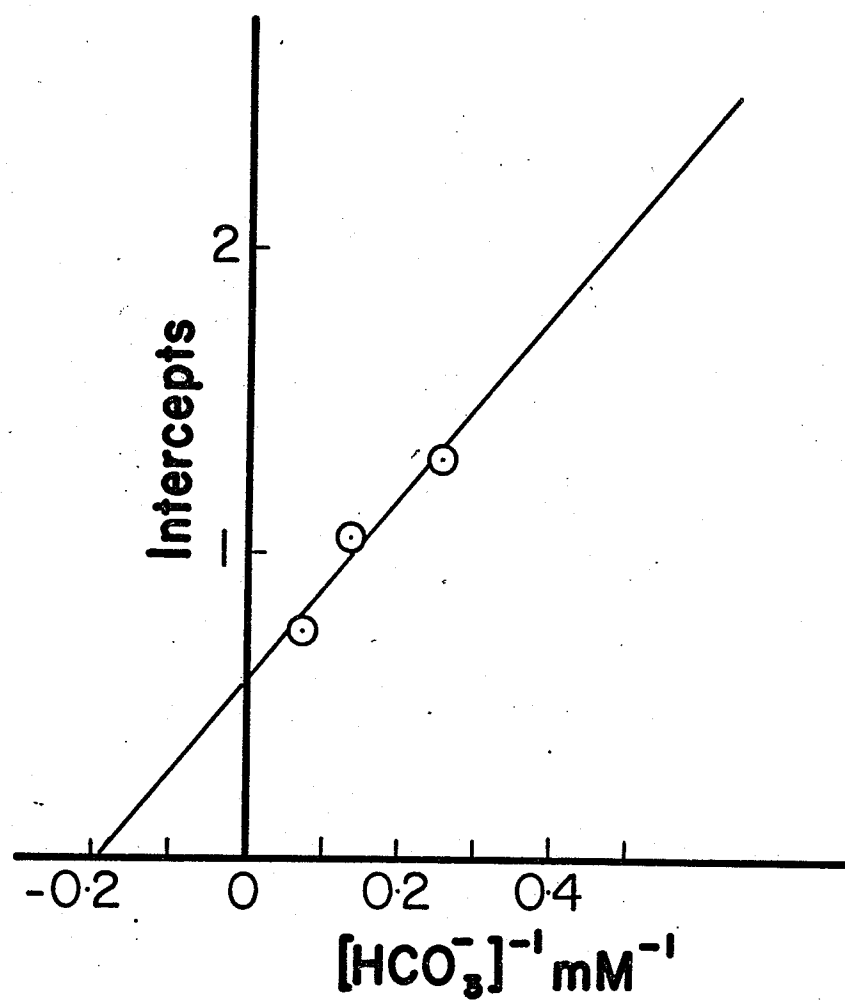


Figure 19A. Replot of intercepts obtained from Figure 19, as a function of the reciprocal of HCO_3^- concentration.



intercepts against reciprocals of propionyl CoA concentrations was linear and yielded a true K_m value of 0.4 mM for propionyl CoA (Fig. 21).

3. MgATP : bicarbonate

With MgATP as the variable substrate and bicarbonate at several fixed concentrations, double reciprocal plots resulted in linear intersecting lines (Fig. 22). Replots of (K_m^{-1}/v^{-1}) and $(1/v^{-1})$ against reciprocals of bicarbonate concentrations were linear (Figs. 23A and 23B). The true K_m for bicarbonate was calculated from the slope replot to be 2.56 mM while that value obtained from the intercept replot was 2.90 mM.

When bicarbonate was varied against several fixed concentrations of MgATP, the double reciprocal plots were linear and intersecting (Fig. 24). Replots of values for slopes and intercepts against reciprocals of MgATP concentrations were also linear (Figs. 25A and 25B). The replot of slopes yielded a true K_m for MgATP of 0.167 mM while a true K_m value for MgATP of 54 μ M was obtained from the replot of intercepts.

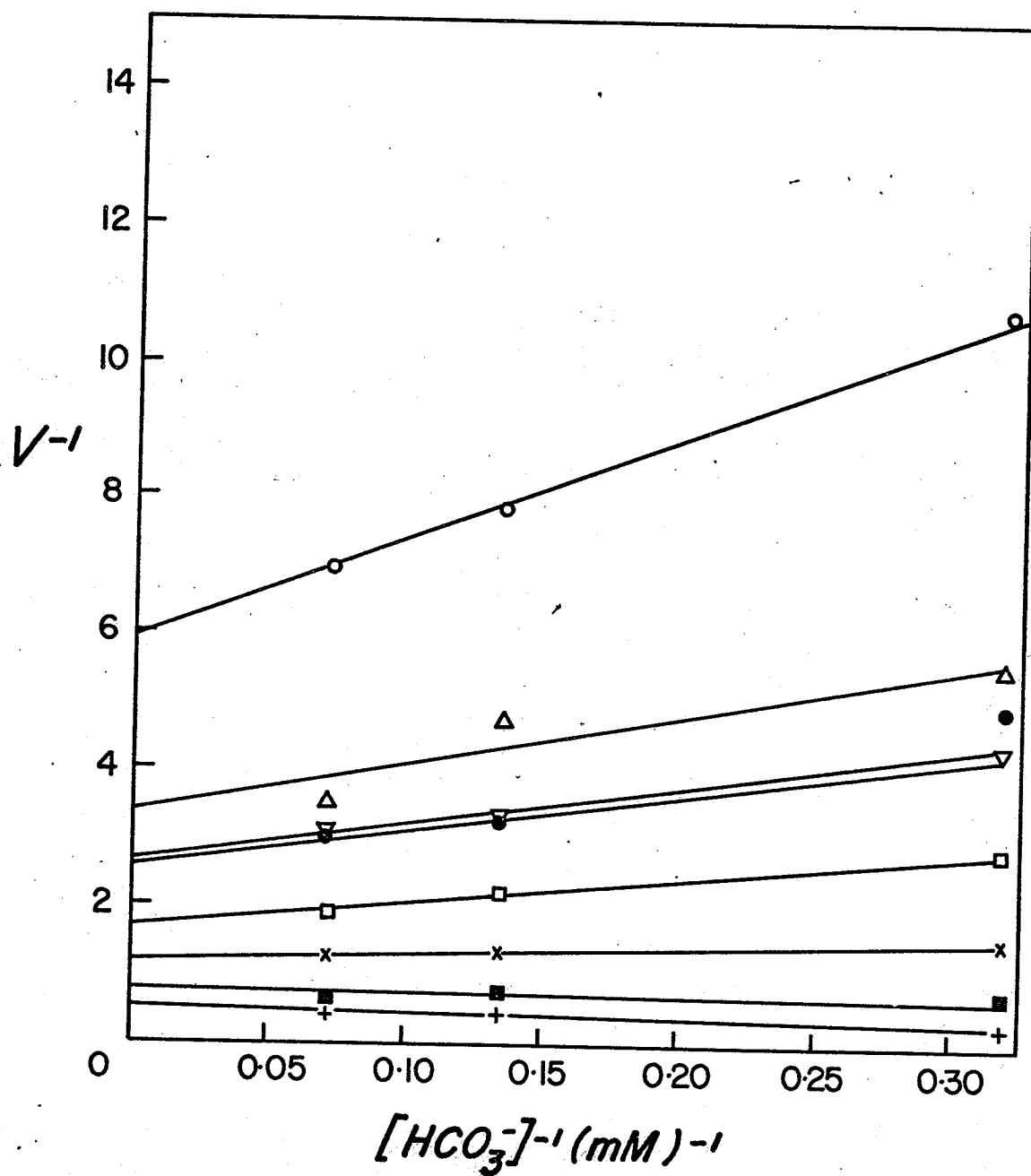
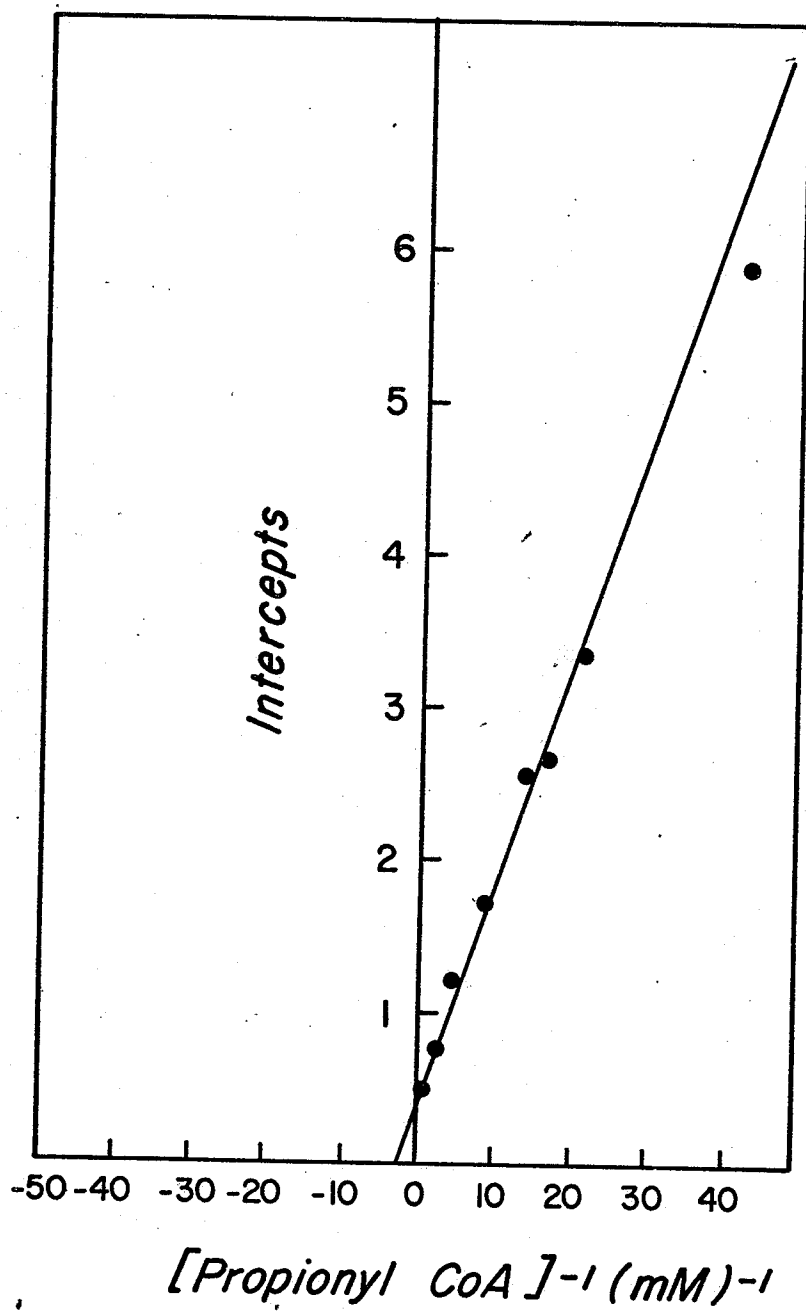


Figure 21. Replot of intercepts obtained from
Figure 20, as a function of the
reciprocal of propionyl CoA
concentration.



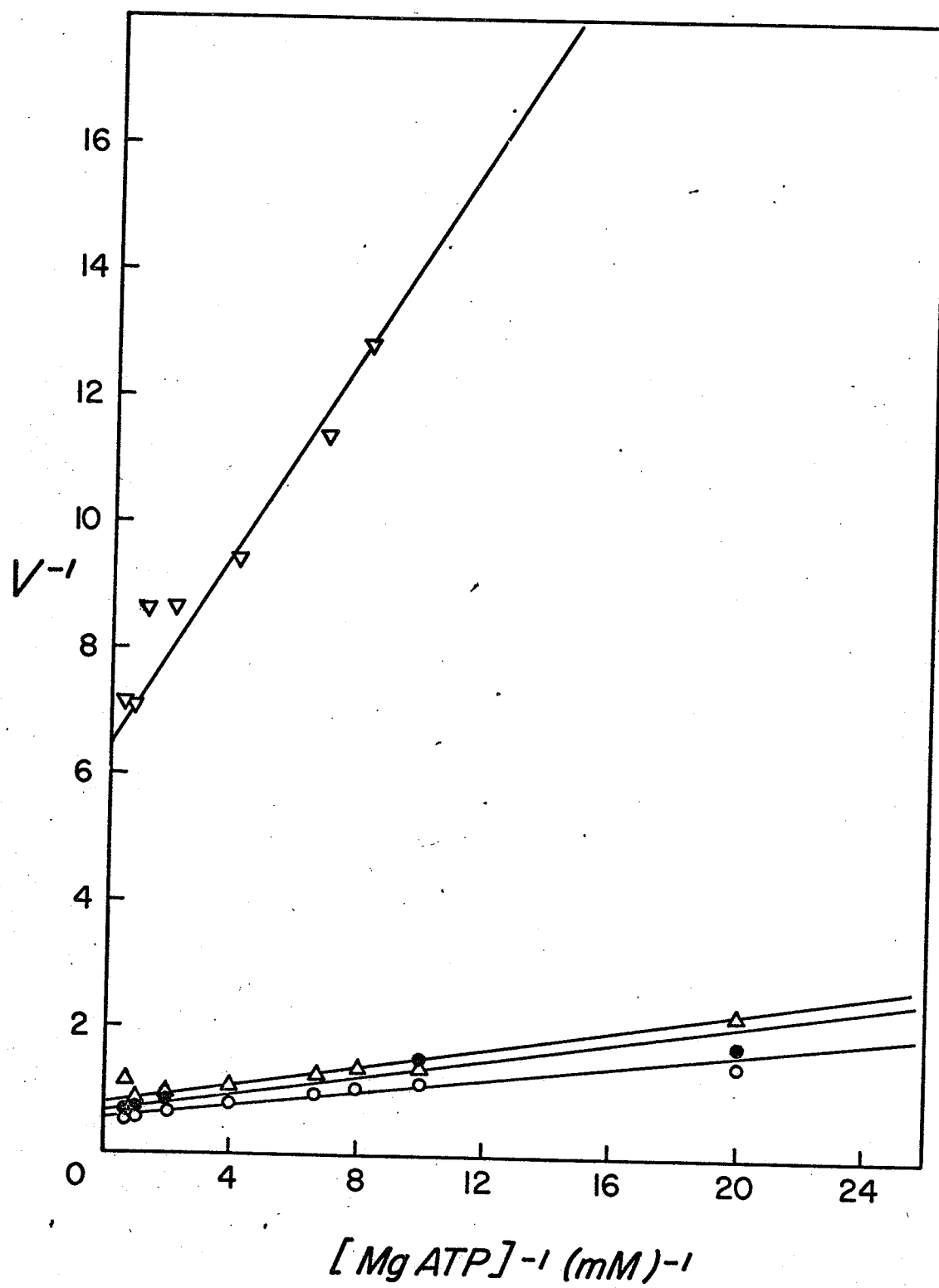


Figure 23. Replots of slopes and intercepts
obtained from Figure 22 as a
function of the reciprocal of
 HCO_3^- concentration.
A, slopes;
B, intercepts.

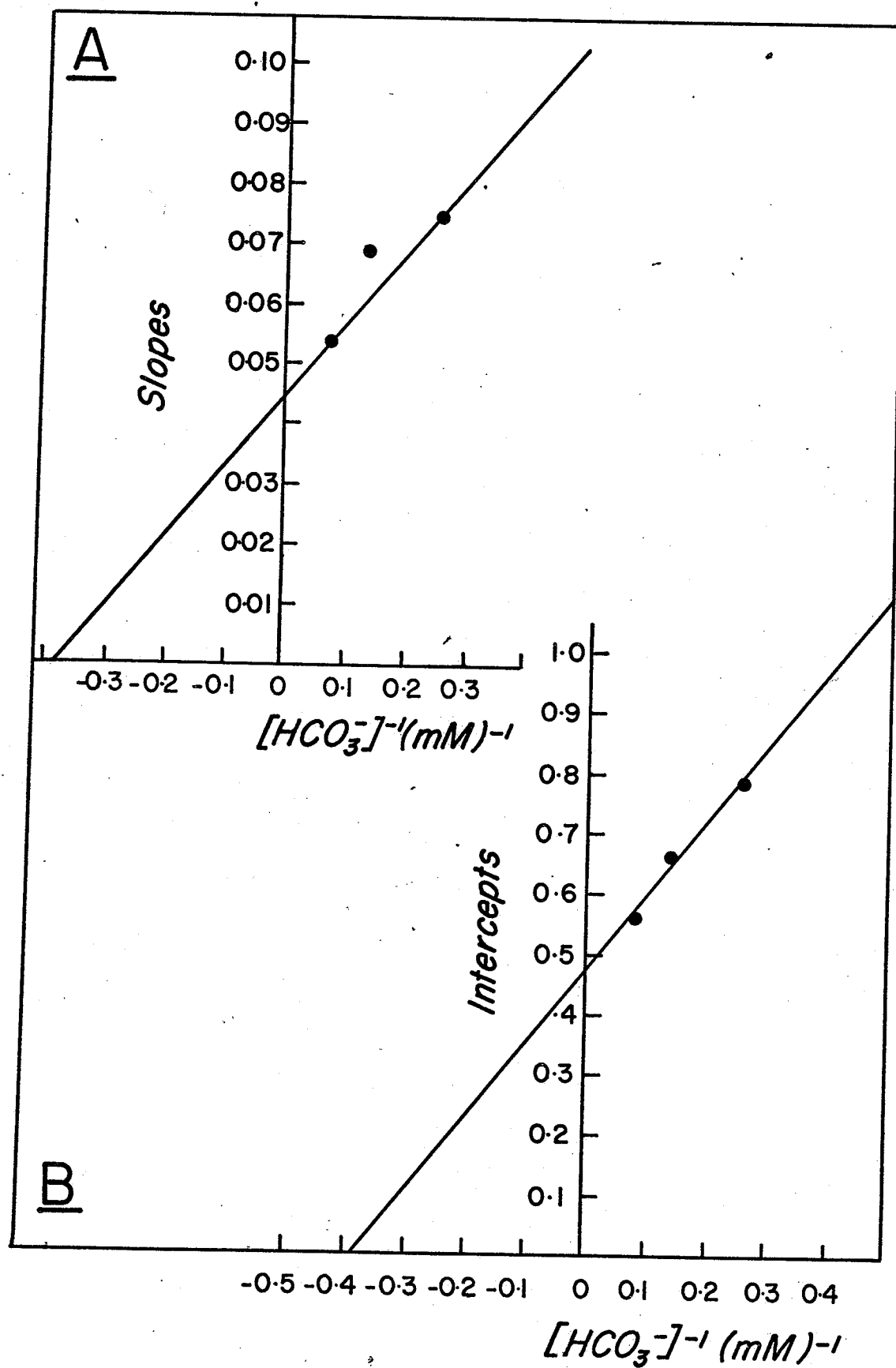


Figure 24. Lineweaver-Burk plots obtained
using HCO_3^- as variable and
MgATP as fixed variable.

○—○, 0.05 mM;

□—□, 0.1 mM;

△—△, 0.9 mM;

▽—▽, 1.35 mM.

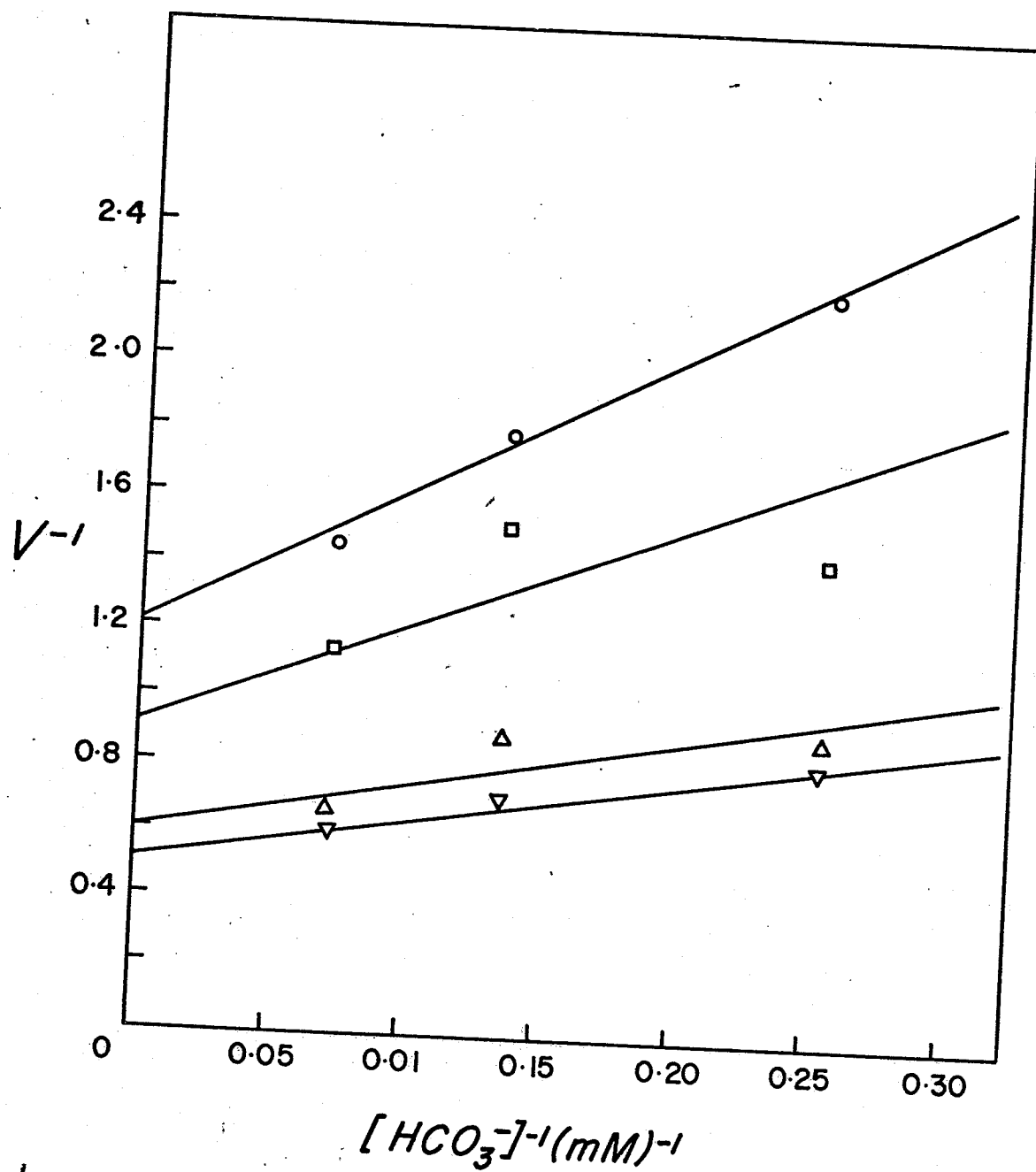
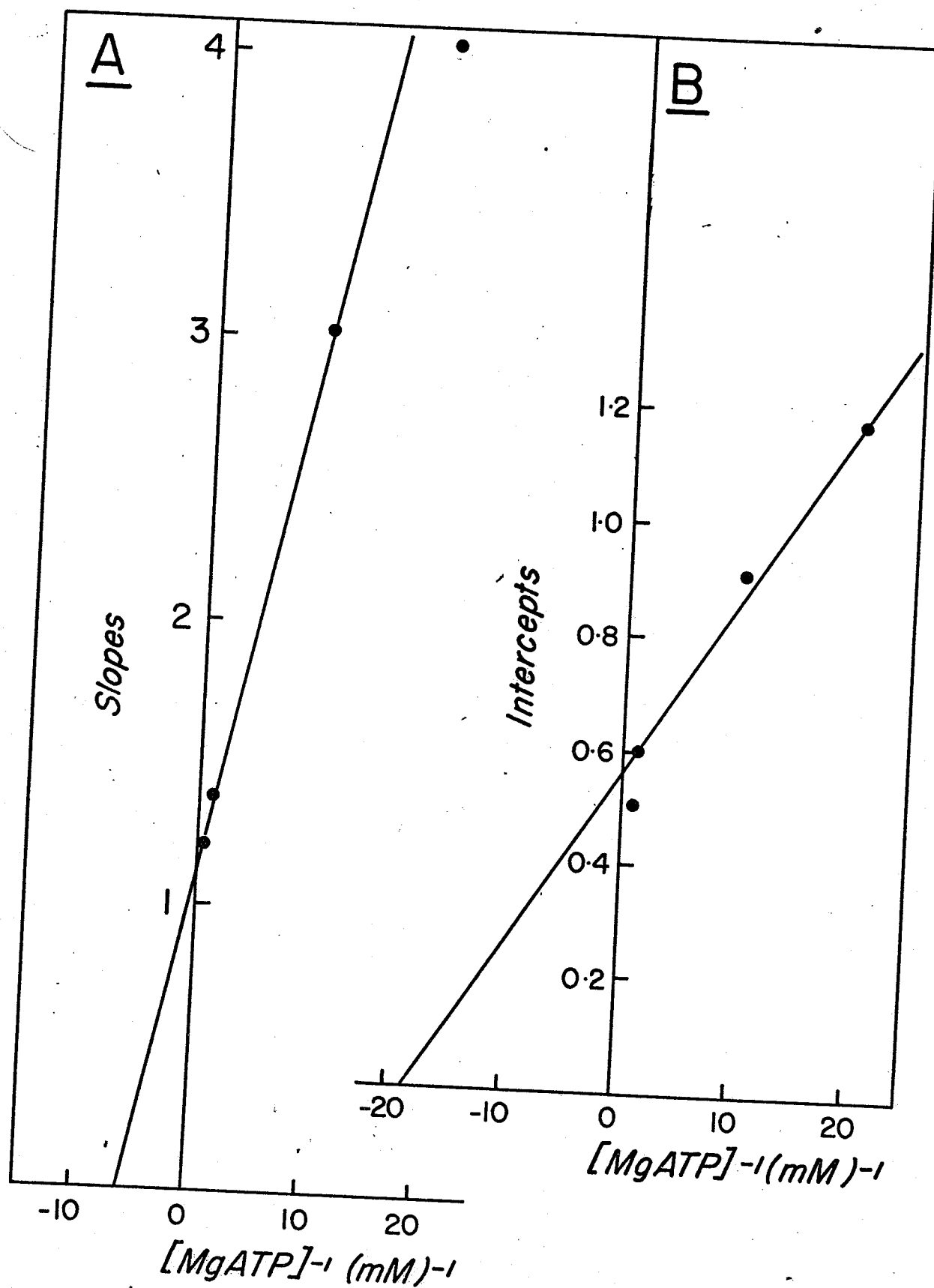


Figure 25. Replots of slopes and intercepts
obtained from Figure 24 as a
function of the reciprocal of
MgATP concentration.

A, slopes;

B, intercepts.



Product Inhibition Studies

Product inhibition studies were carried out with each product in combination with every substrate. Inhibition constants (K_i 's) were determined by measuring initial velocities at varied concentrations of a substrate and several fixed concentrations of the product, while keeping the other substrates at a fixed saturating concentration. From the double reciprocal plots, the intercepts and slopes were re-plotted against inhibitor concentration. K_i values, $K_{i\text{intercept}}$ (K_{iI}) and $K_{i\text{slope}}$ (K_{iS}), were obtained from the intercepts at the horizontal axis.

All terms used to describe the various types of inhibition are those of Cleland (3). Therefore, the inhibition is called competitive if the inhibitor increases the slope but does not affect the vertical intercepts. The inhibition is noncompetitive if the inhibitor increases both the slope and the vertical intercepts and uncompetitive if an increase is observed only on the vertical intercepts.

The conditions used throughout this study were standard conditions as described in "Materials and Methods" with the exception that the $\text{KH}^{14}\text{CO}_3$ final concentration used was approximately 4 mM not 14 mM in the standard conditions.

1. P_i : MgATP

When MgATP was the variable substrate at several fixed concentrations of P_i , the double reciprocal plots were linear (Fig. 26) and indicated competitive inhibition; i.e. only the slopes were increased by addition of inhibitor. The replot for the slopes (Fig. 27) was also linear and yielded a K_{iS} value of 38 mM.

2. P_i : bicarbonate

When bicarbonate was the variable substrate at several fixed concentrations of P_i , double reciprocal plots were linear (Fig. 28) and indicated noncompetitive inhibition; i.e. both the slopes and vertical intercepts were affected by addition of inhibitor. Replots of slopes and intercepts (Figs. 29A and 29B) were linear. The values for K_{iS} and K_{iI} were calculated to be 4.0 mM and 230 mM respectively.

3. P_i : propionyl CoA

When propionyl CoA was varied at several fixed concentrations of P_i , the double reciprocal plots were linear (Fig. 30) and suggested competitive inhibition. The replot for slopes (Fig. 31) was linear and yielded a K_{iS} value of 282 mM.

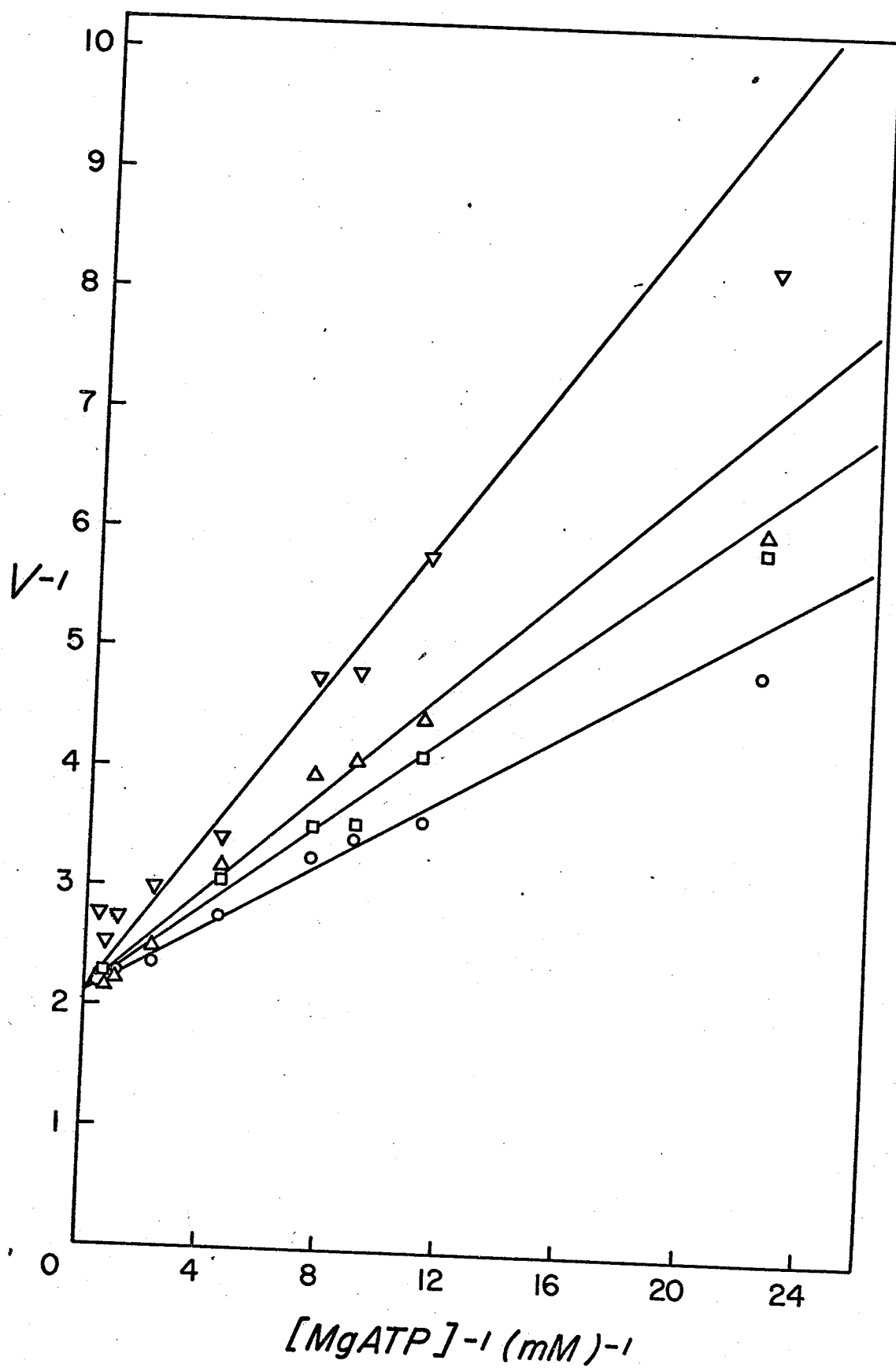


Figure 27. Replot of slopes obtained from
Figure 26, as a function of
phosphate concentration.

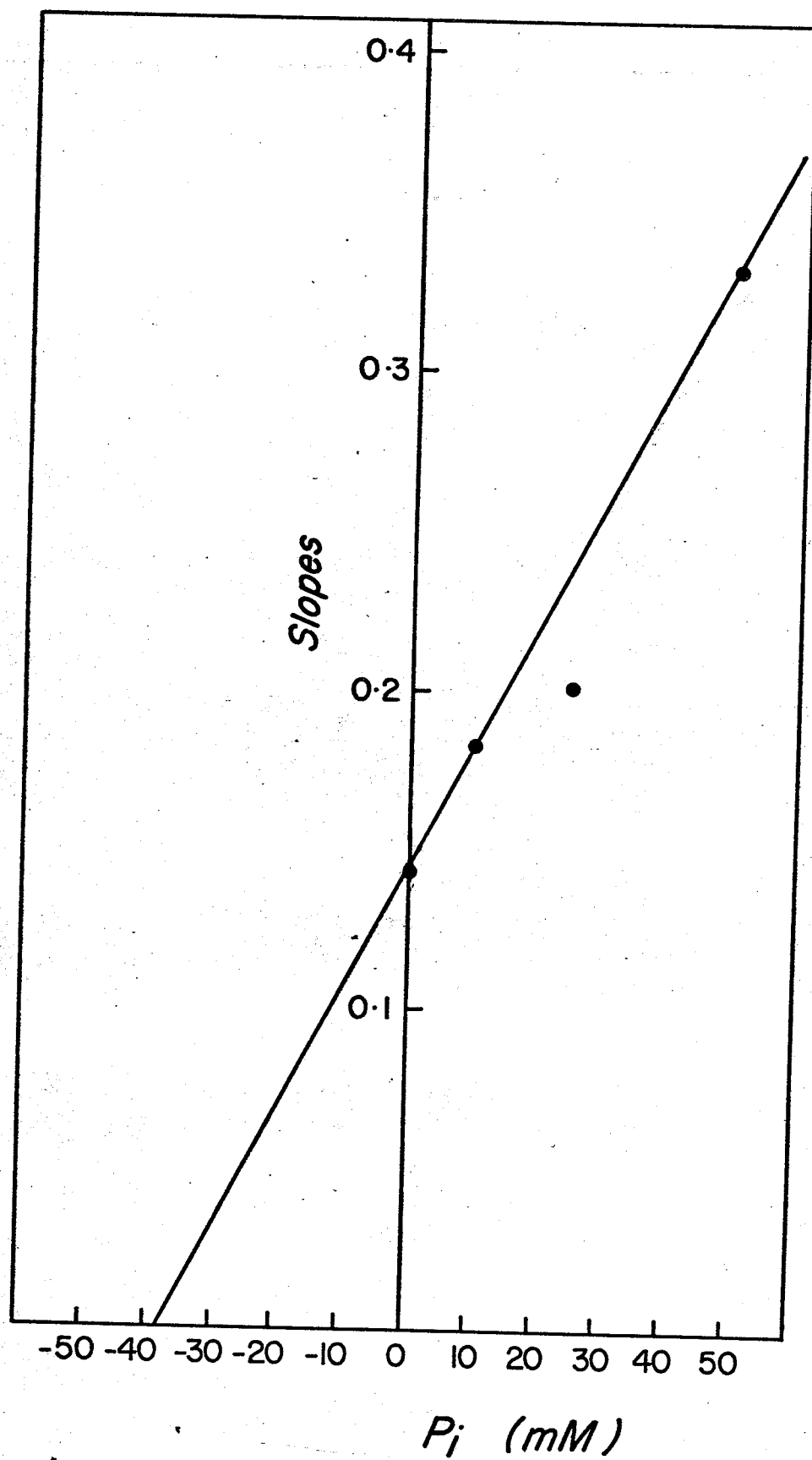


Figure 28. Lineweaver-Burk plots of inhibition by potassium phosphate, using HCO_3^- as variable substrate.

○—○, 0 mM;

□—□, 10 mM;

△—△, 25 mM;

▼—▼, 50 mM.

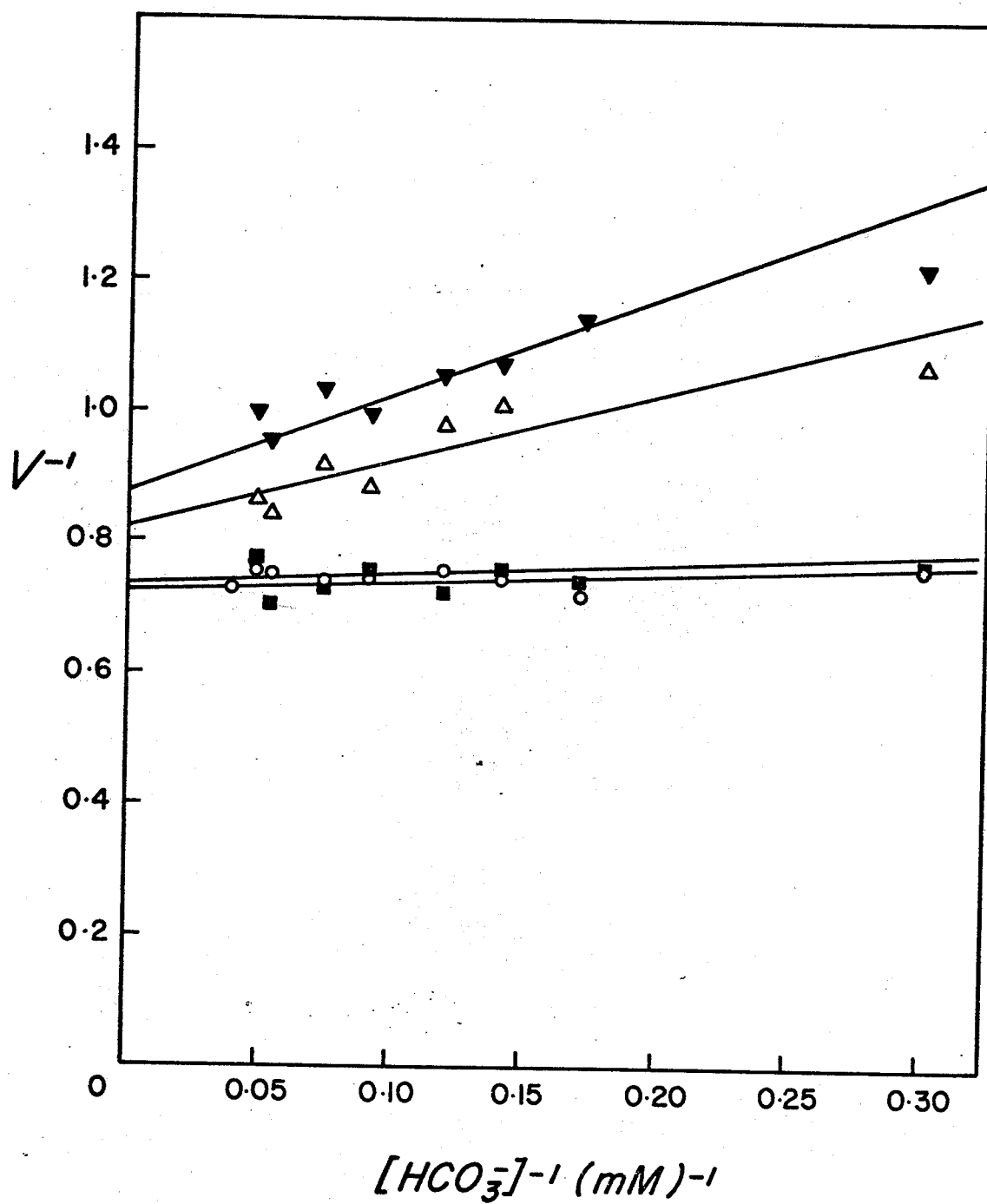


Figure 29. Replots of slopes and intercepts
obtained from Figure 28, as a
function of phosphate concentra-
tion.

A, slopes;

B, intercepts.

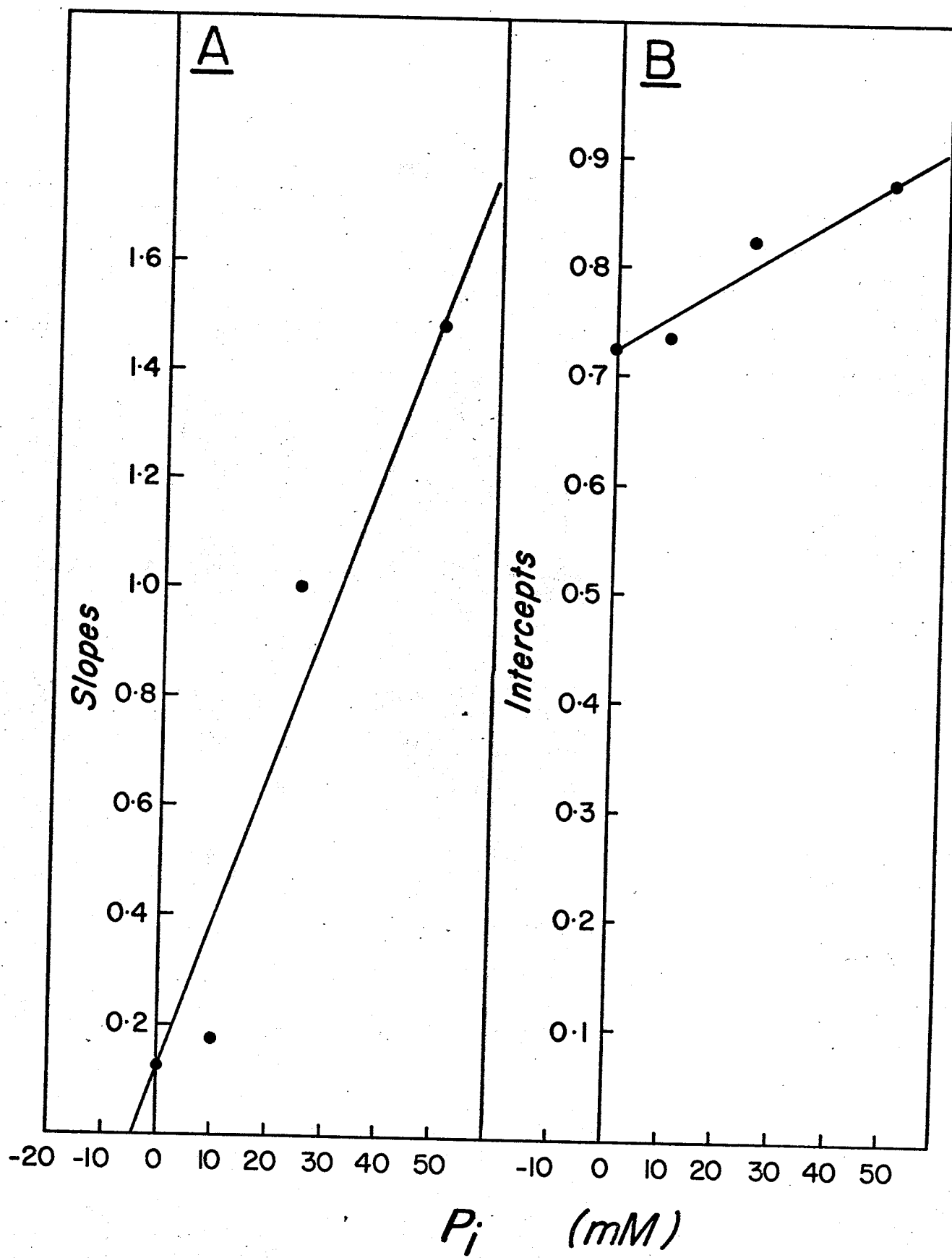


Figure 30. Lineweaver-Burk plots of inhibition
by potassium phosphate, using
propionyl CoA as variable substrate.

○—○, 0 mM;

■—■, 50 mM;

▽—▽, 100 mM.

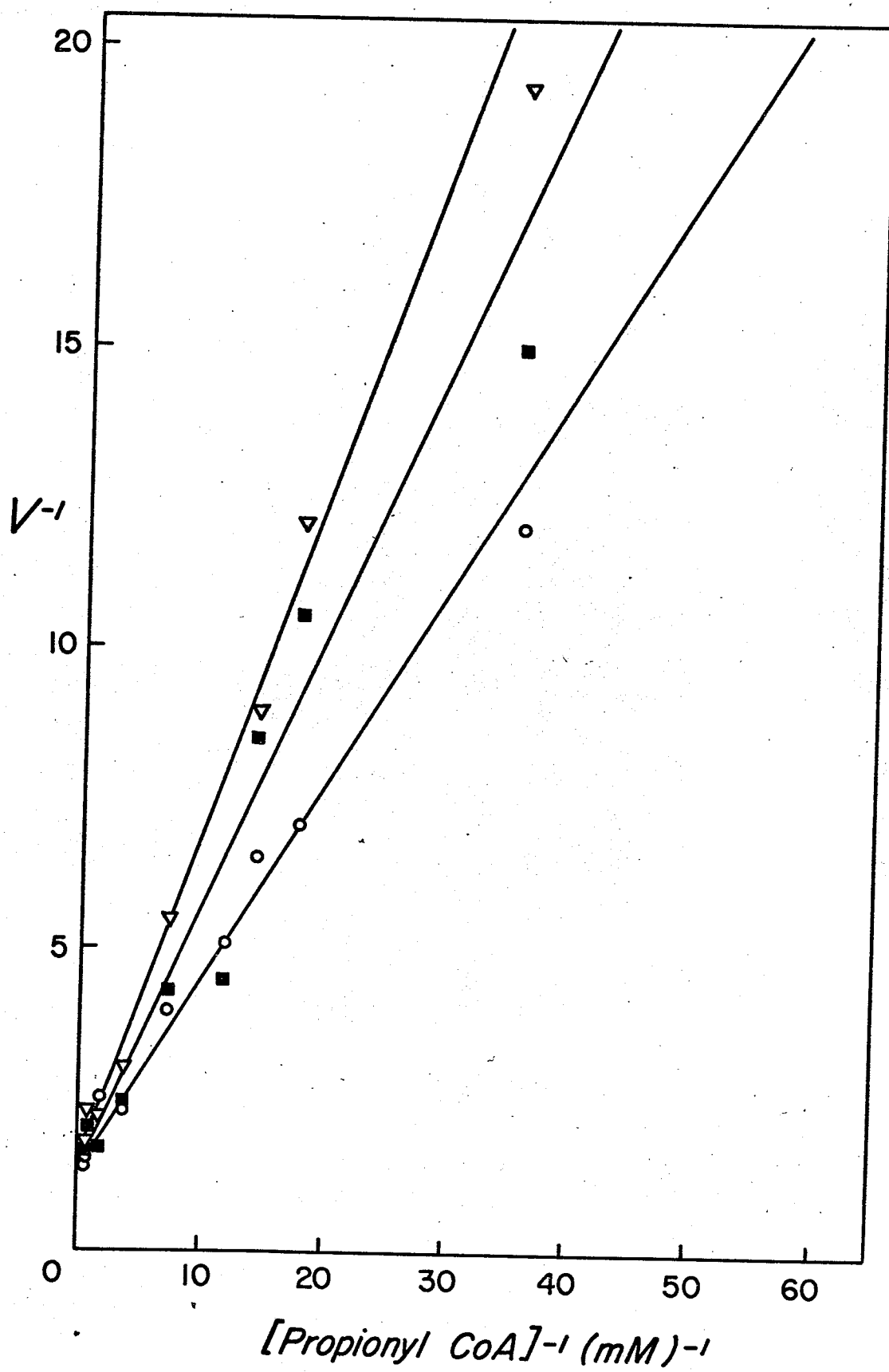
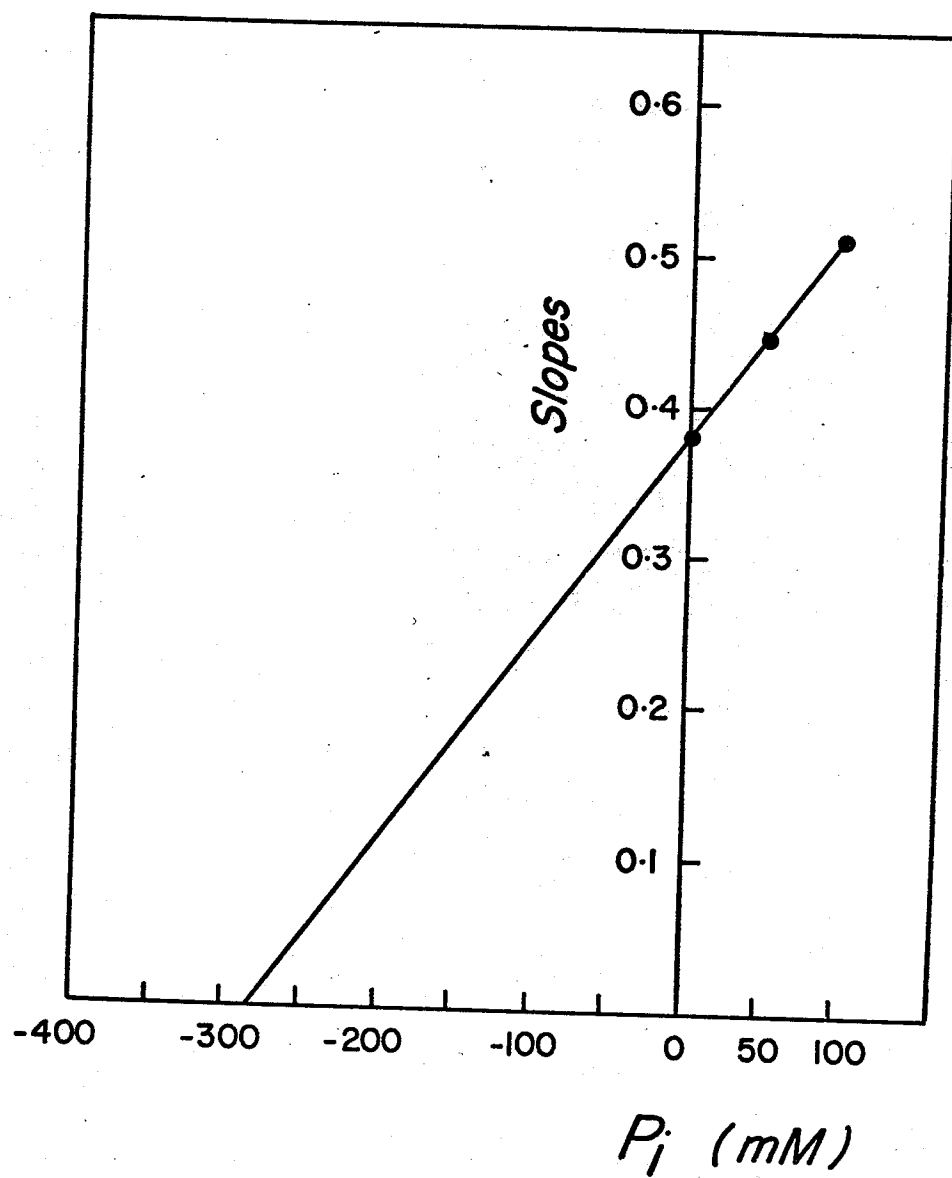


Figure 31. Replot of slopes obtained from
Figure 30, as a function of
phosphate concentration.



4. MgADP : MgATP

When MgATP was varied at several fixed concentrations of MgADP, the double reciprocal plots were linear (Fig. 32) and indicated competitive inhibition. The replot of slopes (Fig. 33) was linear and resulted in a K_{iS} value of 42 μ M.

5. MgADP : bicarbonate

When bicarbonate was the variable substrate at several fixed concentrations of MgADP, the double reciprocal plots were linear (Fig. 34) and demonstrated noncompetitive inhibition. Replots of slopes and intercepts (Figs. 35A and 35B) were linear. The values for K_{iS} and K_{iI} were calculated to be 0.10 mM and 4.15 mM respectively.

6. MgADP : propionyl CoA

When propionyl CoA was varied at several fixed concentrations of MgADP, the double reciprocal plots were linear (Fig. 36) and showed competitive inhibition. The replot of slopes versus MgADP concentration was linear (Fig. 37) and resulted in a K_{iS} of 1.0 mM.

7. Methylmalonyl CoA : MgATP

When MgATP was varied at several fixed concentrations of methylmalonyl CoA, the double reciprocal plots were linear (Fig. 38) and indicated noncompetitive inhibition. The replots of slopes and intercepts (Figs. 39A and 39B) were linear also

Figure 32. Lineweaver-Burk plots of inhibition
by MgADP, using MgATP as variable
substrate.

○—○, 0 mM;

■—■, 1.0 mM;

△—△, 2.5 mM;

▽—▽, 5.0 mM.

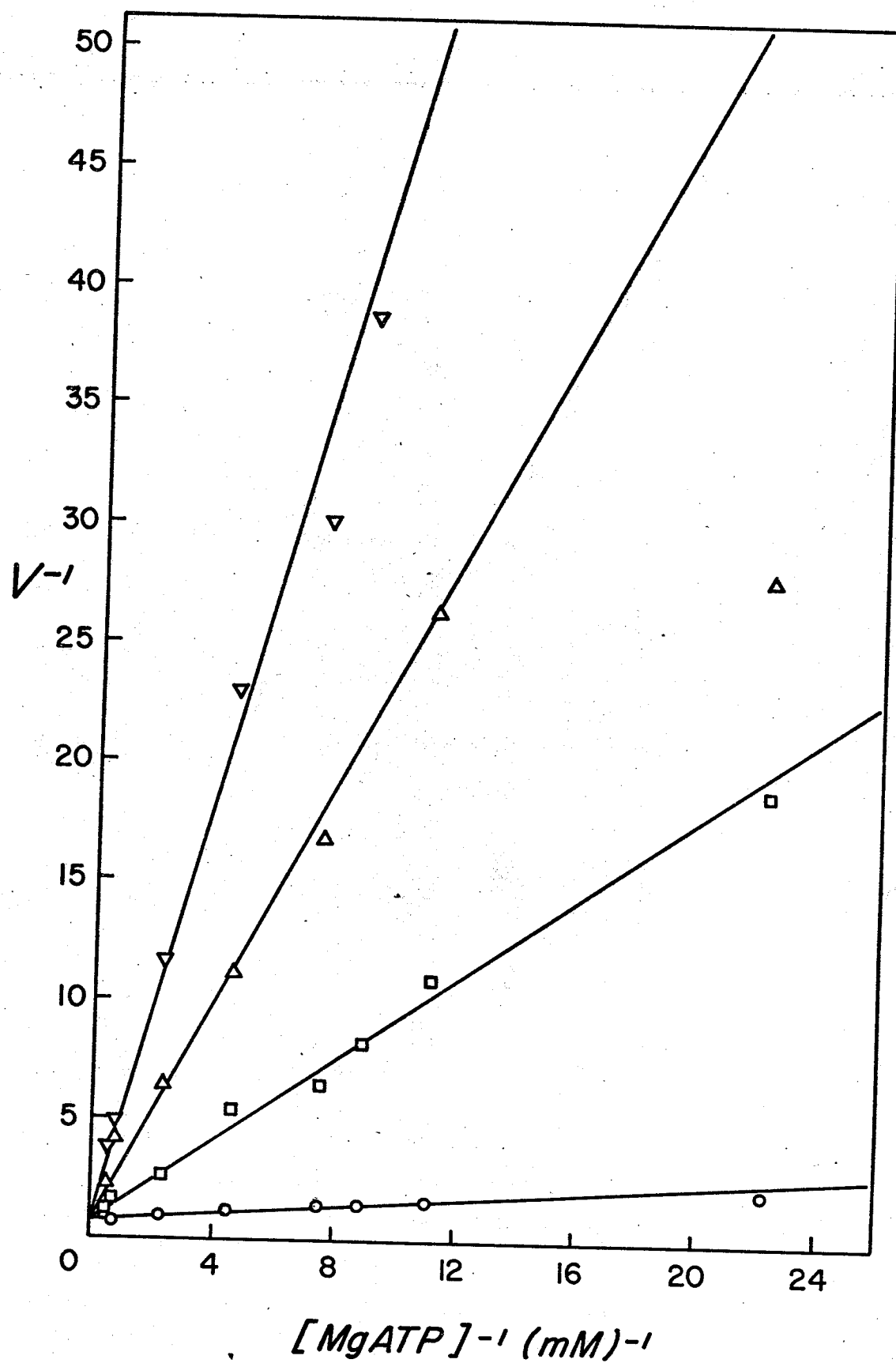


Figure 33. Replot of slopes obtained from
Figure 32, as a function of
MgADP concentration.

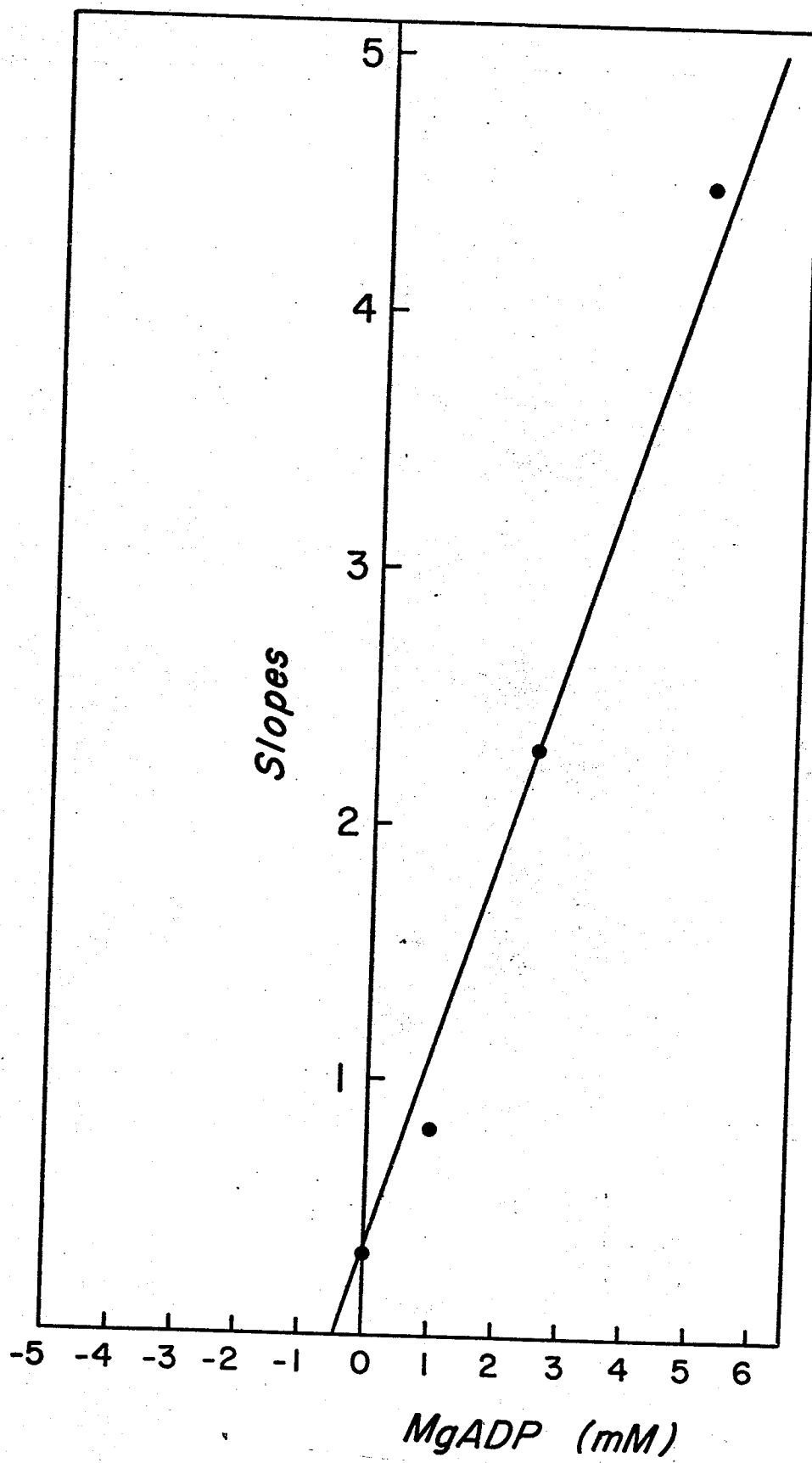


Figure 34. Lineweaver-Burk plots of inhibition by MgADP, using HCO_3^- as variable substrate.

○—○, 0 mM;
□—□, 1 mM;
△—△, 2.5 mM;
▽—▽, 5.0 mM.

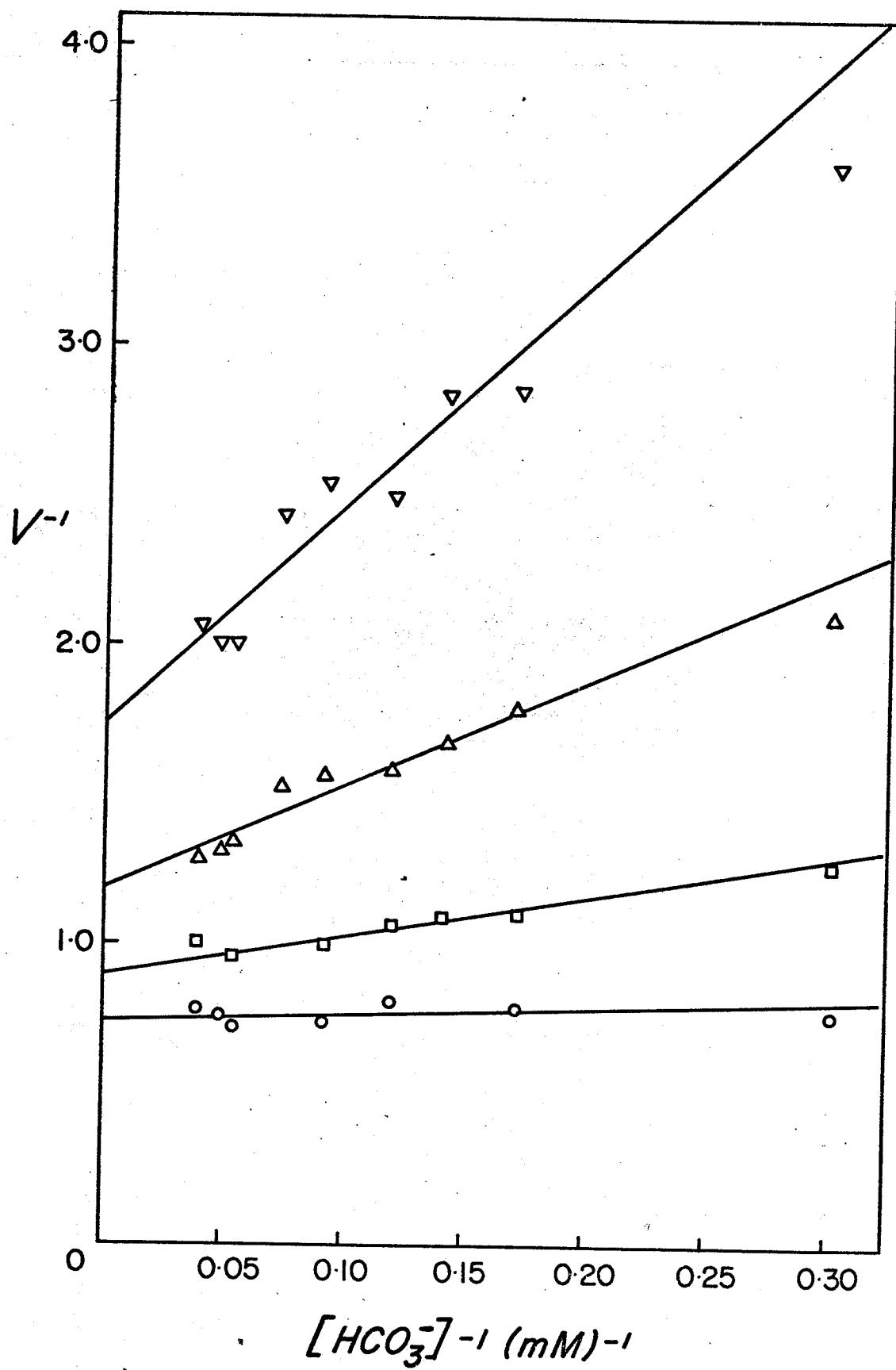


Figure 35. Replots of slopes and intercepts
obtained from Figure 34, as a
function of MgADP concentration.
A, slopes;
B, intercepts.

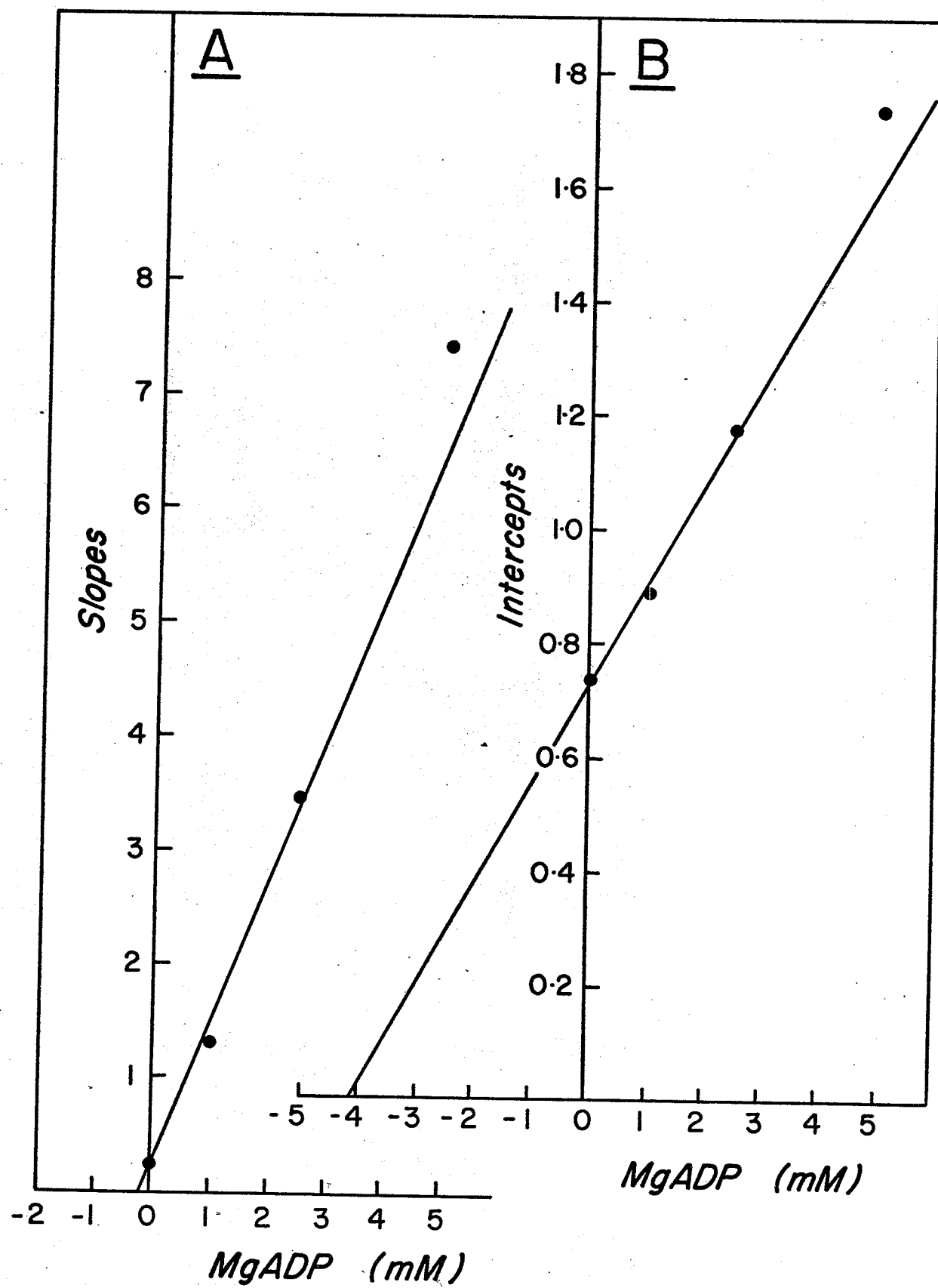


Figure 36. Lineweaver-Burk plots of inhibition
by MgADP, using propionyl CoA as
variable substrate.

○—○, 0 mM;

■—■, 1.0 mM;

△—△, 2.5 mM;

▽—▽, 5.0 mM.

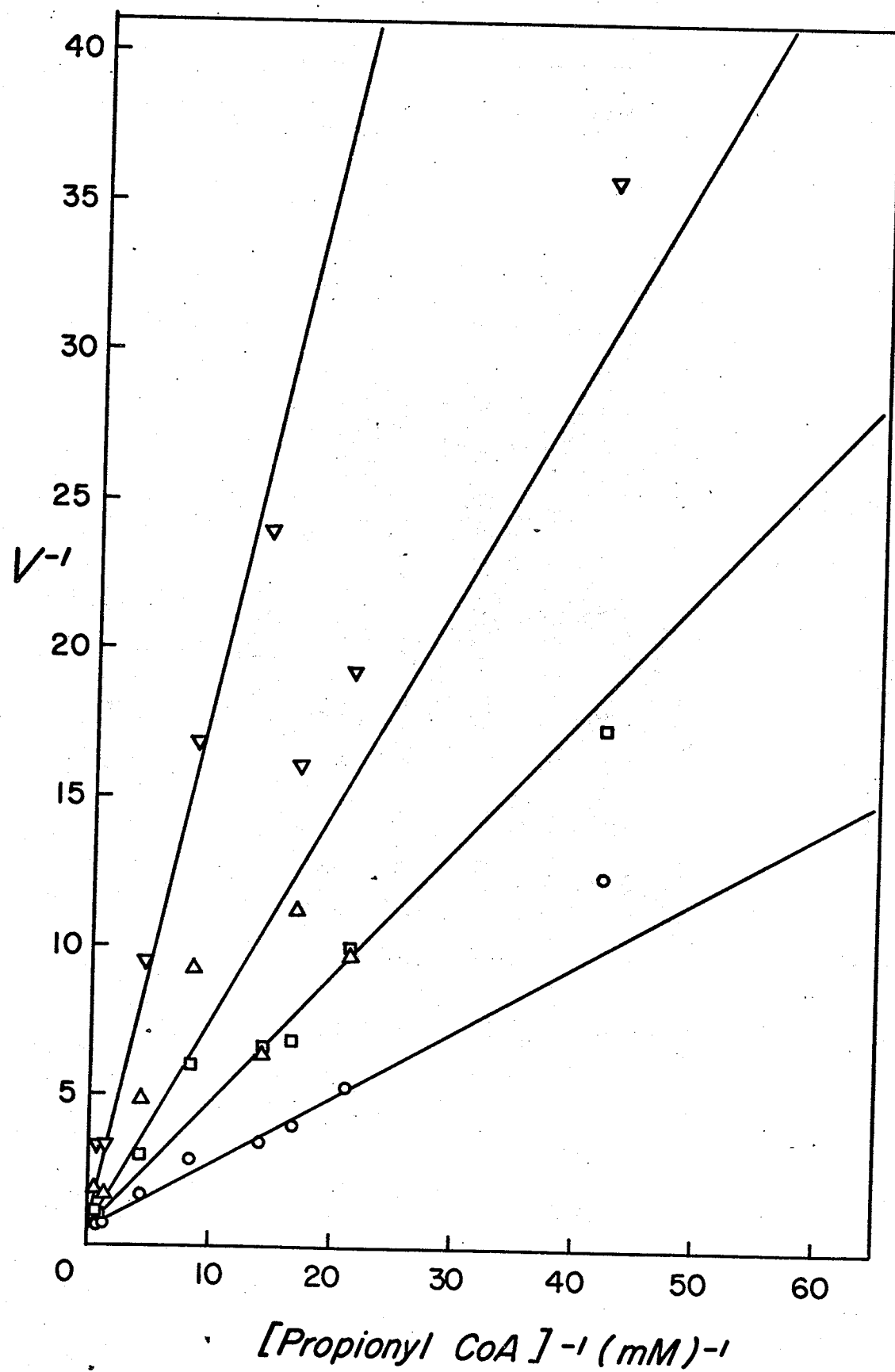


Figure 37. Replot of slopes obtained from
Figure 36 as a function of
MgADP concentration.

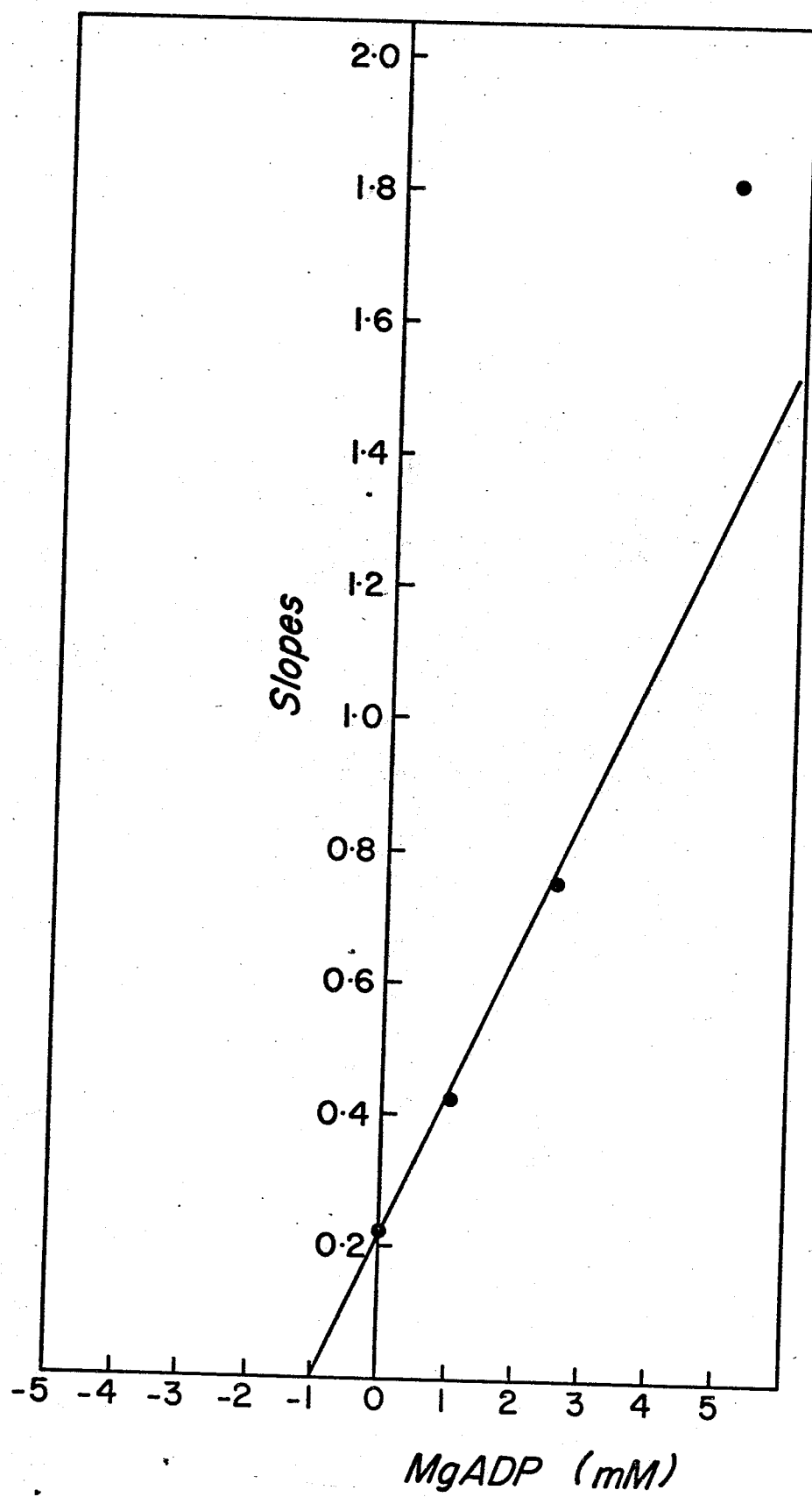


Figure 38. Lineweaver-Burk plots of inhibition by methyl malonyl CoA, using MgATP as variable substrate.

○—○, 0 mM;

■—■, 0.106 mM;

△—△, 0.53 mM;

▽—▽, 1.06 mM;

●—●, 2.05 mM.

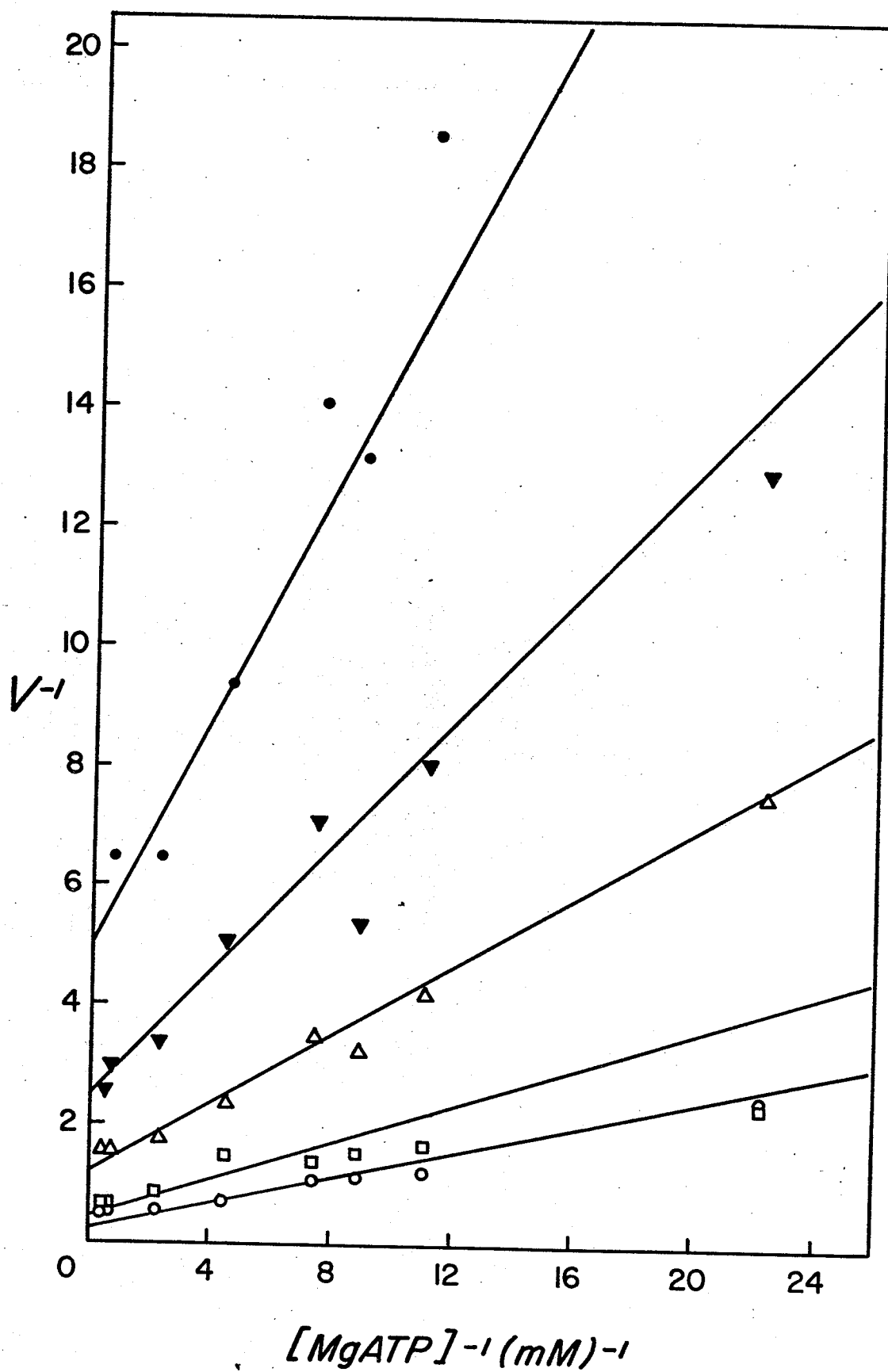
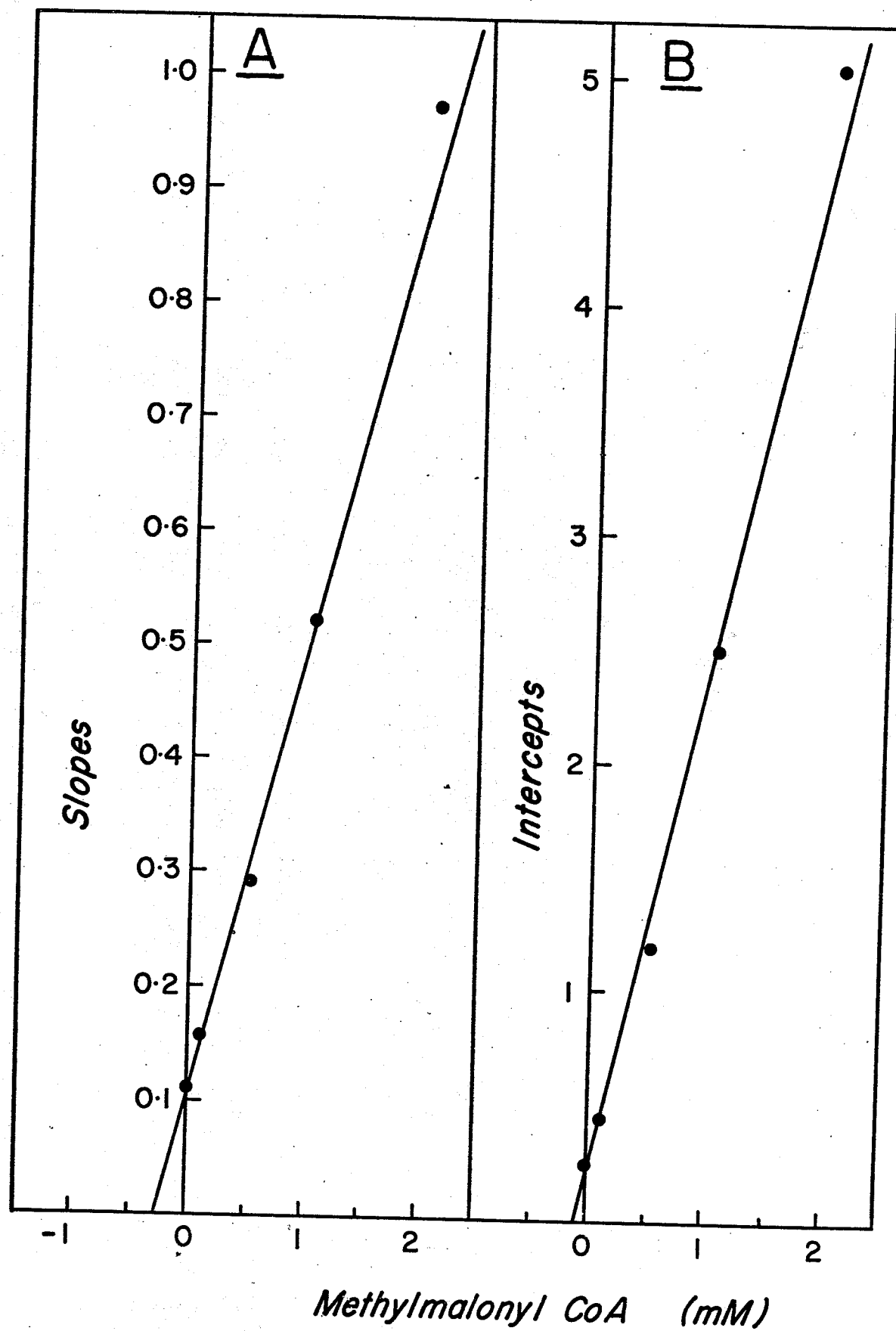


Figure 39. Replots of slopes and intercepts
obtained from Figure 38, as a
function of methyl malonyl CoA
concentration.

A, slopes;

B, intercepts.



and resulted in values for K_{iS} and K_{iI} of 0.28 mM and 0.10 mM respectively.

8. Methylmalonyl CoA : bicarbonate

When bicarbonate was varied at several fixed concentrations of methylmalonyl CoA, the double reciprocal plots were linear (Fig. 40) and indicated noncompetitive inhibition. Replots of slopes and intercepts (Figs. 41A and 41B) were also linear and yielded K_{iS} and K_{iI} values of 0.15 mM and 1.35 mM.

9. Methylmalonyl CoA : propionyl CoA

When propionyl CoA was varied at several fixed concentrations of methylmalonyl CoA, the double reciprocal plots were linear (Fig. 42) and indicated competitive inhibition. A replot of slopes yielded a K_{iS} value of 0.06 mM (Fig. 43).

Figure 40. Lineweaver-Burk plots of inhibition by methyl malonyl CoA, using HCO_3^- as variable substrate.

○—○, 0 mM;

◻—◻, 0.106 mM;

Δ—Δ, 0.53 mM;

▽—▽, 1.06 mM;

●—●, 2.05 mM.

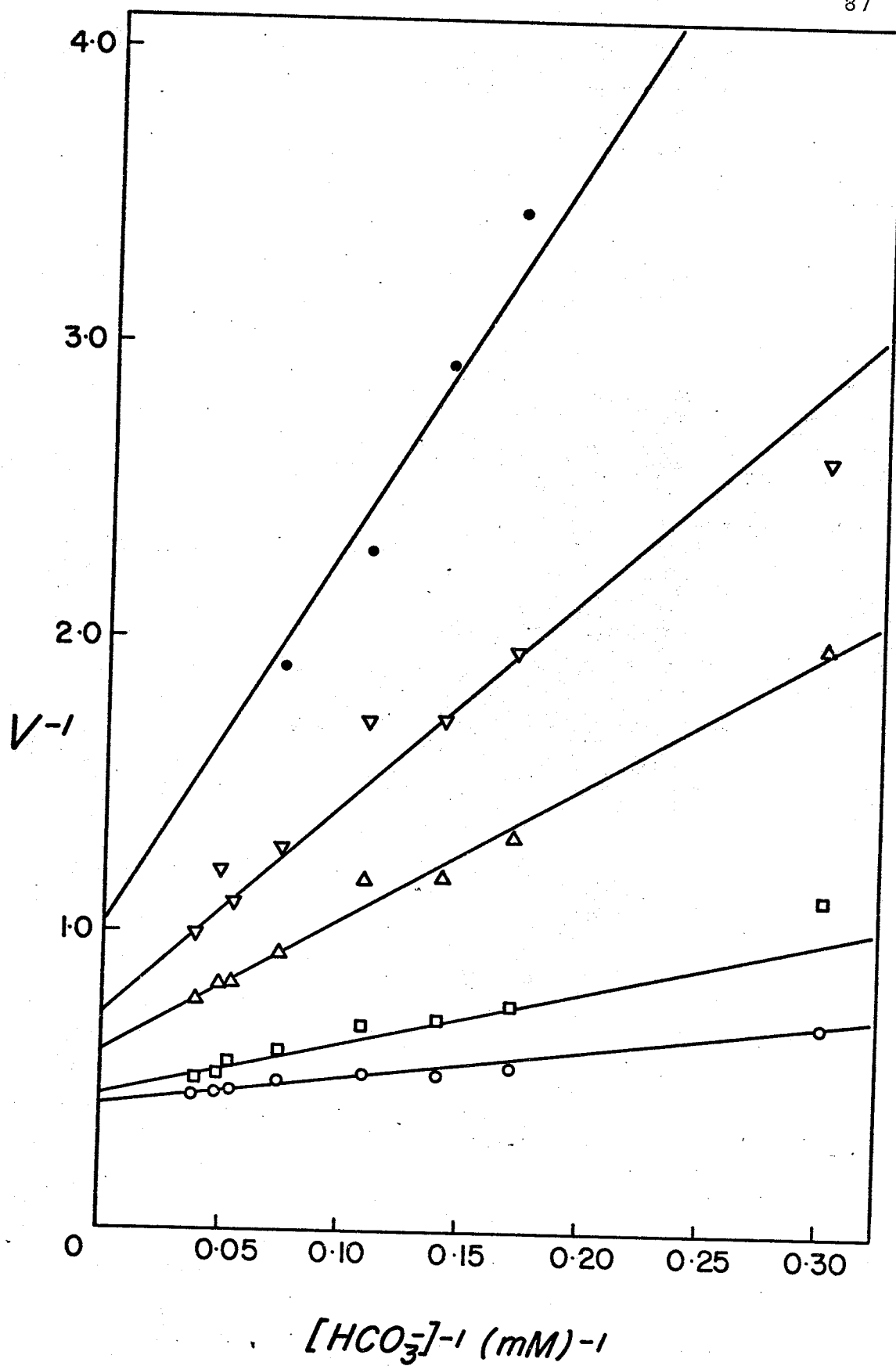


Figure 41. Replots of slopes and intercepts
obtained from Figure 40, as a
function of methyl malonyl CoA
concentration.

A, slopes;

B, intercepts.

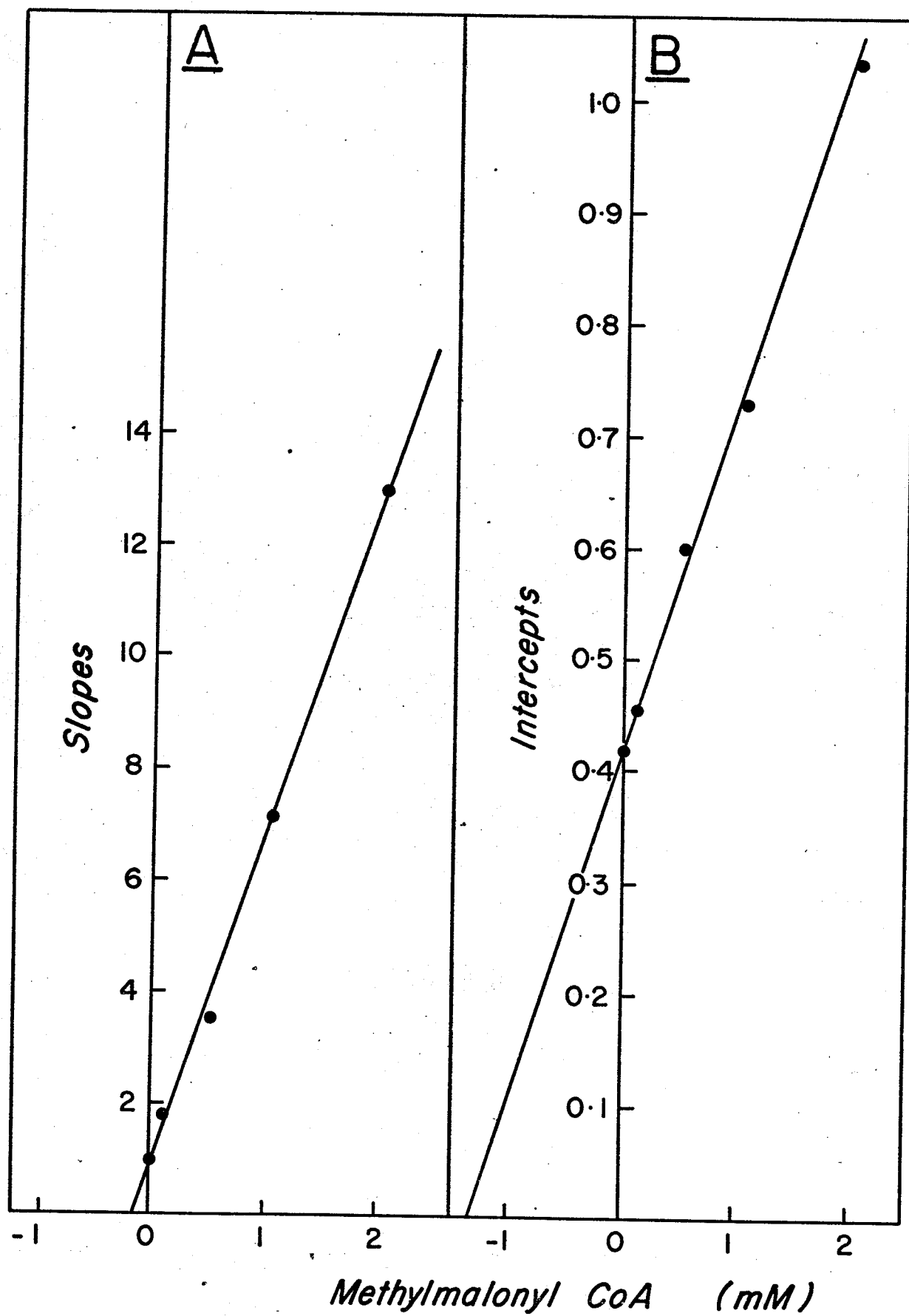


Figure 42. Lineweaver-Burk plots of inhibition by methyl malonyl CoA, using propionyl CoA as variable substrate.

○—○, 0 mM;

□—□, 0.106 mM;

△—△, 0.53 mM;

▽—▽, 1.06 mM;

●—●, 2.05 mM.

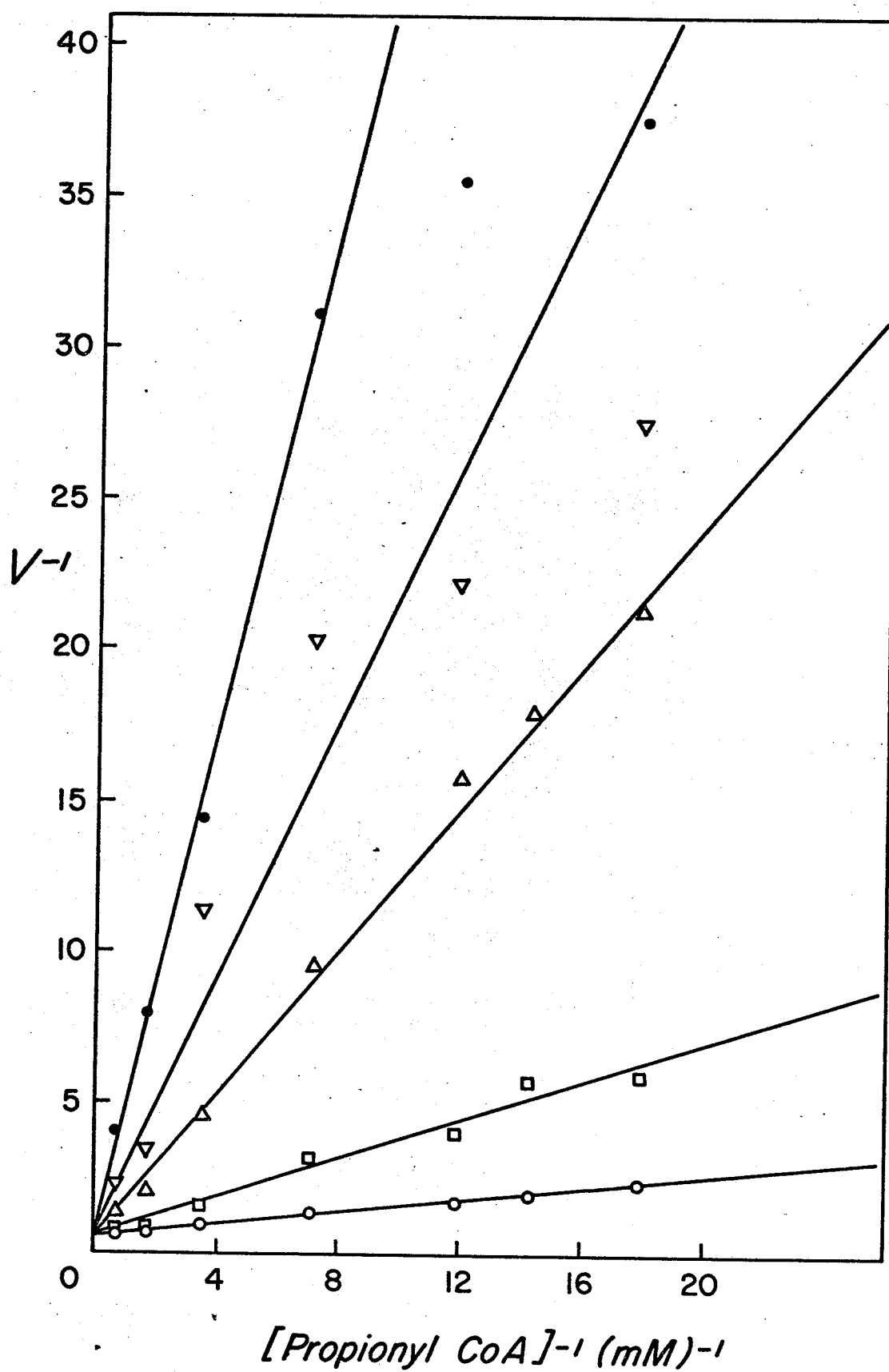
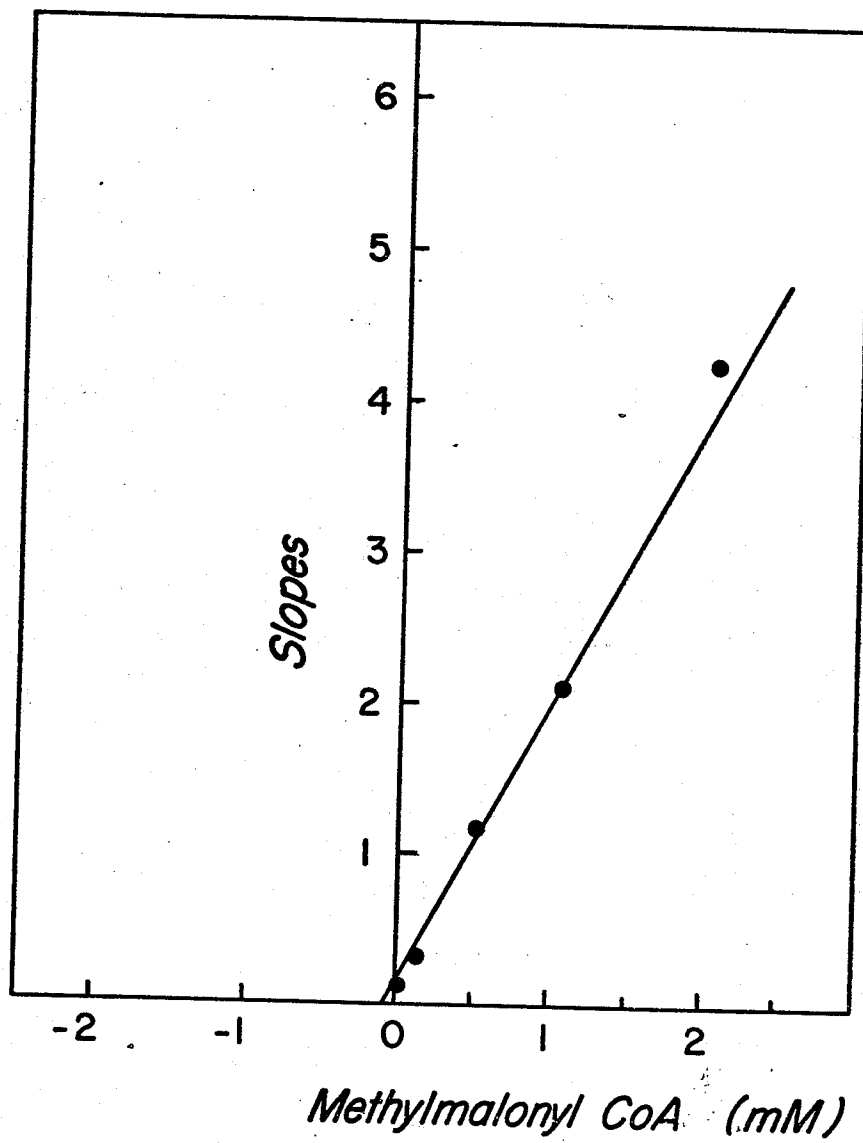


Figure 43. Replot of slopes obtained from
Figure 42, as a function of
methyl malonyl CoA concentration.



GENERAL DISCUSSION

This study was initiated to investigate the physical and kinetic properties of propionyl CoA carboxylase from a prokaryotic source. As discussed previously, the enzyme, propionyl CoA carboxylase, has an anaplerotic function, being a key distributary of the TCA cycle. However, most evidence concerning the physical and kinetic behavior of this enzyme has been presented in studies involving eukaryotic sources. Hence, the results obtained from examining the properties and kinetics of propionyl CoA carboxylase from R. rubrum could be used as a comparison with the aforementioned systems as well as with all biotin carboxylases in general.

Effect of pH on Propionyl CoA Carboxylase Activity

As indicated (Figure 3) the pH optimum of propionyl CoA carboxylase from R. rubrum was 7.9 - 8.1

using standard assay conditions. This value was very close to that obtained from other propionyl CoA carboxylase enzyme systems. A comparison of the results from this study with those obtained from other sources is given in Table V.

Effect of Various Cations and Anions on Propionyl CoA Carboxylase Activity

Propionyl CoA carboxylase from R. rubrum is affected by various cations and anions in different ways (Table III). Na^+ and Cl^- ions seem to have little or no effect on enzyme activity, with Cl^- ions perhaps displaying a slightly inhibitory response. The results however, are more clear cut with respect to other ions. K^+ acted as a strong activator of propionyl CoA carboxylase, resulting in a 18% stimulation of the enzyme. P_i ; a product of the propionyl CoA carboxylase reaction, was expected to be a strong inhibitor and as predicted, P_i caused a 45% inhibition of enzyme activity. The presence of $\text{SO}_4^{=}$ ions; structural analogues of P_i , should also display an inhibitory effect on activity but not to the same extent as P_i . The results clearly verify this prediction with $\text{SO}_4^{=}$ resulting

TABLE V

Comparison of pH optima of propionyl CoA carboxylases from various sources.

Source of enzyme	pH optimum
pig heart ^{a,b,c}	7.8 - 8.2
bovine liver ^{d,e,f}	8.0 - 8.5
<u>Rhodospirillum rubrum</u> ^{g,h}	7.6 - 8.0
<u>Rhodospirillum rubrum</u> ⁱ	7.9 - 8.1
^a Tietz and Ochoa (30)	
^b Kaziro et al (32)	
^c Kaziro (34)	
^d Giorgio and Plaut (93)	
^e Hegre and Lane (40)	
^f Halenz et al (39)	
^g Olsen and Merrick (1)	
^h Knight (19)	
ⁱ Present study	

in a 5% inhibition of the enzyme. However, this inhibitory effect by P_i and $SO_4^{=}$ became less pronounced when K^+ ions were also present in the reaction system. Enzyme inhibition by P_i was reduced from a 45% to 28% inhibition effect by the presence of K^+ in the assay mixture. Furthermore, the $SO_4^{=}$ effect was reversed from a 5% inhibition of the enzyme to a 12% stimulation by the addition of K^+ into the assay mixture. K^+ ion therefore, seems to antagonize the effect of both P_i and $SO_4^{=}$ ions causing a marked reduction in the amount of inhibition of the enzyme by P_i , and a reversal of the inhibitory effects of $SO_4^{=}$. A comparison of the results obtained in this study with those obtained using propionyl CoA carboxylase from other sources is presented in Table VI.

Inhibition by Avidin and Protection by Biotin

As indicated earlier (Table II), propionyl CoA carboxylase isolated from R. rubrum is inhibited by avidin. In addition, preincubation with excess biotin eliminated this inhibitory effect on enzyme activity by avidin. These facts indicate that propionyl CoA carboxylase is one of the biotin-

TABLE VI

Comparison of effects of various ions on propionyl CoA carboxylase from several sources

Source of Enzyme	K ⁺	L _i ⁺	Na ⁺	NH ₄ ⁺	Rb ⁺	Cs ⁺	Br ⁻	Ion I ⁻	ClO ₄ ⁻	Cl ⁻	CH ₃ COO ⁻	SO ₄ ⁻	P _i	tetramethyl ammonium
pig heart ^{a,b,c,d}	+	0	0	+	+	+	0	0	0	0	0	-	-	0
bovine liver ^e	+	0	0	+	+	+								
Rhodospirillum rubrum ^f	+		0							0		-	-	

+ = activates enzyme activity

- = inhibits enzyme activity

0 = little or no effect on enzyme activity

- a Edwards and Keech (95)
 b Tietz and Ochoa (30)
 c Neujahr (96)
 d Neujahr and Mistry (41)
 e Giorgio and Plaut (93)
 f Present study

containing enzymes as are other carboxylases including propionyl CoA carboxylases from all sources thus far tested (33, 39, 94).

Kinetic Constants of Propionyl CoA Carboxylase

The results of initial velocity studies on propionyl CoA carboxylase yielded apparent and true K_m values as determined from the double reciprocal rate-concentration plots (90) for MgATP, HCO_3^- , and propionyl CoA. A comparison of Michaelis constants for propionyl CoA carboxylase from R. rubrum as determined in this study with those from several other sources has been presented in Table VII. The apparent substrate affinity constants for the enzymes isolated from other sources are essentially identical to those obtained in this study (Table VII).

Effect of Free Mg^{++} on Propionyl CoA Carboxylase Activity^a

Allosteric enzymes are characterized by several distinctive features as compared to non-regulatory enzymes. One of these features is the initial velocity pattern obtained in a kinetic analysis of the enzyme. The initial velocity data obtained in the case of non-

^aThe reader is referred to the additional material following page 101 for further discussion of this topic.

TABLE VII

Comparison of Michaelis constants for propionyl CoA carboxylase
from several sources

Source of Enzyme	Michaelis constants (mM)			
	propionyl CoA	bicarbonate	ATP	MgATP
pig heart ^{a,b,c}	0.20 - 0.27	2.5	0.08	
bovine liver ^{d,e}	0.26	1.9	0.04-0.055	
<u>Rhodospirillum</u>	0.13	5.3	0.14	
<u>rubrum</u> ^f				
<u>Rhodospirillum</u>	0.133	2.8		0.176
<u>rubrum</u> ^g				
a Tietz and Ochoa	(30)			
b Kaziro et al	(32)			
c Kaziro	(34)			
d Halenz et al	(39)			
e Hegre and Lane	(40)			
f Olsen and Merrick	(1)			
g Present study				

regulatory enzymes is normally a rectangular hyperbola defined by the Michaelis-Menten equation:

$$v = \frac{VS}{K_m + S}$$

where V = maximum velocity

S = substrate

K_m = Michaelis constant

In the case of regulatory enzymes, a variety of plots are obtained when velocity is measured as a function of substrate concentration. Usually, these plots display different behavior than plots from non-regulatory enzymes.

In this study, normal Michaelis-Menten kinetics were observed with the substrates HCO_3^- and propionyl CoA. The presence or absence of free Mg^{++} in the assay system had little if any effect on the apparent K_m values obtained for these two substrates. However, with MgATP, a striking difference in the v versus S plots was observed if the assay mixture was lacking free Mg^{++} . In the absence of free Mg^{++} , the rate-substrate concentration curve was sigmoidal i.e. it showed cooperative behavior (Fig. 10). Lineweaver-Burk replots were non-linear and the apparent K_m value for MgATP could not be determined. However, the shape of this curve was changed fundamentally in the presence

of free Mg^{++} from the original sigmoid curve to a hyperbolic type of curve (Fig. 11). The double reciprocal plot was now linear and a K_m value for MgATP was obtained (Fig. 12). Thus free Mg^{++} seems to be acting as a positive modulator of propionyl CoA carboxylase with MgATP having a distinct homotropic effect; acting as both a true substrate of the reaction as well as an allosteric effector.

In the present study, MgATP interactions were examined further as to the extent and type of cooperativity observed for R. rubrum propionyl CoA carboxylase. Since the enzyme used throughout this thesis was not totally purified, binding studies were not attempted. However, a series of v versus S plots for MgATP were constructed using varying concentrations of free Mg^{++} in the assay system (Fig. 13). The amount of free Mg^{++} was gradually increased from zero to the standard assay concentration of 2.25 mM. The shapes of the rate-substrate concentration curves concomitantly changed from the sigmoidal type at the zero extreme to the hyperbolic type at the 2.25 mM extreme. Between these two concentration extremes the lines fell between the sigmoidal and hyperbolic types of plots. Therefore, Figure 13 clearly illustrates the existence of positive

cooperativity. These results resembled those obtained by Cazzulo and Stoppani (79) using yeast pyruvate carboxylase.

Knowing that the maximum velocities of the aforementioned curves were the same (see "Results"), the Hill equation was applied to the data (Figs. 14). The results from the Hill plot revealed that n values varied from close to at zero free Mg^{++} concentration to close to 1 at 2.25 mM free Mg^{++} concentration. Clearly, the existence of at least two interacting sites for MgATP had already been suggested by the cooperativity of MgATP (Fig. 13), and the Hill plot provided additional support for this supposition.

As was indicated previously, the true number of catalytic sites for MgATP could not be determined since binding studies could not be attempted without a pure enzyme. However, the data presented above, can be interpreted in terms of at least one model. A basic allosteric model similar to that described by Monod et al (97, 98) can be proposed to explain the homotropic behavior of MgATP.

In this allosteric model, the enzyme; propionyl CoA carboxylase, consists of at least two subunits, each with a catalytic site and possibly an activator site. The enzyme exists in two forms, the inactive

or tight state (T), and the active or relaxed state (R). The equilibrium between the two states is governed by the concentration of ligand present in the system; MgATP or free Mg^{++} . MgATP and Mg^{++} bind better to the R state and shift the equilibrium in the direction of the R state. Hence, when no free Mg^{++} is present in the system, MgATP activity plot shows a distinct homotropic behavior, being sigmoidal in shape. However, if sufficient free Mg^{++} is present in the system along with MgATP, the enzyme is converted completely to the R state, and normal hyperbolic v versus S plots for MgATP result. The n value obtained from the Hill plot from this model, would therefore be any value greater than one and would agree with the observed results.

Alternative models to explain the data could be described, but the one outlined above, has the virtue of simplicity. For example, non-linear reciprocal plots would be predicted on the basis of a non-allosteric model in which the ligand binds twice to the enzyme - at an activator site which must be occupied before catalytic activity is manifested, and at the catalytic site. Analysis of the data using the method of Nakazawa and Hayaishi (99) eliminated this possibility. This model was therefore not considered further.

Additional Material

There is abundant evidence and general agreement that a divalent cation, such as Mg^{++} , is a requirement for the action of biotin carboxylases (34, 86, 101, 102). The exact role of the Mg^{++} ion has however been the subject of considerable debate. The reader is referred to the papers of McClure et al (100), Dugal (80), Cazzulo and Stoppani (79) and Bais and Keech (78), for examples of varying interpretation of the role of Mg^{++} in the action of biotin carboxylases.

In the foregoing discussion it has been assumed that there was no free Mg^{++} in the MgATP preparations used, and that the kinetic observations presented in Figures 10-14 reflected changes in the behaviour of the enzyme in response to known changes in free Mg^{++} levels. These changes have been interpreted as resulting from the action of the Mg^{++} ion as an allosteric activator.

A major difficulty with this interpretation is that it is possible to calculate the free Mg^{++} concentration in MgATP preparations, and such calculations show that under the conditions used in the experiments under discussion, and assuming a stability constant of $80,000 M^{-1}$ (103) for MgATP, a significant quantity (25-30% of the total Mg^{++}) of free Mg^{++} was present in the reaction mixtures used. In fact, when the data of Fig 10 was plotted taking this into account, a less sigmoid plot resulted. While this alone does not negate the

Additional Material(continued)

possibility that Mg^{++} can act as an allosteric activator for propionyl CoA carboxylase, it indicates that the problem is more complex than the earlier discussion has assumed. Additional factors which may further complicate the situation are:-

a) Free ATP could be a strong inhibitor, competitive with MgATP, particularly at low MgATP levels. This in itself could lead to the production of a sigmoid curve.

b) The possible action of ADP as a product inhibitor may complicate the measurement of initial velocities at low MgATP levels. Further, since the stability constant for MgADP is an order of magnitude lower than that for MgATP, free Mg^{++} ions could be released during the reaction, thus affecting the kinetic behaviour.

c) Errors in making exactly equimolar mixtures of $MgCl_2$ and ATP may have been made.

In view of this, it is concluded that there is insufficient data presented in this Thesis to enable the presentation of a reasonable hypothesis concerning the roles of Mg^{++} and MgATP in this enzyme catalyzed reaction. Other experiments, designed to distinguish between the various possibilities mentioned above, must be performed if a clearer view is to be obtained.

Discussion of Mechanism of Action of Propionyl CoA Carboxylase

The major concern when dealing with enzymes and their kinetic patterns has always been to try to set up some type of mechanism for the enzyme's action. A summary of the kinetic patterns obtained in this study is presented in Table VIII. All terminology and analytical methods used in discussing these kinetic results are those of Cleland (2, 3, 4).

In trying to determine an enzyme's mechanism of action, the problem of fitting one's results to suit "classical" enzyme models is usually a major step in analyzing the results. Traditionally, all interpretations of enzyme kinetics for complex reactions, example biotin carboxylases, were assumed to focus on a reaction mechanism where only one active centre enzyme was operative. Furthermore, until the possibility of enzymes having more than

TABLE VIII

Summary of kinetic data for propionyl CoA carboxylase from R. rubrum

Substrates	Predicted Results		Observed Results		Type of Inhibition
	Nonclassical rapid equilibrium	Nonclassical rapid equilibrium with abortive complexes ^a	Intercept	Slope	
MgATP-HCO ₃ ⁻			change	change	
MgATP-Prop. CoA			change	no change ^b	
Prop. CoA-HCO ₃ ⁻			change	no change ^c	
Product inhibition					
MgATP-MgADP	C	C	no change	change	C
MgATP-P _i	C	C	no change	change	C
MgATP-Methylmal-CoA	NC	NC	change	change	NC
HCO ₃ ⁻ - MgADP	C	NC	change	change	NC
HCO ₃ ⁻ - P _i	C	NC	change	change	NC
HCO ₃ ⁻ - Methylmal. CoA			change	change	NC

Table VIII Continued

Substrates	Predicted Results		Observed Results		Type of Inhibition
	Nonclassical rapid equilibrium	Nonclassical rapid equilibrium with abortive complexes ^a	Intercept	Slope	
Prop. CoA - MgADP	UC	UC	no change	change	C d
Prop. CoA - P _i	UC	UC	no change	change	C d
Prop. CoA - Methylmal. CoA	C	C	no change	change	C

Prop. CoA = propionyl CoA

Methylmal. CoA = methylmalonyl CoA

C = competitive

UC = uncompetitive

NC = noncompetitive

^aThe abortive complexes which form at the site of the Bi Bi partial reaction are E-HCO₃⁻-P_i and E-HCO₃⁻ - MgADP.

^bAt high propionyl CoA concentrations, the lines became distinctly curved concave upward; indicating inhibition of MgATP binding at high propionyl CoA concentrations. However these lines resembled parallel lines for the most part.

Table VIII Continued

^cAt low propionyl CoA concentrations, the family of lines displayed an intersecting pattern. At higher propionyl CoA concentrations, the lines became biphasic and showed an additional complex kinetic behavior. The lines became curved concave downward, thereby indicating activation of HCO_3^- binding. The central portion of the curves however, approximated parallel behavior and were used in all initial velocity patterns and analyses, as explained in the text.

^dThe only deviations to a nonclassical rapid equilibrium mechanism with abortive complexes are noted here. The observed results were competitive in nature, while those predicted by the aforementioned mechanism, were uncompetitive.

one active site operating at one time had been only speculative. Even with the findings that the mechanism of action of biotin enzymes involved the formation of intermediate carboxybiotin complexes (45, 64) and that all of the reaction components could form binary complexes with the enzyme (65, 66), the question of more than one operative active site per enzyme had not been seriously considered. In fact, although Cleland (2, 3, 4) had suggested that this possibility could exist, it was not until the studies of Barden et al (67), and McClure et al (68), on pyruvate carboxylase, that attention was focused on the reality of such a possibility.

The kinetic results listed in Table VIII, could not fit any plausible mechanism in which there was only one active site on the enzyme operative at any one time. A mechanism that could satisfactorily explain these kinetic patterns is a "nonclassical" Ping Pong Bi Bi Uni Uni mechanism involving two separate and functionally distinct catalytic sites, presumably linked by the carboxyl carrier; the biotinyl residue. One of the two catalytic sites would bind the reactants of each partial reaction, with the biotinyl residue swinging freely between the two sites regardless of what other molecules were bound there. Inspection of Table VIII

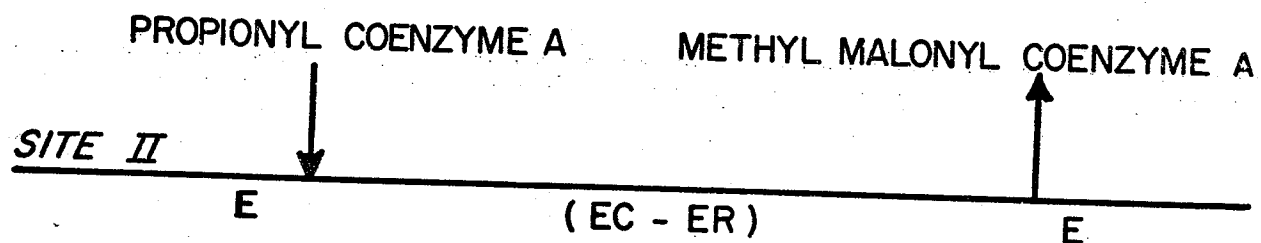
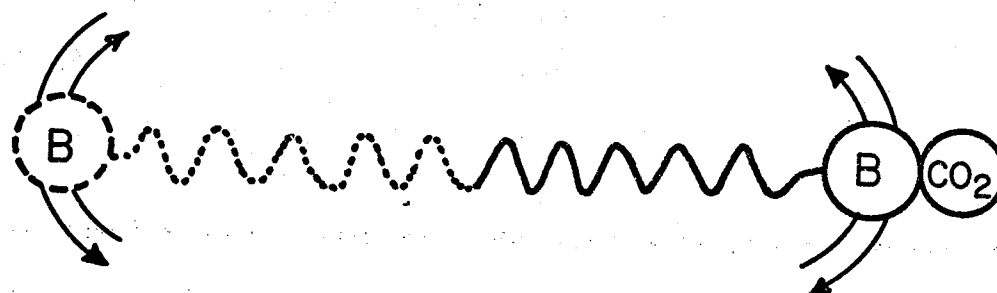
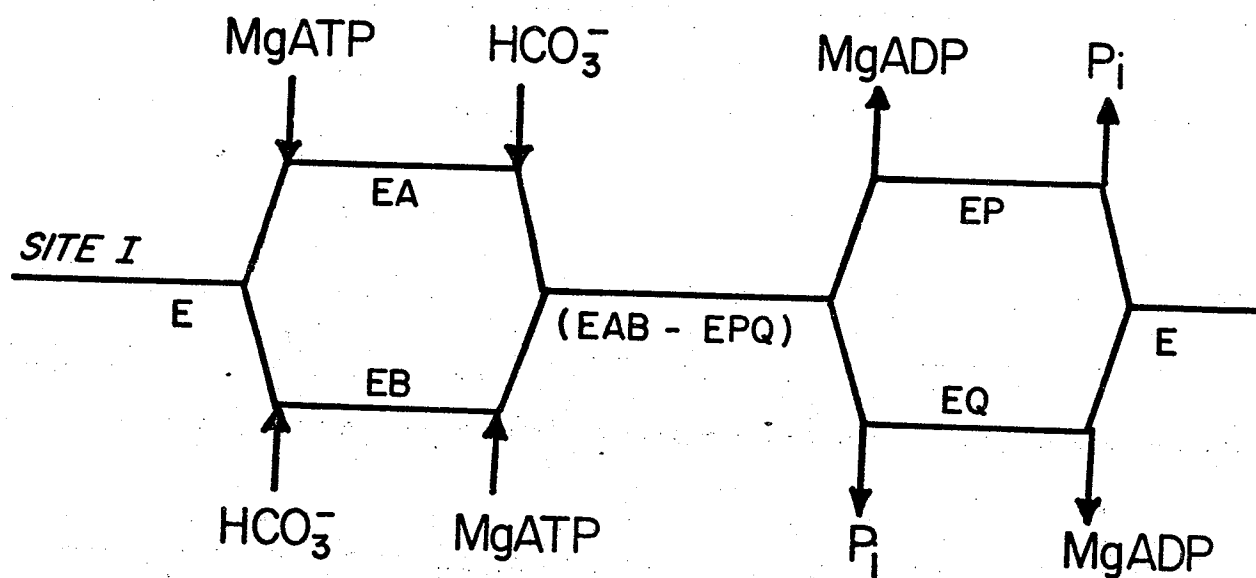
shows that the results obtained in this study are consistent with those predicted for such a mechanism. The exceptions to this consistency are noted in the table and discussed in greater detail below.

The reactant at the Uni Uni site, propionyl CoA, seems not only to act as a substrate, but also exhibits some sort of effect on the affinity for binding of the substrates MgATP and HCO_3^- to the enzyme at the other catalytic site. This mechanistic interpretation would therefore not conflict, in any significant manner, with the previously determined facts concerning biotin carboxylases in general.

If it is assumed that there are two separate and distinct sites, I and II, in analogy with the model proposed for pyruvate carboxylase (67), then the reaction catalyzed by propionyl CoA carboxylase may be visualized as follows (Figure 44).

From Fig. 44, it would be expected that initial velocity patterns for the interaction of substrates at site I (that is MgATP - HCO_3^- interactions) would be intersecting, using Cleland's method of analysis (4). The results as shown in Table VIII, verify this prediction. Furthermore, interaction of the substrates of site I (either MgATP or HCO_3^-) with the substrate of site II (propionyl

Figure 44. Diagramatic representation of the
proposed kinetic mechanism for
propionyl CoA carboxylase from
R. rubrum.



CoA) would result in parallel initial velocity patterns. This prediction does not concur fully with the observed data. The deviations from predicted behavior will now be discussed: (a) MgATP - propionyl CoA interactions: (See Fig. 15). The lines become concave upward at high propionyl CoA concentration, and also deviate from linearity at very low propionyl CoA concentration. The lines nevertheless appear to be essentially parallel. (b) HCO_3^- - propionyl CoA interactions: (See Fig. 19). The lines are not parallel, rather showing an intersecting pattern. However, they more closely approximate a parallel pattern at higher HCO_3^- concentrations, and become concave downwards at high propionyl CoA concentrations. It should also be noted that it is difficult to obtain reliable data when HCO_3^- is a varied substrate, particularly at low HCO_3^- concentrations. This is a result of the nature of the assay, and the problem of the presence of endogenous HCO_3^- in the system.

Therefore, propionyl CoA seems to not only act as a substrate at site II, but also affects the affinity of site I for MgATP and HCO_3^- at high propionyl CoA concentrations. Activation of HCO_3^- binding, and inhibition of MgATP binding to site I, seem to be a direct consequence of the higher propionyl CoA concentrations present in the reaction system. The question however, arises as to how propionyl CoA might affect

the binding of both HCO_3^- and MgATP to the enzyme, and both in a different manner. Possibly, as was suggested in the case of pyruvate carboxylase from rat liver (68) and from chicken liver (67), at high concentrations, propionyl CoA combines with the enzyme a second time in the vicinity of site I in such a way that HCO_3^- binding is increased and MgATP binding is decreased. The binding affinity for HCO_3^- and MgATP would then depend on the fractional occupancy of site II by propionyl CoA, regardless of the degree of carboxylation of biotin. The observed initial velocity patterns, while not being in complete agreement with predicted results, may be regarded as being consistent with the postulated mechanism (Fig. 44), as discussed above.

The reaction at site I is essentially a rapid equilibrium random Bi Bi reaction with MgATP and HCO_3^- as substrates, and P_i and MgADP as products. Site I reactants combine at a common catalytic site on the enzyme. The results of product inhibition studies predicted for such a scheme would therefore be competitive inhibition patterns for MgATP or HCO_3^- with P_i or MgADP . Only competitive inhibition would be suggested since the product inhibitor and the variable substrate are involved in the same partial reaction.

However, the observed results display competitive inhibition patterns with $\text{MgATP} - \text{P}_i$ or $\text{MgATP} - \text{MgADP}$ interactions but not with $\text{HCO}_3^- - \text{P}_i$ or $\text{HCO}_3^- - \text{MgADP}$ ^{which} patterns/display noncompetitive product inhibition relationships. Therefore one might suspect the existence of a third catalytic site for the carboxylation of the enzyme as was suggested for pyruvate carboxylase from A. niger (70). However, the observed data can be interpreted in terms of the two-site scheme of Fig. 44, by assuming that HCO_3^- and P_i or MgADP form abortive enzyme-reactant complexes, simultaneously binding to the enzyme in the forms $\text{E-HCO}_3^- - \text{P}_i$ and $\text{E-HCO}_3^- - \text{MgADP}$. Therefore the observed results would be consistent with the predicted patterns for the site I reaction.

The reaction at site II is a Uni Uni reaction with propionyl CoA as substrate and methylmalonyl CoA as product. Thus propionyl CoA and methylmalonyl CoA share a common catalytic site, with this site being separate from that used by the reactants at site I. Product inhibition patterns for this partial reaction should therefore be competitive in nature between propionyl CoA and methylmalonyl CoA, since the variable substrate and the product inhibitor bind the same enzyme form. The results in Table VIII, clearly verify this prediction.

Now what about the predicted product inhibition patterns between product inhibitors and variable substrates of the two different catalytic sites? If methylmalonyl CoA is the product inhibitor and the variable substrate is either MgATP, or HCO_3^- , the predicted inhibition pattern should be uncompetitive. However, the observed inhibition pattern is non-competitive. This apparent discrepancy can be explained if the rate of the reaction in the direction of methylmalonyl CoA decarboxylation is not solely dependent on the interconversion of the central complex, but also limited in part by the release of MgATP. Under such conditions HCO_3^- could react with E-MgATP and biotin to regenerate carboxybiotin. This would result in an inhibition of the reaction, yielding a noncompetitive pattern. Similar results were seen in work done on pyruvate carboxylase by Barden et al (67). Product inhibition patterns between P_i or MgADP, and propionyl CoA, should also be uncompetitive. However, the observed results show competitive inhibition patterns for these interactions. This discrepancy can be explained by the overlap of propionyl CoA from site II to the vicinity of site I, thus competing with the product inhibitors, P_i or MgADP, at site I. The observed results now can be explained by the mechanism shown in Fig. 44.

The following summation can be used to explain the mechanism of reaction of propionyl CoA carboxylase from R. rubrum. A two site mechanism is proposed for this enzyme. Initial velocity patterns and substrate-inhibitor relationships with the enzyme provide sufficient evidence in making such a proposal. Furthermore, the kinetic behavior of HCO_3^- with either P_i or MgADP, suggests that abortive enzyme-reactant complexes are formed. Hence, HCO_3^- and either P_i or MgADP could simultaneously bind to the enzyme producing the forms $\text{E-HCO}_3^- - \text{P}_i$ and $\text{E-HCO}_3^- - \text{MgADP}$. This is supported by previous work performed on pyruvate carboxylase by Scrutton and Utter (66). In this two-site mechanism, the Bi Bi partial reaction displays a rapid equilibrium random mechanism as has been seen in other related enzyme mechanisms (67, 68). The overall reaction of the enzyme is defined as the sum of the two partial reactions and is described by a Ping Pong Bi Bi Uni Uni mechanism in which separate catalytic sites exist for the reactants of each partial reaction. The results therefore, agree with work previously done on acetyl CoA carboxylase by Alberts et al (54, 55) where the individual subunits of the enzyme carry out specific parts of the reaction. Furthermore, independence of one site from the other seems to be lost at higher

propionyl CoA concentrations. This may be a direct result of the overlap of site I by propionyl CoA bound at site II. This fractional occupancy by propionyl CoA at or around the two sites of the enzyme seems also to affect the binding affinity for the two substrates of the Bi Bi reaction, and both in a different manner. Therefore, minor differences, from a mechanistic point of view, may be observed between the present study and previous work done on pyruvate carboxylase systems from eukaryotic sources (67, 68, 70). The

The evidence for the proposed mechanism of action of propionyl CoA carboxylase from R. rubrum is not absolutely conclusive. The question of changes in the binding of MgATP and HCO_3^- to the enzyme at different propionyl CoA concentrations should be subjected to further examination. In addition, a rate equation has not yet been set up for the reaction. However, the application of Cleland's analytical principles (4) to kinetic studies of initial velocity and product inhibition patterns, seemed to prove successful in illuminating the reaction mechanism of a complex system in the present study.

REFERENCES

1. Olsen, I. and Merrick, J. M. (1968). J. Bacteriol. 95: 1774.
2. Cleland, W. W. (1963). Biochim. Biophys. Acta. 67: 104.
3. Cleland, W. W. (1963). Biochim. Biophys. Acta. 67: 173.
4. Cleland, W. W. (1963). Biochim. Biophys. Acta. 67: 188.
5. Kaziro, Y. and Ochoa, S. (1964). In "Advances in Enzymology", Vol. 26, 312-378 (Nord, F. F., ed.) Interscience Publishers, New York.
6. Ringer, A. I. (1912). J. Biol. Chem. 12: 511.
7. Lorber, V., Lifson, N., Sakami, W. and Wood, H. G. (1950). J. Biol. Chem. 183: 531.
8. Larsen, H. (1951). J. Biol. Chem. 193: 167.
9. Lardy, H. A. and Peanasky, R. (1953). Physiol. Rev. 33: 560.
10. Flavin, M. and Ochoa, S. (1957). J. Biol. Chem. 229: 965.
11. Flavin, M., Castro-Mendoza, H. and Ochoa, S. (1956). Biochim. Biophys. Acta. 20: 591.

12. Flavin, M., Castro-Mendoza, H. and Ochoa, S. (1957).
J. Biol. Chem. 229: 981.
13. Elsdon, S. R. and Ormerod, J. G. (1956). Biochem.
J. 63: 691.
14. Ormerod, J. G. (1956). Biochem. J. 64: 373.
15. Clayton, R. K. (1957). Arch. Mikrobiol. 26: 29.
16. Clayton, R. K., Dettmer, F. H. and Robertson, A. E.
(1957). Arch. Mikrobiol. 26: 20.
17. Elsdon, S. R. (1958). Abstr. 7th Int. Congr.
Microbiol., Stockholm 71.
18. Gibson, J. and Knight, M. (1961). Biochem. J.
78: 8p.
19. Knight, M. (1962). Biochem. J. 84: 170.
20. Burton, D. N. (1971). Unpublished observations.
21. Hsia, Y. E., Scully, K. J. and Rosenberg, L. E.
(1969). Lancet I: 757.
22. Hsia, Y. E., Scully, K. J. and Rosenberg, L. E.
(1971). J. Clin. Invest. 50: 127.
23. Gompertz, D., Storrs, C. N., Bau, D. C. K., Peters,
T. J. and Hughes, E. A. (1970). Lancet I: 1140.
24. Barnes, N. D., Hull, D., Balgobin, L. and Gompertz, D.
(1970). Lancet II: 244.
25. Lynen, F. and Tada, M. (1961). Angew. Chem.
73: 513.

26. Wawszkiewicz, E. J. and Lynen, F. (1964).
Biochem. Z. 340: 213.
27. Kanada, T. and Corcoran, J. W. (1961). Federation
Proc. 20: 273.
28. Grisebach, H., Achenbach, H. and Hofheinz, W.
(1960). Z. Naturforsch. 15b: 560.
29. Evans, M. C. W., Buchanan, B. B. and Arnon, D. I.
(1966). Proc. Nat. Acad. Sci. U.S.A. 55: 928.
30. Tietz, A. and Ochoa, S. (1959). J. Biol. Chem.
234: 1394.
31. Kaziro, Y., Leone, E. and Ochoa, S. (1960).
Proc. Nat. Acad. Sci. U.S.A. 46: 1319.
32. Kaziro, Y., Ochoa, S., Warner, R. C. and Chen, Y.-J.
(1961). J. Biol. Chem. 236: 1917.
33. Kaziro, Y., Grossman, A. and Ochoa, S. (1965).
J. Biol. Chem. 240: 64.
34. Kaziro, Y. (1969). In "Methods in Enzymology",
Vol. 13, 181-190 (Lowenstein, J. M., ed.)
Academic Press, New York.
35. Kaziro, Y. and Ochoa, S. (1961). J. Biol. Chem.
236: 3131.
36. Halenz, D. R. and Lane, M. D. (1960). J. Biol.
Chem. 235: 878.
37. Lane, M. D., Halenz, D. R., Kosow, D. P. and
Hegre, C. S. (1960). J. Biol. Chem. 235: 3082.

38. Lane, M. D. (1962). In "Methods in Enzymology",
Vol. 5, 576-581. (Colowick, S. P. and Kaplan,
N. O., eds.) Academic Press, New York.
39. Halenz, D. R., Feng, Y.-J., Hegre, C. S. and
Lane, M.D. (1962). J. Biol. Chem. 237: 2140.
40. Hegre, C. S. and Lane, M. D. (1966). Biochim.
Biophys. Acta. 128: 172.
41. Neujahr, H. Y. and Mistry, S. P. (1963). Acta.
Chem. Scand. 17: 1140.
42. Allen, S. H. G., Jacobson, B. E. and Stjernholm,
R. (1964). Arch. Biochem. Biophys. 105: 494.
43. Bangh, C. L., Bates, D. S., Claus, G. W. and
Werkman, C. H. (1961). Enzymologia 23: 15.
44. Alberts, A. W. (1970). Unpublished observations,
as cited in Reference 63.
45. Ochoa, S. and Kaziro, Y. (1961). Federation Proc.
20: 982.
46. Kosow, D. P. and Lane, M. D. (1961). Biochem.
Biophys. Res. Commun. 4: 92.
47. Kosow, D. P. and Lane, M. D. (1961). Biochem.
Biophys. Res. Commun. 5: 191.
48. Kosow, D. P. and Lane, M. D. (1962). Biochem.
Biophys. Res. Commun. 7: 439.
49. Lynen, F., Knappe, J., Lorch, E., Jutting, G. and
Ringelmann, E. (1959). Angew. Chem. 71: 481.

50. Waite, M. and Wakil, S. J. (1962). J. Biol. Chem. 237: 2750.
51. Shive, W. and Rogers, L. L. (1947). J. Biol. Chem. 169: 453.
52. Wood, H. G., Allen, S. H. G., Stjernholm, R. and Jacobson, B. (1963). J. Biol. Chem. 238: 547.
53. Lynen, F., Knappe, J., Lorch, E., Jutting, G., Ringelmann, E. and Lachance, J. P. (1961). Biochem. Z. 335: 123.
54. Alberts, A. W., Nervi, A. M. and Vagelos, P. R. (1969). Proc. Nat. Acad. Sci. U.S.A. 63: 1319.
55. Alberts, A. W. and Vagelos, P. R. (1968). Proc. Nat. Acad. Sci. U.S.A. 59: 561.
56. Fall, P. R. and Vagelos, P. R. (1973). J. Biol. Chem. 248: 2078.
57. Nervi, A. M., Alberts, A. W. and Vagelos, P. R. (1971). Arch. Biochem. Biophys. 113: 401.
58. Dimroth, P., Guchhait, R. B., Stoll, C. and Lane, M. D. (1970). Proc. Nat. Acad. Sci. U.S.A. 67: 1353.
59. Guchhait, R. B., Moss, J. D., Sokolski, W. and Lane, M. D. (1971). Proc. Nat. Acad. Sci. U.S.A. 68: 653.
60. Guchhait, R. B., Polakis, S. E., Dimroth, P., Stoll, E., Moss, J. D. and Lane, M. D. (1974). J. Biol. Chem. 249: 6633.

61. Dimroth, P., Guchhait, R. B. and Lane, M. D. (1971).
Hoppe-Seyler's Z. Physiol. Chem. 352: 351.
62. Guchhait, R. B., Zwergel, E. E. and Lane, M. D.
(1974). J. Biol. Chem. 249: 4776.
63. Scrutton, M. C. and Young, M. R. (1972). In "The
Enzymes", Third Edition, Vol. VI, 1-35 (Boyer, P. D.,
ed.), Academic Press, New York.
64. Green, N. M. (1963). Biochem. J. 89: 585.
65. Mildvan, A. S., Scrutton, M. C. and Utter, M. F.
(1966). J. Biol. Chem. 241: 3488.
66. Scrutton, M. C. and Utter, M. F. (1965). J. Biol.
Chem. 240: 3714.
67. Barden, R. E., Fung, H.-C., Utter, M. F. and
Scrutton, M. C. (1972). J. Biol. Chem. 247:
1323.
68. McClure, W. R., Lardy, H. A., Wagner, M. and
Cleland, W. W. (1971). J. Biol. Chem. 246:
3579.
69. McClure, W. R., Lardy, H. A. and Cleland, W. W.
(1971). J. Biol. Chem. 246: 3584.
70. Feir, H. A. and Suzuki, I. (1969). Can. J.
Biochem. 47: 697.
71. Ashman, L. K. and Keech, D. B. (1975). J. Biol.
Chem. 250: 14.
72. Moss, J. D. and Lane, M. D. (1971). In "Advances
in Enzymology", Vol. 35, 321-442 (Meister, A.,
ed.), Interscience Publishers, New York.

73. Lane, M. D., Moss, J. D. and Polakis, S. E. (1974).
In "Current Topics in Cellular Regulation",
Vol. 8, 139 (Horecker, B. L. and Stadtman, E. R.,
eds.), Academic Press, New York.
74. Lane, M. D., Moss, J. D., Ryder, E. and Stoll, E.
(1971). In "Advances in Enzyme Regulation",
First Edition, Vol. 9, 237-251. (Weber, G., ed.),
Pergamon Press, New York.
75. Lane, M. D. and Moss, J. D. (1971). In "Metabolic
Pathways", Third Edition, Vol. 5, 23-54.
(Vogel, H. J. ed.), Academic Press, New York.
76. Polakis, S. E., Guchhait, R. B. and Lane, M. D.
(1973). J. Biol. Chem. 248: 7957.
77. Barden, R. E. and Scrutton, M. C. (1974). J. Biol.
Chem. 249: 4829.
78. Bais, R. and Keech, D. B. (1972). J. Biol. Chem.
247: 3255.
79. Cazzulo, J. J. and Stoppani, A. O. M. (1969).
Biochem. J. 112: 747.
80. Dugal, B. S. (1973). Biochem. Biophys. Res.
Commun. 54: 1603.
81. Simon, E. J. and Shemin, D. (1953). J. Am. Chem.
Soc. 75: 2520.
82. Cohen-Bazire, G., Sistrom, W. R. and Stanier, R. Y.
(1957). J. Cellular Comp. Physiol. 49: 25.

83. Burton, D. N. (1972). Personal communications.
84. Bray, G. A. (1960). Anal. Biochem. 1: 279.
85. Lowry, O. H., Rosebrough, N. J., Farr, A. L. and Randall, R. J. (1951). J. Biol. Chem. 195: 265.
86. Keech, D. B. and Utter, M. F. (1963). J. Biol. Chem. 238: 2609.
87. Gailiusis, J., Rinne, R. W. and Benedict, C. R. (1964). Biochim. Biophys. Acta. 92: 592.
88. Seubert, W. and Remberger, U. (1961). Biochem. Z. 334: 401.
89. Ling, A.-M. and Keech, D. B. (1966). Enzymologia. 30: 367.
90. Lineweaver, H. and Burk, O. (1934). J. Am. Chem. Soc. 56: 658.
91. Howden, R. L. (1970). M.Sc. Thesis, Univ. of Manitoba.
92. Florini, J. R. and Vestling, C. S. (1957). Biochim. Biophys. Acta. 25: 575.
93. Georgio, A. J. and Plaut, G. W. E. (1967). Biochim. Biophys. Acta. 139: 487.
94. Lane, M. D. and Lynen, F. (1963). Proc. Nat. Acad. Sci. U.S.A. 49: 379.
95. Edwards, J. B. and Keech, D. B. (1968). Biochim. Biophys. Acta. 159: 167.

96. Neujahr, H. Y. (1963). Acta. Chem. Scand. 17:
1777.
97. Monod, J., Changeux, J. P. and Jacob, F. (1963).
J. Mol. Biol. 6: 306.
98. Monod, J., Wyman, J. and Changeux, J. P. (1965).
J. Mol. Biol. 12: 88.
99. Nakazawa, A. and Hayaishi, O. (1967). J. Biol.
Chem. 242: 1146.
100. McClure, W.R., Lardy, H.A. and Kneifel, H.P. (1971).
J. Biol. Chem. 246, 3569.
101. Gregolin, C., Ryder, E., Kleinschmidt, A.K.,
Warner, R.C. and Lane, M.D. (1966). Proc. Nat. Acad.
Sci. U.S.A. 56, 148.
102. Coon, M.J. (1962), in "Methods in Enzymology" Vol 5,
896. (Colowick, S.P. and Kaplan, N.O. ed.), Academic
Press, New York.
103. O'Sullivan, W.J. and Perrin, D.D. (1964). Biochemistry
3, 18.